ADRENERGIC REGULATION OF REGIONAL FAT METABOLISM

Konstantinos Manolopoulos
Green Templeton College

A thesis submitted to the Faculty of Clinical Medicine
at the University of Oxford
for the degree of Doctor of Philosophy

Trinity Term 2011

Oxford Laboratory of Integrative Physiology
Oxford Centre for Diabetes, Endocrinology and Metabolism
Nuffield Department of Medicine
University of Oxford

ACKNOWLEDGEMENTS

I would like to thank all members of the Oxlip research group who have helped in making this work possible. Jane Cheeseman and Louise Dennis for continuous help and support with the recruitment, organisation and execution of all studies. Marj Gilbert, Pauline Sutton and Sandy Humphreys for handling and biochemical analysis of countless samples. Leanne Hodson and Barbara Fielding, together with Marj Gilbert and Jenny Collins, for the handling and analysis of the isotope tracer samples, and for stimulating and very helpful discussions. Matt Neville and Jenny Collins for the handling, preparation and analysis of the molecular biology samples, as well as for the many hours of good fun and chatting. Karin Harnden for help with the food diaries and Claire Colley for secretarial support and help. To all of you – thank you. Your dedication and commitment made my time in the group both very enjoyable and a great experience.

I am deeply grateful to my supervisors, Keith Frayn and Fredrik Karpe. Both have been – and are – a source of great inspiration and guidance. They gave me the opportunity to come to Oxford and included me in the Oxlip family from the very first day. They taught me unique methodologies for the investigation of human metabolism and sparked my interest in adipose tissue physiology. Above all, they taught me that it is the combination of academic excellence and personal warmth that makes for successful progress.

I would also like to thank my family for their understanding and support during the times of research and writing up of this thesis. The arrival of our daughter Danae marked one of the happiest days in December 2009 – it was a day that started with a study at OCDEM and ended with a baby at the John Radcliffe Hospital. However, it also marked the start of a difficult personal balance between work and family life. I thank my wife Io, who has been supporting me with her selfless attitude.

Finally, I am honoured by being Keith Frayn's last D.Phil. student. To you, Keith, I dedicate this thesis. You truly are a great mentor.

MEMORANDUM

The collation, analysis and interpretation of the work presented in this thesis are my original work carried out under the supervision of Professor Keith Frayn and Dr Fredrik Karpe in the Nuffield Department of Clinical Medicine at the University of Oxford.

Various members of the staff assisted with the clinical studies, particularly the nursing staff, Jane Cheeseman and Louise Dennis. The processing and biochemical analysis of blood samples was done by members of the laboratory staff (Sandy Humphreys, Marje Gilbert, Pauline Sutton). Mass spectrometry was performed by Marje Gilbert, Leanne Hodson, Jenny Collins and Barbara Fielding. Molecular biology methods were performed by Jenny Collins and Matt Neville. I was responsible for collation and analysis of the data. Sandy Humphreys advised on appropriate statistical analysis.

ABSTRACT

Adrenergic regulation of regional fat metabolism

Konstantinos Manolopoulos

Green Templeton College, D. Phil. Thesis, Trinity Term, 2011

Introduction: An increased gluteofemoral adipose tissue (AT) mass is associated with a protective cardiovascular and metabolic risk profile, and effective fatty acid retention in femoral AT has been proposed as a possible mechanism. Catecholamines are important regulators of AT lipolysis and blood flow (ATBF). The aim of the thesis was to investigate regional differences in the adrenergic regulation of fatty acid release and ATBF between abdominal and femoral AT *in vivo*. Furthermore, *in vivo* regional fatty acid trafficking was studied in a physiological setting over 24 h.

Methods: Regional fatty acid trafficking, along with the measurement of ATBF, was studied with the arterio-venous difference technique and stable isotope tracers in healthy volunteers. Adrenergic agonists (isoprenaline, adrenaline) were infused either locally by microinfusion, or systemically. Local microinfusion of adrenoreceptor antagonists (propranolol, phentolamine) was used to characterize specific adrenoreceptor subtype effects. The trafficking of dietary fatty acids was studied over a 24 h period involving three meals containing stable isotope-labelled fatty acids along with intravenous infusions of another labelled fatty acid.

Results: Femoral ATBF and lipolysis was less responsive to adrenergic stimulation with adrenaline compared to abdominal AT. This was due to increased femoral α-adrenoreceptor responsiveness. When studied over 24 h, femoral AT showed a lower lipolysis rate compared to abdominal AT, while dietary fatty acids were extracted more avidly by abdominal AT. Uptake of non-dietary fatty acids (derived from very-low-density lipoproteins or unbound non-esterified fatty acids) was comparable between abdominal and femoral AT.

Conclusion: There are fundamental differences in response to adrenergic stimuli between abdominal and gluteofemoral tissues and the ability of femoral AT to trap non-dietary fatty acids may provide protection of other tissues from ectopic fatty acid deposition.

PUBLICATIONS

Publications of material arising from work related to this thesis:

Manolopoulos KN, Karpe F, Frayn KN. Gluteofemoral fat as a determinant of metabolic health. Int J Obesity. 2010;34:949-959

Manolopoulos KN, Karpe F. Functional genetic effect of the ADRB2 Arg16Gly polymorphism in the LARGE trial (Correspondence). Lancet. 2010;375:724-725

McQuaid SE, **Manolopoulos KN**, Dennis AL, Cheeseman J, Karpe F, Frayn KN. Development of an arterio-venous difference method to study the metabolic physiology of the femoral adipose tissue depot. Obesity. 2010;18:1055-1058

Published abstracts of material arising from work related to this thesis:

Manolopoulos KN, Karpe F, Frayn KN. Gluteofemoral fat as a determinant of metabolic health: differential adrenergic regulation of regional lipolysis and adipose tissue blood flow *in vivo* (American Diabetes Association meeting, 2010). Diabetes. 2010;59:A391

Manolopoulos KN, Cheeseman J, Dennis AL, Frayn KN, Karpe F. Increased lipolytic activity of the gluteofemoral adipose tissue is a feature of the female pattern of fat distribution (International Congress of Obesity, 2010). Obesity Reviews. 2010;11 (Suppl. 1):175

TABLE OF CONTENTS

ABBREVIATIONS

A	Arterial
ADR	Adrenaline
ANOVA	Repeated measures analysis of variance
ANP	Atrial natriuretic peptide
ART	Artery
ATBF	Adipose tissue blood flow
ATGL	Adipose triglyceride lipase
AUC	Area under the curve
AV	Arterio-venous
BMI	Body mass index
bpm	Beats per minute
cAMP	Cyclic adenosine 3', 5'-monophosphate
cDNA	Complementary deoxyribonucleic acid
CS	Cushing's syndrome
CsI	Cesium iodide
DAG	Diacylglycerol
ddct	Delta delta cycle threshold
DNA	Deoxyribonucleic acid
DXA	Dual X-ray absorptiometry
ECG	Electrocardiogram
FAME	Methyl esters of fatty acids
FFA	Free fatty acids
FFM	Fat-free mass
FoxO1	Forkhead box „Other" 1 transcription factor
GC	Gas chromatography
HC	Hip circumference
HDL	High density lipoprotein
HR	Heart rate
HSL	Hormone-sensitive lipase
Hz	Hertz
IL-6	Interleukin 6
IP_3	Inositol triphosphate
IRMS	Isotope-ratio mass spectrometry
ISO	Isoprenaline

LDF	Laser Doppler flowmetry
LDL	Low density lipoprotein
LPL	Lipoprotein lipase
M	Molar
MBq	Mega-Becquerel
MS	Mass spectrometry
mW	Milli-Watt
NaCl	Sodium chloride
NEFA	Non-esterified fatty acid(s)
NO	Nitric oxide
OBB	Oxford BioBank
PCR	Polymerase chain reaction
PET	Positron emission tomography
PKA	Protein kinase A
R_a	Rate of appearance
RNA	Ribonucleic acid
SAL	Saline
SEM	Standard error of the mean
SERCA	Smooth endoplasmic reticulum Ca^{2+}-ATPase
SNPs	Single nucleotide polymorphisms
SR	Sarcoplasmic reticulum
TG	Triglyceride(s)
TNF-α	Tumour necrosis factor α
TTR	Tracer/tracee ratio
V	Venous
VLDL	Very low density lipoprotein
WC	Waist circumference
WHR	Waist to hip ratio
Xe	Xenon

1 Introduction

1.1 Introduction

Lipids, and the fatty acids they contain, are one of the macronutrient components of food. Fatty acids are also an important metabolic fuel for many tissues. Fatty acid trafficking is a complex metabolic process under hormonal regulation that involves the gut, where dietary lipids are first taken up, the skeletal muscles and the liver, where fatty acids are metabolised further, and adipose tissue. Adipose tissue is the dedicated organ for storing fatty acids in the form of triglycerides (TG) in the human body. It plays a pivotal role in daily metabolism, by taking up dietary fatty acids in the postprandial period and by releasing them as non-esterified fatty acids (NEFA) during the postabsorptive period or exercise. Adipose tissue mass and distribution is closely related to cardiovascular risk and insulin resistance. In this Chapter, the physiology of adipose tissue fatty acid trafficking, the health implications of regional differences in adipose tissue distribution and function, and how they relate to the aims of this thesis, are discussed.

1.2 Adipose tissue fatty acid trafficking

1.2.1 Fatty acid uptake and release

The rate of fatty acid uptake, primarily taking place after meals, the rate of release (lipolysis) during fasting/exercise, and the blood flow in the tissue beds are important determinants of local adipose tissue fatty acid trafficking (1, 2).

Within an hour after a meal, dietary lipids enter the circulation via the lymphatic system in the form of chylomicrons – a process that peaks 3-4 hours postprandially. Chylomicrons are large lipoprotein particles with a diameter of up to 1 µm containing dietary fat, of which TG is the main component. After entering the adipose tissue beds, chylomicrons come into contact with lipoprotein lipase (LPL). LPL is the enzyme responsible for the hydrolysis of TG into fatty acids for entry into the adipocytes. Its location on the luminal side of the capillary endothelial cells facilitates this process. LPL is produced by the adipocytes and transported to the endothelial cells; a process that is induced by insulin, which is abundant at high concentrations postprandially (3). The fatty acids that have been hydrolysed by LPL enter the adipocyte by diffusion or helped by a specialized transporter protein, the so-called fatty acid translocase (also known as CD36) (4). At the same time, insulin

suppresses fat mobilization by several different mechanisms. Firstly, it inhibits the activity of hormone-sensitive lipase (HSL), the major acutely-regulated enzyme of adipocyte lipolysis (discussed in more detail below). The activation of the insulin-receptor pathway leads to the phosphorylation and activation of a phosphodiesterase, which in turn breaks down cyclic adenosine 3',5'-monophosphate (cAMP) (5). The consequent decrease in cellular cAMP concentrations results in reduced activity of protein kinase A and thus dephosphorylation and inactivation of HSL. In the longer term, insulin also inhibits the activity of adipose triglyceride lipase (ATGL), a further lipase of the lipolytic pathway of adipocytes, in a mechanism involving the transcription factor FoxO1 (6). Finally, insulin promotes the re-esterification of fatty acids into TG within the adipocyte (2, 7).

In the postabsorptive period, e.g. during an overnight fast, net adipose tissue fatty acid trafficking switches from fatty acid uptake to lipolysis. This switch is driven by the low plasma insulin concentration during the postabsorptive period and the consecutive predominance of catecholamine-dependent effects. Fatty acids are released as NEFA, after the TG stored in the adipocyte lipid droplet has been hydrolysed by intracellular lipases. The process involves ATGL and HSL, as well as a monoacylglycerol lipase (7, 8). ATGL hydrolyses TG into diacylglycerol (DAG), HSL hydrolyses TG into DAG and DAG into monoacylglycerol, while the latter is hydrolysed into a (non-esterified) fatty acid and a glycerol molecule by the monoacylglycerol lipase. Activation of HSL is the result of β-adrenergic stimulation (see Section 1.2.3) and leads to the translocation of HSL to the surface of the lipid droplet (9). However, in order for ATGL and HSL to access the TG stored in the droplet, perilipin, a so-called lipid-droplet protein, has to change its conformation (10, 11). This is because perilipin, in its dephosphorylated state, coats the lipid droplet, thus preventing the lipases from coming into contact with the stored TG (9). Phosphorylation of perilipin is again dependent on β-adrenergic stimulation, which results in a conformational change – perilipin moves away from the droplet allowing the lipases to access its content (11). Overall, the hydrolysis of TG results in three NEFA molecules (and a glycerol molecule) which diffuse into the capillaries. Once there, they are transported in the circulation bound to albumin (12). A small portion of NEFA might not leave the adipocyte and is re-esterified into TG, although this pathway is mostly induced by insulin (13).

Other, non-adrenergic stimulators of lipolysis are known (14). Amongst them, atrial natriuretic peptide (ANP) has been described more recently (15). ANP increases

adipocyte lipolysis via a cyclic guanosine monophosphate (cGMP)-dependent pathway that is not antagonised by insulin. However, since ANP appears to play mostly a role in exercise-related lipolysis, this will not be discussed further here.

1.2.2 Adipose tissue blood flow

Adipocytes depend on the capillary bed for delivery of substrate after a meal (chylomicrons), but also for distribution of lipolysis-derived NEFA during the postabsorptive period and exercise. Thus, adipose tissue blood flow (ATBF) is an important determinant of adipose tissue physiology (16).

Fasting ATBF is around 3 $ml.min^{-1}.100\ g\ tissue^{-1}$ and may increase markedly (up to 4-fold from baseline) shortly after a meal (10, 17). Fasting ATBF is determined on the one hand by nitric oxide (NO), a potent vasodilator synthesized in the endothelium by endothelial nitric oxide synthase (18). At the same time, the effect of NO is counterbalanced by angiotensin II, which has vasoconstrictor properties (19). Thus, fasting ATBF is mainly determined by the balance between the local NO and angiotensin II signal. In contrast, the postprandial ATBF rise is the result of catecholamine-mediated vasodilatation (discussed in more detail in Section 1.2.3.) (18). The postprandial ATBF response is blunted in obesity and insulin resistance, which could lead to the assumption that insulin is involved in ATBF regulation (20, 21). However, insulin does not appear to have a direct ATBF effect, but to act indirectly via sympathetic activation (22). Finally, there is recent evidence that ATBF might also be under transcriptional control of certain genes involved in vasodilatation (23).

The exact integration of ATBF into daily metabolic physiology remains unclear, because of methodological limitations in the study of ATBF (see Section 2.1). When studied over 24 h with three meals given, ATBF increases after each meal (2). Using the microdialysis technique (see Section 2.1), it was found that ATBF increases steadily during the night (24). During early starvation (i.e. 14-20 h postprandially), ATBF does not change significantly, despite an observed increased efflux of NEFA from adipose tissue (25). However, there is evidence for a moderate ATBF increase during prolonged starvation (10, 26). As one would expect, ATBF increases significantly during exercise, driven by the increase in plasma catecholamines (27).

1.2.3 Adrenergic regulation of adipose tissue function

Adrenaline and noradrenaline are the two endogenous catecholamines exerting peripheral effects in various organs of the human body. Both are synthesized from the common precursor dopamine. In noradrenergic neurons, noradrenaline is derived from dopamine, catalysed by dopamine-β-hydroxylase. In the adrenal medulla, adrenaline is the product of methylation of noradrenaline by phenylethanolamine-N-methyl transferase. The two catecholamines reach the peripheral tissues by different means: adrenaline in a humoral way as a plasma hormone, noradrenaline via neuronal secretion from sympathetic synapses that are located within the tissue (28, 29).

Catecholamines bind to G-protein-coupled adrenergic receptors which are divided in two groups: the α-adrenoceptor family comprises the subtypes α_1 and α_2, and the β-adrenoceptor family has three members termed β_1, β_2 and β_3. The β_3-adrenoceptor has been implicated in lipolysis in adipocytes derived from rodents; however, its role in human adipose tissue is debated (14, 28). Therefore, β_3-adrenoceptors will not be considered further here. Noradrenaline stimulates primarily α-adrenoceptors and in higher concentrations β_1-adrenoceptors (30). In low concentrations, adrenaline primarily stimulates α-adrenoceptors, while there is an affinity-shift towards both β-adrenoceptor subtypes at medium and higher concentrations. Upon stimulation, α- and β-adrenoceptors often exert opposite cellular effects. Since both receptor subtypes are present in most tissues, the final effect depends on the concentration and receptor affinity of the agonist and the distribution pattern of adrenoceptor subtypes (see Table 1.1) (28, 29).

Adrenergic stimulation of adipose tissue exerts effects both on adipocytes and the vascular bed. Adipocytes express both β-adrenoceptor subtypes, α_2-adrenoceptors and, in low quantities, α_1-adrenoceptors (28, 31). Due to their low expression levels in white adipocytes, α_1-adrenoceptors are not regarded as playing a major role in the adrenergic regulation of lipolysis. However, when doxazosin, a selective α_1-adrenoceptor blocker, was given to healthy volunteers, a decrease of adipose tissue vascular resistance and an increase in fasting lipolysis *in vivo*, compared to placebo, was seen (32).

Table 1.1: Adrenergic receptors and tissue-specific effects

Receptor	*General effects*	*Adipose tissue effects*
α_1	Inhibition of gut motility Vasoconstriction Bronchoconstriction Contraction of uterus	Decreases ATBF *(low expression in adipocytes)*
α_2	Inhibition of sympathetic activity (e.g. lowers blood pressure) Inhibition of salivation Inhibition of insulin secretion	Decreases ATBF Inhibition of lipolysis
β_1	Increases heart rate Increases cardiac ejection fraction Increases renal renin secretion	Increases lipolysis
β_2	Vasodilatation Bronchodilatation Dilatation of uterus Increases insulin and glucagon secretion	Increases ATBF Increases lipolysis
β_3	Unclear in humans	Unclear in humans Increases brown fat thermogenesis and white adipose tissue lipolysis in rodents

In lipolysis, β-adrenergic stimulation leads to the activation of adenylyl cyclase by a stimulatory G-protein. The generation of cAMP results in the activation of protein kinase A (PKA) that in turn phosphorylates HSL (28, 33). The increased intracellular cAMP concentrations lead also to the phosphorylation of perilipin. The catecholamine-dependent lipolytic pathway is described further in Section 1.2.1.

Activation of α_2-adrenoceptors inhibits adenylyl cyclase activity via an inhibitory G-protein. The consequent decrease in intracellular cAMP concentrations results in the inhibition of HSL activity and the dephosphorylation of perilipin (34). This process is mediated on the one hand by constitutively active phosphatases, which dephosphorylate HSL directly (35). However, it is important to note that the major antagonist of lipolysis is insulin. As described in Section 1.2.1, insulin promotes the degradation of intracellular cAMP by phosphorylating phosphodiesterase-3B in a phosphatidylinositol-3-kinase/protein kinase B-dependent mechanism (36). Thus, the overall decrease in cAMP concentrations results in a net dephosphorylation, and inactivation, of HSL with consecutive inhibition of lipolysis.

As noted above, noradrenaline is secreted via sympathetic nerve terminals into adipose tissue. Although little work has been carried out in human adipose tissue, it is clear that these nerve terminals come into contact with the vascular bed and, to

some extent, with adipocytes (37, 38). Animal work showed that the density of sympathetic innervation varies between fat depots (39) and that nerves in different fat depots derive from different areas of the sympathetic chain (40). Sympathetic denervation led to an increase in fat mass due to a change in adrenoceptor density and an increase in adipocyte precursor cells (41). Together with the presence of parasympathetic (cholinergic) nerve terminals, adipose tissue sympathetic innervation is an important determinant of adrenergic regulation of adipose tissue function (10, 42).

The lipolytic effect of β-adrenergic stimulation and the anti-lipolytic effect of α-adrenergic stimulation in adipocytes are accompanied by a concomitant effect on blood flow. ATBF increases due to vasodilatation during β-adrenergic stimulation (18). In pre-capillary sphincters, activation of vascular β-adrenoceptors increases intracellular cAMP concentrations via adenylyl cyclase activation as discussed above. cAMP activates PKA which in turn stimulates a Ca^{2+}-pump located on the sarcoplasmic reticulum (SR). This smooth endoplasmic reticulum Ca^{2+}-ATPase (known as SERCA) reduces the intracellular Ca^{2+}-concentration by sequestrating Ca^{2+} into the SR. In addition, PKA hyperpolarises the cell membrane resulting in the closing of voltage-gated Ca^{2+} channels. Thus, intracellular Ca^{2+} concentrations are further decreased and the pre-capillary sphincters relax (29).

In contrast, stimulation of α-adrenoceptors has the effect of phospholipase C activation and the generation of inositol trisphosphate (IP_3) and DAG. IP_3 leads to the release of Ca^{2+} stored in the SR and DAG opens so-called receptor-operated channels that allow entry of Ca^{2+} ions from the extracellular space. Eventually, the intracellular increase in Ca^{2+} concentration results in vasoconstriction (29).

As discussed in Section 1.2.2, ATBF is only partly under adrenergic control and other potent vasoactive agents are present *in vivo*.

1.2.4 *ADRB2* haplotypes

The β_2-adrenoceptor is encoded on chromosome 5q31-32 in the *ADRB2* gene. Several single-nucleotide polymorphisms (SNPs) have been identified in humans, some of them with implications for asthma and cardiovascular disease (43). Of specific relevance to the adrenergic regulation of fatty acid trafficking are *ADRB2* SNPs that are organised in three haplotypes. These haplotypes of interest are termed *2*, *4* and *6* and are part of a group of twelve *ADRB2* haplotypes identified (see

Table 1.2). Haplotypes *2*, *4* and *6* are the most common in Caucasians, with a reported allele frequency of 48.3%, 33.0% and 13.2% respectively. Moreover, they show functional effects in terms of receptor expression and response to β_2-agonist treatment in humans (44). Asthma patients homozygous for haplotype *2* showed a better improvement of their forced expiratory volume (FEV_{1s}) after β_2-agonist treatment than patients carrying haplotype *4_4*. This was linked to a lower β_2-adrenoceptor expression in HEK293 cells transfected with a haplotype *4* β_2-adrenoceptor transcript (44).

More importantly, haplotype-specific effects have been observed in isolated human adipocytes (45). Eriksson *et al*. showed that β_2-adrenoceptor selective stimulation of adipocytes with terbutaline resulted in significant differences in lipolysis between haplotypes: *4_4* showed lower and *6_6* higher lipolysis rates compared to *2_2* (45). Given the impact on lipolysis *in vitro* and the described role of β_2-adrenoceptors in ATBF-regulation, one of the aims of my thesis is to investigate the effect of these specific haplotypes on fatty acid trafficking *in vivo* to seek for possible explanations of interindividual differences in lipolysis and systemic NEFA concentrations (see Section 1.5).

Table 1.2: Overview of ADRB2 haplotypes of interest (adapted from (44))

Nucleotide	-1023	-709	-654	-468	-406	-367	-47	-20	46	79	252	491	523	
Alleles	G/A	C/A	G/A	C/G	C/T	T/C	T/C	T/C	G/A	C/G	G/A	C/T	C/A	
Haplotype														Freq. Cau.
2	A	C	G	G	C	C	C	C	G	G	G	C	C	48.3
4	G	C	A	C	C	T	T	T	A	C	G	C	C	33.0
6	G	C	G	C	C	T	T	T	G	C	A	C	A	13.2

Nucleotide no. based on first nucleotide of start codon being +1; *Freq*, Frequency in %, *Cau*, Caucasians

1.3 Regional fat distribution and health

Adipose tissue, as discussed above, plays an integral part in normal human metabolic physiology. However, adipose tissue mass is also associated with disease – especially when it is increased in obesity (46). Traditionally, the body mass index (BMI) is used to define obesity (BMI>30 $kg.m^{-2}$) and an increased BMI is strongly correlated with a high risk of cardiovascular disease and diabetes (47). The BMI is not necessarily determined by adipose tissue mass only, since it is calculated using the body weight (and height), which includes other tissues as well (e.g. muscle). Furthermore, when obesity-related health risks are expressed based on BMI, it is not clear *where* the additional fat mass has been accumulated in the body. This is not as a trivial piece of information as it appears for two reasons.

Firstly, in the 1950s, Vague noticed the importance of fat distribution in relation to health and disease risk (48). His observations led to the development of the "apples and pears" terminology, describing abdominal and gluteofemoral adipose tissue accumulation respectively. Following Vague's initial report of abdominal obesity predisposing to cardiovascular risk, there is now a large body of evidence showing that regional fat distribution is an important determinant of health. This is discussed further in Section 1.3.1.

Secondly, it is now widely accepted that there are different adipose tissue depots in the human body that display distinct differences in their function, regulation and – most importantly – association to cardiovascular and metabolic risk (49-51). A large number of studies have focussed on the properties of visceral adipose tissue and its association to cardiovascular and metabolic risk (52). Visceral fat accumulation correlates strongly with abdominal subcutaneous fat mass and becomes apparent when abdominally obese individuals are studied with imaging techniques (53-55). Visceral adipocytes display a much higher lipolytic activity when compared to subcutaneous adipocytes *in vitro* (56). The anatomical proximity of visceral adipose tissue to the liver, by means of venous drainage into the portal vein, has led to the hypothesis that NEFA released from visceral adipose tissue are particularly involved in the development of hepatic insulin resistance (57). However, when different adipose tissue depots (including the visceral) were studied *in vivo*, visceral adipose tissue contributed least to the systemic or the portal NEFA pool (58, 59). In fact, the depot with the largest contribution to both systemic and portal NEFA concentrations

was that of abdominal subcutaneous adipose tissue. Hence, the importance of visceral adipose tissue *in vivo* has been challenged (60-62). In Section 1.4 the differential properties of abdominal and gluteofemoral adipose tissue are discussed further, while visceral adipose tissue will not be considered further in this thesis.

1.3.1 Fat distribution and health - epidemiological evidence

Body fat distribution can be expressed by the waist-to-hip-ratio (WHR) which is also widely used to assess cardiovascular and metabolic risk. An increased WHR correlates with obesity-associated diseases and mortality and, interestingly, proves to be a stronger cardiovascular risk marker than BMI (63-65).

This is supported by several population studies showing that obesity-associated health risks depend on the accumulation of abdominal fat. Abdominal obesity is associated with increases in blood pressure and plasma TG concentrations (63, 64). A large abdominal fat mass predicts also the development of type 2 diabetes independently of BMI (66).

In contrast to abdominal fat, it is the *protective* role of gluteofemoral fat that is striking. The protective properties of gluteofemoral adipose tissue have been confirmed in many studies conducted in subjects with a wide range of age, BMI and co-morbidities (for a summary of studies see Table 1 in Appendix). Gluteofemoral fat mass, expressed as thigh circumference, hip circumference or leg adipose tissue mass, is independently associated with a healthy blood lipid profile: lower total- and LDL-cholesterol, and total- and VLDL-TG concentrations, and higher HDL-cholesterol concentrations (67-72). Direct effects on vascular health that might convey atherosclerotic protection have also been reported. An increased gluteofemoral fat mass is associated with lower aortic calcification and arterial stiffness (73-75), as well as with a decreased progression of aortic calcification (76). Leg adipose tissue mass change, as a result of a 14-week intervention study with diet and exercise, is inversely associated with diastolic blood pressure and LDL-cholesterol concentrations (77). In terms of metabolic health, gluteofemoral fat is inversely associated with fasting insulin concentrations and insulin concentrations after an oral glucose load, and positively associated with insulin sensitivity (67, 72, 78-80). Finally, in healthy overweight and obese women, hip circumference and thigh adipose tissue mass are associated with a lower HbA1c and higher leptin concentrations (81).

Large population studies also confirm the protective effect of gluteofemoral adipose tissue. In the AusDiab study, a larger hip circumference was associated with a lower prevalence of undiagnosed diabetes mellitus and dyslipidaemia (82). In the INTERHEART study, a large epidemiological study with 27,000 participants, an independent association between larger hip circumference and lower risk for myocardial infarction was established (65). In the prospective EPIC-Norfolk study, larger hip circumference was associated with a lower hazard ratio for coronary heart disease (83). In the same study, hip circumference was positively associated with plasma concentrations of ascorbic acid, an anti-oxidative factor thought to contribute to endothelial protection (84).

1.3.2 Gluteofemoral fat loss and disease

A further perspective underlining the protective features of gluteofemoral adipose tissue is to elucidate what happens when substantial amounts of gluteofemoral fat mass are *lost*. Indeed, gluteofemoral adipose tissue loss is associated with metabolic abnormalities, as explained below in the cases of glucocorticoid excess and partial lipodystrophy.

Cortisol is the main glucocorticoid in humans and is secreted by the cortex of the adrenal glands. Cortisol has important catabolic functions in fuel metabolism and as such impacts on adipose tissue mass. In the state of glucocorticoid excess, as seen in Cushing's syndrome (CS), a marked fat re-distribution of adipose tissue is pathognomonic. Typically, the body fat distribution phenotype in CS is that of abdominal obesity with peripheral fat mass loss (85). Glucocorticoid excess reduces the mass of the gluteofemoral adipose tissue depot, but also changes adipocyte function in the abdominal depot (86). Mechanistically, an increase in abdominal LPL-activity and a decreased lipolytic capacity of the enlarged abdominal adipocytes has been described (87). Furthermore, cortisol decreases abdominal adipose tissue lipolysis *in vivo* (88). Abdominal fat accumulation in CS has been attributed to a redistribution of peripheral fat to the visceral fat depot (89, 90). Although the increase of visceral adipose tissue mass might provide a mechanism for the increased metabolic and cardiovascular risk associated with CS (91, 92), it is interesting to note that visceral fat accumulation in CS does not correlate with lipid and glucose profiles (93). The direct association of gluteofemoral adipose tissue loss and metabolic health in CS has not been studied yet. However, the *relative* mass loss due to fat

redistribution might provide a plausible mechanism for the adverse effect of glucocorticoid excess on metabolic and cardiovascular risk.

Another example of the impact of gluteofemoral fat loss on health is that of partial lipodystrophy. Lipodystrophy is a disease characterised by the partial or total absence of adipose tissue and can be either inherited or acquired (94). The loss of adipose tissue, the dedicated storage organ, leads to the body using alternative areas of storing TG in a process called ectopic fat deposition (95). Ectopic fat deposition occurs in the liver, pancreas and muscle – organs that are not dedicated to store large amounts of TG – and this is thought to cause insulin resistance and increase cardiovascular risk (96, 97). Depending on the type of lipodystrophy and whether there is any adipose tissue present at all, there may be fat accumulation in specific non-atrophic fat depots, for instance the neck (94, 95).

One such example of partial adipose tissue loss is the autosomal dominant familial partial lipodystrophy Dunnigan-type. These patients primarily lose the subcutaneous adipose tissue of their arms and legs (95) and suffer from severe insulin resistance, hyperlipidaemia, hypertension and, often, diabetes (98-100). Several gene mutations of the *LMNA* and *PPARG* genes were identified as the molecular mechanism responsible for the development of familial partial lipodystrophy (94). The *PPARG* mutations provide a possible link between adipose tissue dysfunction and the metabolic profile associated with this type of lipodystrophy, given that in these patients adipose tissue appears to be unresponsive to physiological regulatory mechanisms (100).

In contrast, patients with the acquired partial lipodystrophy form (Barraquer-Simons' syndrome), in which there is a progressive loss of adipose tissue from the face and upper-body but retained fat in the gluteofemoral region, only display mild insulin resistance and have a lower prevalence of diabetes compared to other lipodystrophic syndromes (94, 101).

In summary, body fat distribution is a major determinant of metabolic health and gluteofemoral adipose tissue accumulation is associated with an improved metabolic and cardiovascular risk profile. One key question is therefore, whether functional differences in the regulation of fatty acid trafficking are the basis for the differential association of abdominal and gluteofemoral adipose tissue with health and disease.

1.4 Regional adipose tissue physiology

Supporting the hypothesis of distinct adipose tissue depots with specific differential regulation patterns, there are marked differences between abdominal and gluteofemoral adipose tissue in terms of fatty acid trafficking, ATBF and adrenergic regulation.

Subcutaneous abdominal adipose tissue was the major contributor of systemic NEFA and displayed a higher lipolysis rate when compared to the gluteofemoral fat depot (58, 59). Lipolysis was lower in the gluteal than the abdominal depot (102). Starvation for 72 h resulted in increased lipolysis in abdominal but not gluteofemoral adipose tissue (103). When studied with radioactive tracers and timed biopsies, abdominal adipose tissue appeared to take up fatty acids more avidly than gluteofemoral adipose tissue in the postprandial period (104, 105).

Recent *in vivo* studies suggest that regional fatty acid trafficking is complex and that there might be distinct VLDL- and NEFA-turnover pathways. Using stable isotope tracers, it was found that femoral adipose tissue preferentially sequesters VLDL-derived TG, while abdominal adipose tissue takes up chylomicron-derived TG more avidly after a meal (106). A recent study investigating fatty-acid uptake in abdominal adipose tissue over a 24 h period and comparing lean and abdominally obese men found that chylomicron-derived fatty acid uptake was blunted in obesity (107). The regulation of long-term (e.g. in 24 h) fatty acid deposition in the gluteofemoral adipose tissue depot is little understood and is studied as part of this thesis.

ATBF changes in abdominal adipose tissue have been well-studied in different settings (see Section 1.2.2). In contrast, little is known about ATBF regulation in gluteofemoral fat and findings are conflicting. Gluteal fat was shown to have a lower basal (postabsorptive) ATBF rate (102). In one study, following a meal, ATBF increased in both the abdominal and femoral depots in women, but only in the abdominal depot in men (105). However, this study had limited time resolution. More recently, similar increases in femoral and abdominal ATBF after a meal have been shown in men and women (106).

Consistent with this, regional differences between abdominal and gluteofemoral adipose tissue depots have been observed with regards to adrenergic regulation. *In vitro* studies showed that the lipolytic effect of noradrenaline was greater in abdominal than gluteal adipocytes (108). This was due to an increased lipolytic

sensitivity of β-adrenoceptors in abdominal adipocytes compared to gluteal. Further, both β-adrenoceptor subtypes were more highly expressed in abdominal adipocytes, with no difference between β_1- and β_2-expression or density (108, 109). The α_2-adrenoceptor was expressed at similar levels in abdominal and gluteal adipocytes, in men and women. However, gluteal adipocytes were more sensitive to the anti-lipolytic effects of clonidine (an α_2-adrenoceptor agonist) than abdominal adipocytes in women (108). The presence of a strong α-adrenoceptor effect in gluteofemoral fat was further shown in a study of adipocytes derived from the thigh where selective β-stimulation with isoprenaline resulted in increased lipolysis *in vitro* (110). In contrast, adrenaline did not elicit any lipolytic response in these cells, unless the α-adrenoceptor blocker phentolamine was added.

There are few *in vivo* studies comparing differences in the regional adipose tissue response to adrenergic stimulation. During adrenaline stimulation, abdominal lipolysis appeared to be higher than femoral lipolysis, when measured as glycerol release by microdialysis in women (111). Palmitate release, a direct marker of lipolysis, was lower in leg fat compared to the abdominal depot during systemic β-adrenoceptor stimulation in women (112). In lean women, femoral ATBF showed an attenuated increase during systemic adrenaline stimulation compared to abdominal fat (111). With respect to sex-specific differences, one study showed a blunted lipolytic response of leg palmitate release in response to adrenaline in women compared to men (113).

1.5 Aims of thesis

It is clear that adipose tissue is the dedicated organ for fatty acid storage and *in vivo* studies have shown a remarkable adaptation of postprandial fatty acid uptake to ensure “safe” deposition of dietary fatty acids during the day (2). The importance of this becomes evident in obesity, where the observed impairment of postprandial fatty acid uptake provides a possible mechanism for ectopic fat deposition (114). In view of the differential association between abdominal and gluteofemoral adipose tissue depots and cardiovascular and metabolic risk, it seems plausible that gluteofemoral adipose tissue conveys some protective properties that go beyond (or perhaps are an expansion of) “healthy” adipose tissue function (51). Overall, it has been suggested that gluteofemoral adipose tissue acts as a “metabolic sink” that traps fatty acids and prevents ectopic fatty acid deposition (115). This hypothesis is supported by the recent finding of preferential uptake of VLDL-derived TG in femoral adipose tissue, as opposed to the preferential uptake of chylomicron-derived TG in abdominal

adipose tissue (106). Abdominal adipose tissue buffers the daily influx of dietary-derived fatty acids, while gluteofemoral adipose tissue traps “un-buffered” fatty acids that have been re-circulated by the liver. Lower lipolysis rates under many conditions would also support this role of gluteofemoral fat as a long-term “metabolic sink”.

The exact *in vivo* mechanisms that render gluteofemoral adipose tissue protective are not clear yet. Catecholamines are important regulators of fatty acid trafficking as they influence lipolysis and ATBF. The regional differences in adrenergic regulation discussed above warrant further investigation *in vivo*, as they might provide a possible mechanism for the protective properties of gluteofemoral adipose tissue.

Therefore, the specific aims of this thesis are the following:

1. To study α- and β-adrenoceptor-dependent regulation of lipolysis and ATBF in abdominal and femoral adipose tissue *in vivo*.

2. To study the molecular mechanisms and the impact of genetic adrenoceptor-variation on β-adrenoceptor-regulated lipolysis.

3. To study fatty acid trafficking in abdominal and femoral adipose tissue over a 24 h period.

2 Methods and method development

Fatty acid trafficking comprises the processes of fatty acid uptake, lipolysis and ATBF (see Section 1.2). The measurement of all three dimensions *in vivo* is possible by applying integrative physiology techniques. These techniques are described in the following.

2.1 ATBF measurement

ATBF measurements are important indicators of adipose tissue activity and used for the calculation of substrate fluxes (see Section 2.6). Several methods for the measurement of ATBF have been described in the literature. The ^{133}xenon (^{133}Xe) washout technique, the measurement of ethanol escape by microdialysis, Laser Doppler Flowmetry (LDF), positron emission tomography (PET) and contrast-enhanced ultrasound have been used in humans. While microdialysis, LDF and contrast-enhanced ultrasound measure relative ATBF changes, ^{133}Xe washout and PET are useful for an absolute measurement of ATBF.

The measurement of ethanol escape by microdialysis involves the insertion of a microdialysis probe into adipose tissue with ethanol included in the perfusion solution (116). As ethanol itself has no effect on ATBF, its removal rate from the dialysate is proportional to the tissue blood flow. By measuring the ethanol concentration in the perfusate, it is possible to monitor ATBF changes. Microdialysis has been and is used extensively for the study of ATBF in different settings (117, 118). However, this method is less responsive and sensitive to physiological ATBF changes than the ^{133}Xe washout method (119). Furthermore, although microdialysis has been used for the calculation of some metabolite fluxes such as glycerol and lactate (120, 121) it cannot be used for fatty acid fluxes, because only water-soluble small molecules can be recovered by dialysis.

LDF utilises the change in wavelength when a laser light hits moving erythrocytes (122). This method is discussed in more detail in Section 2.1.3, since the comparison to the ^{133}Xe washout technique was part of the method development in my research work.

PET has the advantage that in addition to subcutaneous ATBF, visceral ATBF can be measured (123). However, simultaneous physiological observations require that

studies are performed within the PET scanner. This may pose restrictions on what physiological situations can be studied. Furthermore, PET equipment is not widely available, the technique involves a high radiation burden for researchers and participants, and it is expensive.

The use of contrast-enhanced ultrasound has been described in the measurement of ATBF recently (124). The technique involves the intravenous injection of ultrasound contrast agent and the measurement of changes in the signal intensity captured by the ultrasound probe. As with all ultrasound based techniques, the quality of the data is operator-dependent and very prone to movement artefacts. Furthermore, ATBF cannot be monitored easily over prolonged time periods as ultrasound contrast agent needs to be injected repeatedly (or constantly) (125). Currently, contrast-enhanced ultrasound is not used as a standard technique for the measurement of ATBF.

In my studies, I used the ^{133}Xe washout technique for the measurement of abdominal and femoral ATBF. The technique is reproducible (21), allows for the continuous monitoring of ATBF over long periods of time and provides quantitative measurements. The disadvantages are mainly the use of a radioactive gas and its regulatory and health implications for researchers and volunteers. However, given that only small doses of ^{133}Xe are used in each experiment, the personal burden is negligible.

2.1.1 Measurement of ATBF with the ^{133}Xe washout technique

Inert gases diffuse freely across cell membranes and can therefore be used for assessing local tissue blood flow. Their clearance from the tissue is directly proportional to tissue blood flow (126). ^{133}Xe is an inert gas and its use in the measurement of ATBF has been first described by Larsen *et al*. (127). It is an ideal substance for the measurement of ATBF, as it is lipid-soluble (128).

Absolute ATBF is the product of the partition coefficient (λ) and the fractional rate of loss of radioactivity (127):

$$ATBF_{(ml \cdot 100g^{-1} \cdot min^{-1})} = \text{slope of semilog plot}_{(\log \text{counts/second})} \times \lambda_{(ml/g)} \times 100_{(g)} \times 60_{(sec)}$$

The partition coefficient (λ) is a measure of the relative solubility of ^{133}Xe between adipose tissue and blood. Bülow *et al.* showed that the partition coefficient depends on the lipid content of the adipose tissue depot under investigation (129). For

subcutaneous adipose tissue, the measured partition coefficient was 8.2±1.2 $ml.g^{-1}$ and there were no significant differences between abdominal and femoral adipose tissue. Others have estimated the partition coefficient of ^{133}Xe between blood and adipose tissue using the haematocrit and the calculated lipid fraction (130). Using such algorithms, the partition coefficient was 5.3±0.2 $ml.g^{-1}$ for lean and 7.4±0.2 $ml.g^{-1}$ for obese subjects. I used a theoretical partition coefficient of 10 $ml.g^{-1}$ derived from oil/water interphase studies (128). This value was initially described (131, 132) and has been widely used in physiological studies (18, 19, 133, 134). Assuming that there is little variation in the partition coefficient within an adipose tissue depot and that there are no differences between abdominal and femoral fat, the value of 10 $ml.g^{-1}$ seems appropriate, even if it may be too high for certain adipose tissue depots (129).

The partition coefficient of ^{133}Xe is dependent on temperature and haematocrit (135). In order to minimise fluctuations, all studies were performed in a temperature-stable room and haematocrit and skin temperature were measured regularly.

2.1.2 Injection of ^{133}Xe

Gaseous ^{133}Xe (IDB Holland, Naarle-Nassau, Netherlands) was injected into subcutaneous abdominal and femoral adipose tissue at the site of the most abundant subcutaneous fat. In abdominal adipose tissue, it was injected 5 cm lateral to the umbilicus, and in femoral adipose tissue it was injected into the upper part of the middle third of the anterior aspect of the thigh. Both injections were given within the drainage area of the cannulated veins (see Section 2.2). In lean participants, where there is the possibility of injecting ^{133}Xe into tissue layers below the subcutaneous adipose tissue, injection was performed under ultrasound guidance to ensure that the gas was always injected into proper adipose tissue. The injection was performed slowly over 1 min, taking care to withdraw the needle slowly enough, in order to prevent any ^{133}Xe reflux along the needle track. After injection, an equilibrium period of at least 45 min followed before the start of the study, to allow for tissue equilibration of ^{133}Xe. The dose of ^{133}Xe was 1-2 MBq for each injection site and the total dose injected into each participant never exceeded 4 MBq. An independent medical physics risk assessment, carried out as part of the ethics application for my studies, showed that the maximum dose for participants, depending on the number of ^{133}Xe injections, is 0.004 mSv, which is regarded as tolerable with negligible health risks (see Table 2 in Appendix).

^{133}Xe washout and the concomitant decrease in radioactivity were measured with caesium iodide detectors (John Caunt Scientific, Oxford) that were taped over the injection sites (136). Caesium iodide (CsI) acts as the scintillator, emitting fluorescence when hit by the ionising radiation from ^{133}Xe. The fluorescence is amplified and converted into an electrical signal which eventually is processed by a computer. The registered scintillation counts are used for the calculation of ATBF (see Section 2.1.1).

2.1.3 Laser Doppler Flow - an alternative to ^{133}Xe?

The ^{133}Xe washout is an established method for the measurement of ATBF. However, the need for an alternative is required for several reasons. Firstly, to remove the radiation burden on participants and researchers, together with the need of maintaining dedicated radiation control areas for the use and storage of ^{133}Xe. Furthermore, the clinical use of ^{133}Xe declines constantly as its main application in diagnostics is replaced by other more sensitive methods, e.g. spiral computed tomography. This likely threatens the future availability of ^{133}Xe for clinical, and thus research, usage. Finally, the subcutaneous injection of ^{133}Xe is an invasive procedure and, despite its low risk, can be a stress factor for participants.

Any alternative method for measuring ATBF should fulfil the same criteria as the ^{133}Xe washout method currently does. It should be reproducible, of low risk, easily applicable, quantitative and allow for monitoring over long periods of time. Of the alternative methods described above (see 2.1), LDF is the one that might fulfil some of these requirements.

LDF is based on the Doppler shift principle, where a laser light beam is directed to the tissue of interest and changes its wavelength after hitting the moving erythrocytes. The change of wavelength is registered and the magnitude and frequency of the Doppler shift is directly proportional to the number and velocity of the erythrocytes. LDF is frequently used for the analysis of skin blood flow in the area of plastic surgery, but its use in the measurement of ATBF has been limited. This is mostly due to the low penetration of the laser light used, making the use of LDF probes that are taped on the skin inappropriate. Alternative probes that can be introduced percutaneously were developed and were used in ATBF measurements (137). Despite a reasonable correlation between LDF and ^{133}Xe washout, this invasive method did not prove to be a good alternative. The LDF probe is very prone to movement which introduces artefacts in the analysis and there is an issue with

sterility and health safety in terms of using the same percutaneous probe in different participants (F. Karpe, personal communication).

Recently, the company Moor (Moor Instruments, Axminster) developed a LDF meter that produces a high energy laser light (20 mW, wavelength 785 nm). The laser light is emitted through a specially designed probe that is taped on the skin. The higher laser energy means the laser beam is penetrating deeper into tissues than merely reflecting the very superficial skin layers (138). The design of the probe head features a wider-than-usual distance between the transmitting and receiving fibres which, according to the manufacturer, should eliminate skin contribution from the signal. Thus, the manufacturer claimed that this method might be useful in subcutaneous ATBF measurement. I undertook a series of experiments to evaluate the equipment and test its suitability as an alternative to ^{133}Xe washout.

The ATBF response to a glucose stimulus is well-documented and a simple physiological manoeuvre (119). I measured ATBF responses after a 75 g glucose drink in 5 healthy volunteers using ^{133}Xe washout and LDF simultaneously. The ^{133}Xe was injected in abdominal adipose tissue as described before, and the LDF probe was taped to the skin on the contralateral side. Before taping the LDF probe, I took care to avoid superficial subcutaneous veins by checking the area with a light source and ultrasound (see Section 2.2.1). LDF is measured in relative units of flux and can be recorded continuously. However, the recorder's sample rate of 40 Hz generates a vast amount of data that is not necessarily useful. I decided to take recordings of 1 min duration, each 10 min apart. During the LDF recordings, the participants were asked to remain as still as possible and obvious movement artefacts were excluded from the analysis later.

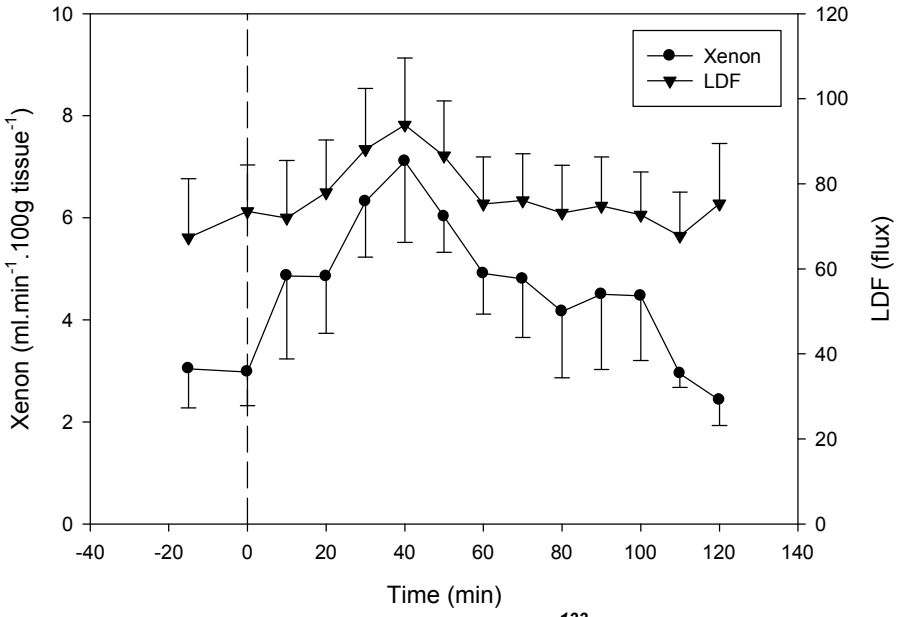

Figure 2.1: Comparison of ATBF measured by ^{133}Xe washout (circles) and LDF (triangles). A 75 g glucose drink was given at 0 min (n=5).

The collated results of this study are shown in Figure 2.1. The oral glucose load resulted in a 3-fold increase of ATBF, as measured with ^{133}Xe. In contrast, according to the LDF data, the increase from baseline was only 1.4-fold. Although it was possible to register the ATBF response using LDF, the magnitude of response seemed underestimated. Interestingly, the initial increase in ATBF in the first 20 min after glucose, as measured by ^{133}Xe, is not registered by LDF at all. This is most probably due to signal interference from skin.

Skin thickness does not affect LDF measurements when used for skin circulation studies (139). However, signal distortion with increasing thickness is to be expected when studying fluxes of deeper tissues, e.g. ATBF. I measured skin thickness with ultrasound and correlated the measurements with basal ATBF as measured by ^{133}Xe and LDF. While ^{133}Xe measurements are independent of skin thickness (Pearson r^2=0.062), LDF-derived flux decreases with increasing skin thickness (Pearson r^2=0.485). The lower signal indicates distortion masking physiological ATBF changes that can be measured by ^{133}Xe as shown above.

A further factor affecting LDF measurements is skin temperature. Small changes in skin temperature have a large effect on skin blood flow (140), but a small effect on ATBF when measured by ^{133}Xe (141). A major concern using the Moor LDF system was that its measurement is influenced by skin blood flow. In a series of studies I

measured skin temperature during a basal LDF reading (data not shown). There was no correlation between skin temperature and flux (r^2=0.015).

In summary, I showed that LDF can be used for measuring ATBF in principle, when a more powerful laser with a modified probe head is used. However, despite the associated increased penetration, there appears to be residual distortion from the skin layers, confounding the measurement ATBF changes. Moreover, subtle physiological ATBF changes remain undetected by LDF. The method still has other major disadvantages compared to ^{133}Xe washout: recordings are very prone to movement artefacts, and it is not a quantitative measure, as only relative ATBF changes can be recorded. Furthermore, it is not sensitive enough and probably the recorded flow is not linear to ATBF. For these reasons, LDF cannot replace the ^{133}Xe washout technique currently, although future technological advances might change this picture.

2.1.4 Manipulation of ATBF with microinfusion

The microinfusion technique was developed by Karpe *et al*. (22) as a means of manipulating ATBF on a local level. It is based on the local delivery of pharmacological agents directly into adipose tissue, and the simultaneous measurement of ATBF using the ^{133}Xe washout technique. This is achieved by the use of subcutaneous infusion catheters (Medtronic Quick-Set, Northridge, CA, USA) originally designed for the continuous delivery of insulin from insulin pumps. These catheters are inserted percutaneously. With the tip reaching a depth of 6 mm, the delivery of vasoactive (or other) agents directly into adipose tissue is achieved by a precision microinfusion pump (CMA-100, CMA Microdialysis, Solna, Sweden). The pump operates at a constant infusion rate of 2 μl.min^{-1}. At the start of each study, ^{133}Xe is first injected slowly through a dedicated injection port located on the top of the catheter. Thus, ^{133}Xe is injected into the exact area where the later infusion of pharmacological agents may take place. The CsI detectors are taped on top of the catheters and after an equilibration period of at least 45 min it is possible to monitor ATBF changes during the microinfusion.

This methodology has been validated and used for studying preprandial and postprandial ATBF regulation previously (18). I used microinfusion to study the direct effect of adrenergic stimuli in ATBF and the exact role of adrenoceptors in ATBF regulation (see Chapters 3 and 5).

2.1.5 Pharmacological agents used for microinfusion

In order to study the effect of different adrenergic agonists on local ATBF, the following pharmacological agents were used for microinfusion (Table 2.1):

Isoprenaline

Isoprenaline (non-proprietary, South Devon Healthcare, UK) is a β-selective adrenoceptor-agonist that binds equally to β_1- and β_2-adrenoceptors. Isoprenaline was sequentially diluted in 0.9% NaCl (Baxter, Deerfield, IL, USA) under sterile conditions to achieve final concentrations of 10^{-8} M, 10^{-6} M and 10^{-4} M.

Table 2.1: Pharmacologic agents used and their properties

Agent	Properties	Adrenoceptor affinity
Isoprenaline	Agonist	$\beta_1=\beta_2$
Adrenaline	Agonist	α, β_1, β_2 (dose-dependent)
Phentolamine	Antagonist	α
Propranolol	Antagonist	β

Phentolamine

Phentolamine is an α-selective adrenoceptor blocker commonly used in the treatment of phaeochromocytoma (a catecholamine-producing tumour). Phentolamine (Alliance Pharmaceuticals, Chippenham) was diluted under sterile conditions in 0.9% NaCl to a final concentration of 10^{-5} M.

Propranolol

Propranolol is a β-selective adrenoceptor blocker used in the treatment of hypertension. For the purposes of microinfusion, propranolol (AstraZeneca, Luton) was diluted under sterile conditions in 0.9% NaCl to achieve a final concentration of 10^{-5} M.

The microinfusion technique and the small doses chosen, result in effective local concentrations without any systemic pharmacological effects (18). As shown in Chapter 3, local ATBF effects are observed during microinfusion without changes in systemic haemodynamic parameters, e.g. heart rate and blood pressure. In a series of experiments, both propranolol and phentolamine were infused into the abdominal

adipose tissue depot of the same participant (see Section 5.2). In order to avoid cross-talk effects, the agents were infused into contralateral sides of the umbilicus. The clear difference in ATBF effect seen between those sites, confirms that microinfusion achieves only local effects (see Figure 5.4).

2.2 Arterio-venous difference technique

Regional tissue substrate trafficking can be assessed based on the arterial and venous concentrations of a particular substrate, and the blood flow. If all three variables are known, substrate flux, i.e. the net rate of extraction/uptake from or release into the circulation, can be calculated. Net extraction of a metabolite is expressed in a positive arterio-venous (AV) difference in concentration, while net release is implied by a negative AV difference (or positive VA difference).

Frayn *et al.* first described the use of the AV difference technique for the study of human adipose tissue in 1989 (142). In this seminal study, the AV difference in NEFA and glucose concentrations was measured across the superficial epigastric vein and an arterialized venous sample. Using the same technique, several other metabolites and adipose tissue-derived peptides, e.g. IL-6, TNF-α and leptin, as well as different metabolic situations, have been studied since (13, 103, 143-145).

Fatty acid release from the gluteofemoral adipose tissue depot was first studied using an AV difference technique in 1957 (146). In this study, Gordon *et al.* investigated the release of NEFA (and the changes in release induced by glucose and insulin) in blood samples taken from the great saphenous vein. Jensen *et al.* used the AV difference technique and tracers across the leg for the measurement of basal palmitate release (58), the uptake and release of palmitate after a meal (59) and leptin release (147). It is important to note that in these studies the venous samples were taken from the external iliac vein. Thus, the venous effluent is not selective for adipose tissue but contains also blood drained from the leg musculature, providing a much more “crude” measurement of leg adipose tissue metabolites. More recently, Tan *et al.* studied selectively gluteal fat by cannulating a gluteal vein and comparing the AV difference of NEFA and TG to those across abdominal adipose tissue (102). They showed that gluteal fatty acid release was 87% lower than in the abdomen. A current study by McQuaid *et al.* investigated the differences in postprandial fatty acid trafficking between femoral and abdominal fat (106). Femoral adipose tissue was

shown to extract TG at a lower rate than abdominal fat, and to have a preference for VLDL-derived over chylomicron-derived TG.

Jensen *et al.* has published on the effects of adrenaline on leg palmitate release in men and women using the external iliac vein cannulation technique (113). He reported an increase in leg palmitate release during adrenaline stimulation in men but not in women. A following study using isoprenaline in women showed a blunted response in leg palmitate release and concluded that the differences seen between men and women in leg palmitate release are not related to α-adrenoceptor activity (112). The AV difference technique has not been applied to study the metabolic effects of adrenergic stimulation selectively on gluteofemoral fat. Furthermore, the role of gluteofemoral fatty acid trafficking in response to sequential feeding over a 24 h period is unclear to date.

2.2.1 Cannulation of a vein draining abdominal adipose tissue

The aponeurosis of the obliquus externus abdominis muscle separates subcutaneous abdominal adipose tissue from the underlying structures. Because of the lack of any perforating veins, the superficial epigastric veins anatomically drain mostly adipose tissue. This was confirmed by Frayn *et al.* when they developed a technique for the cannulation of veins draining adipose tissue, e.g. the superficial inferior epigastric vein and its branches (142). The veins were cannulated in an anterograde fashion and care was taken to place the tip of the catheter above the inguinal ligament in order to minimize blood contribution from the deep leg veins. The AV difference for NEFA and TG confirmed that with the exception of a small contribution from skin, these veins drain subcutaneous abdominal adipose tissue (148).

For the purpose of my studies, I identified superficial abdominal veins using a fibre-optic light source (KL2500, Schott, Mainz, Germany) and ultrasound. Under ultrasound guidance, and after injection of a local anaesthetic (Lidocaine hydrochloride, Antigen Pharmaceuticals, Ireland), I inserted a 20-gauge central venous catheter (BD Careflow, Franklin Lakes, NJ, USA) with the Seldinger technique. I used the anterior superior iliac spine and the projected pubic symphisis as reference points for the inguinal ligament. Using a tape measure, I made sure that the tip of the catheter was placed proximal to the inguinal ligament. After successful cannulation and placement, the catheter was taped on the skin and perfused with 0.9% NaCl solution.

2.2.2 Cannulation of a vein draining femoral adipose tissue

I was involved in the recent development of a cannulation technique of a vein draining femoral adipose tissue for the study of gluteofemoral adipose tissue metabolism (see this Section and (149)). Initially, it was attempted to cannulate veins draining gluteal adipose tissue (102). Although successful in principle, it proved that the blood in these veins clots easily and that they are not suitable for the study of adipose tissue over longer periods. Using veins draining the subcutaneous adipose tissue of the leg is an alternative means of studying this adipose tissue depot.

In my studies, I identified suitable veins located in the medial aspect of the middle third of the thigh. Usually, the saphenous vein or one of its branches was cannulated. After local anesthetic injection, I inserted a 22 gauge cannula (Abbocath T, Hospira venisystems, Lake Forest, Illinois, USA) under ultrasound guidance. After insertion, the catheter was taped to the skin and perfused with 0.9% NaCl solution.

This cannulation is performed with the participants lying on their side resulting in a low filling pressure of the superficial leg veins (as opposed to standing). Therefore, the standard “blood flash back” method for inserting a cannula is of limited use. This problem is overcome by attaching a polyethylene extension tube (Lectrocath, Vygon, Cirencester) and a 1ml syringe to the catheter before insertion. Once the tip of the cannula has penetrated the skin, suction is applied through the syringe. The appearance of blood indicates the moment the cannula has reached the lumen of the vein.

Using this method it was possible to achieve a very high rate of success for the cannulation of veins draining femoral adipose tissue. A refinement of this method for the use in studies of 24 h duration is described in the next Section.

2.2.3 Catheterisation of a vein draining femoral adipose tissue for use over 24 h

The method for obtaining blood samples from veins draining femoral adipose tissue described above is applied without difficulties in studies of short duration. I used this method in the studies described in Chapters 3 and 4. However, the use of the Abbocath catheter in the 24 h studies (see Chapter 6) proved to be problematic. The stiffness of the catheter caused a series of problems: with prolonged use the catheter appeared to irritate the veins considerably, resulting in vasoconstriction and loss of samples. Further, after the ambulatory periods specified in the study protocol, the

catheter was often dislocated, making further blood sampling impossible. The insertion of a further catheter, most likely in the contralateral leg, can be very stressful for a participant after having spent a considerable time in the research unit. Thus, this should be avoided on ethical but also methodological grounds, as stress might affect metabolite concentrations (150).

Two factors had to be considered in my search for an alternative catheter: the stiffness of the catheter and its length. The softer the catheter material, the less likely to cause vein irritation, even during movement. Further, the longer the catheter, the less likely to dislocate during exercise. Based on the Hagen-Poiseuille's Equation, the resistance to blood flow in a single vessel is determined by vessel diameter and length and blood viscosity (151). Unfortunately, the specification of commercially available catheters is that longer catheters have usually a smaller lumen. The resulting higher resistance to blood flow leads to clotting in the catheter. On the other side, larger lumen catheters are stiffer and lead to more tissue damage, resulting in vein irritation and vasoconstriction.

Several catheters of different lumen size, length and stiffness were examined and I discussed product availability and suitability with an expert (Dr Rhys Evans, Department of Anaesthetics, John Radcliffe Hospital, Oxford). A 22 gauge catheter with 40 mm of length (Leaderflex, Vygon, Cirencester) was chosen for running a pilot experiment. The purpose of the pilot experiment was to test the insertion procedure and to answer the question of whether metabolite concentrations vary depending on the depth of insertion. This question arose because of the anatomical considerations regarding leg muscle drainage, discussed in 2.2.4.

The insertion of the catheter proved to be straightforward: under ultrasound guidance, the catheter was inserted using the Seldinger technique. Despite the presumed presence of vein valves, no insertion problems were observed either with the guide wire or with the catheter. Because of the depth of the cannulation, this procedure was carried out under sterile conditions.

In order to assess the effect of cannulation depth on metabolite concentration, blood samples were taken using a longer catheter, normally used for arterial cannulations (20G, Leadercath, Vygon, Cirencester), from three different depths: fully inserted (15 cm), half-way inserted (7.5 cm) and at 2.5 cm (for comparison, the 22 gauge catheter used in the studies of short duration has a length of 3.2 cm). The experiment was

carried out in a healthy volunteer during the late morning, about three hours after breakfast. I compared plasma creatinine, NEFA and glucose concentrations between venous samples taken at the three different depths and arterialised venous samples (Figures 2.2-2.4). There were no differences between the three depths regarding metabolite levels. Creatinine concentrations between the venous samples were comparable (Figure 2.2). This suggests there is minimal contribution from muscle drainage irrespective of the cannulation depth. Furthermore, the clear presence of elevated NEFA concentrations in the venous samples shows that, irrespective of catheter depth, adipose tissue drainage is sampled (Figure 2.3).

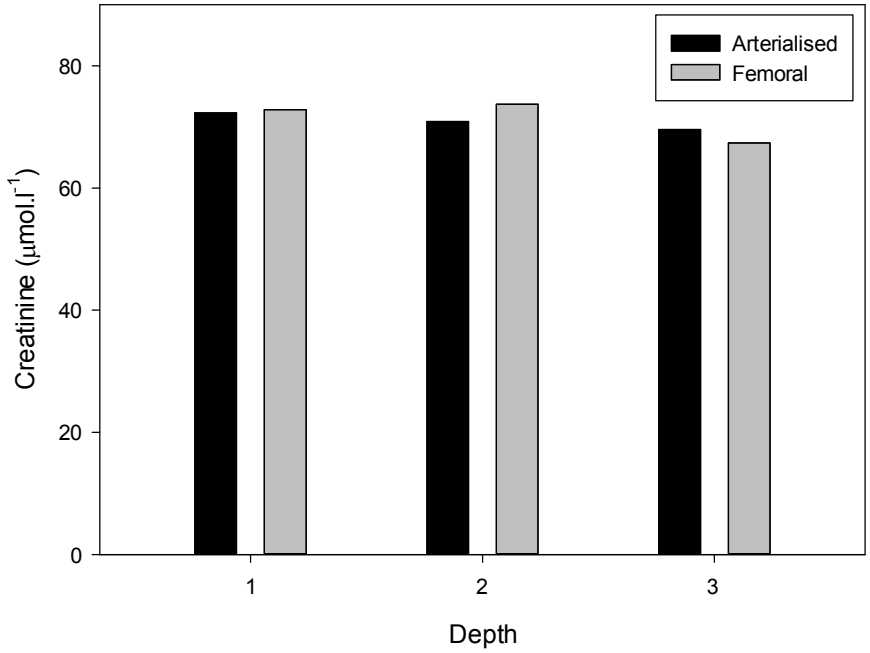

Figure 2.2: Plasma creatinine concentrations in arterialised and venous samples from a vein draining femoral adipose tissue, taken at different cannulation depths (1=15 cm, 2=7.5 cm, 3=2.5 cm; n=1).

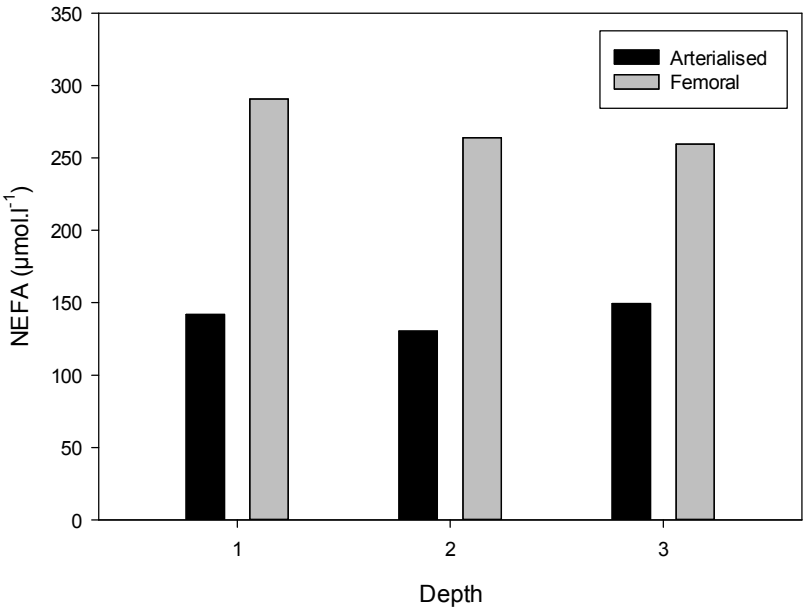

Figure 2.3: Plasma NEFA concentrations in arterialised and venous samples from a vein draining femoral adipose tissue, taken at different cannulation depths (1=15 cm, 2=7.5 cm, 3=2.5 cm; n=1).

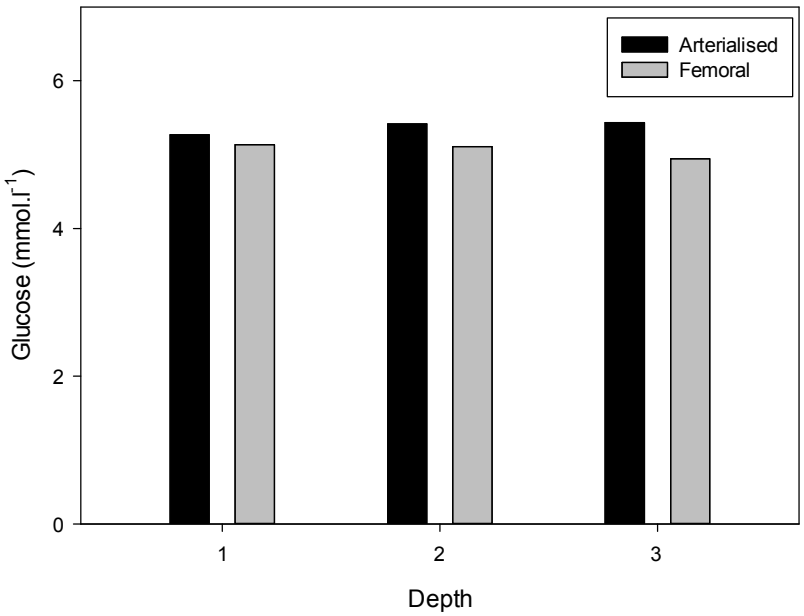

Figure 2.4: Plasma glucose concentrations in arterialised and venous samples from a vein draining femoral adipose tissue, taken at different cannulation depths (1=15 cm, 2=7.5 cm, 3=2.5 cm; n=1).

2.2.4 Specificity of blood samples from the saphenous vein

Blood samples from the epigastric vein are representative for abdominal fat, due to the anatomic properties of the abdominal venous drainage system (142). However, because of the large leg muscles and the presence of superficial to deep venous communications (the perforating vein system), contamination of venous drainage

from muscle should be considered when taking venous blood samples from superficial leg veins. I undertook some methodological studies in order to investigate the question of tissue specificity of saphenous vein blood sampling.

The perforating veins connect the deep leg veins with the superficial saphenous vein, which normally drains the superficial leg and thigh tissues, i.e. skin and fat. From a clinical perspective this is only an issue if there is valve insufficiency, as seen in chronic vein diseases (personal communication Dr. Linda Hands, Department of Vascular Surgery, John Radcliffe Hospital, Oxford). This is because valves direct blood from the superficial to the deep venous system of the leg. Thus, given that in my studies I used only healthy volunteers, there should be little contamination from deep veins.

In an approach to clarify whether the leg musculature is contributing to the venous effluent of the superficial saphenous vein, I measured concentrations of creatinine, a specific muscle marker, during basal conditions and during stimulation of lipolysis with isoprenaline (Figure 2.5, for details on the study population and isoprenaline infusion protocol see Section 3.3).

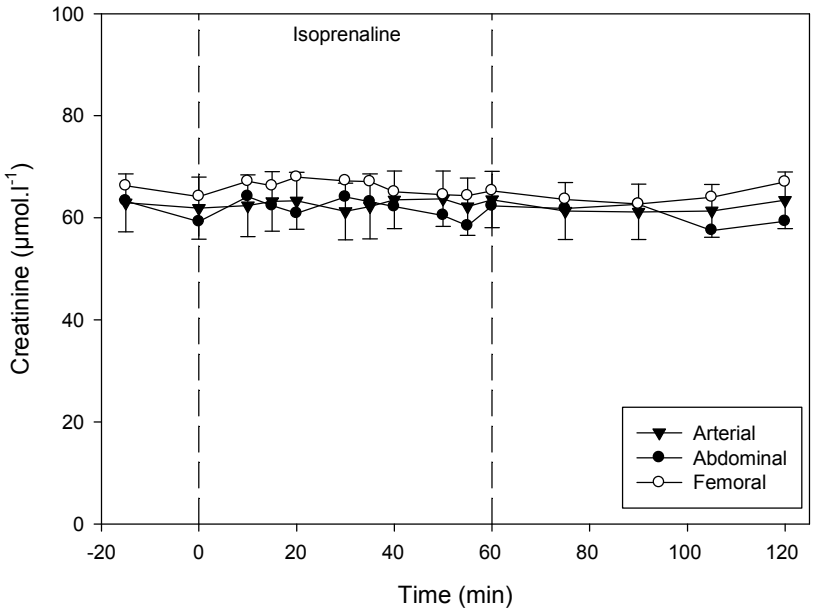

Figure 2.5: Plasma creatinine concentrations in arterial and abdominal and femoral venous samples (n=7; Isoprenaline infusion from 0 to 60 min at 20 ng.min^{-1}.kg fat-free mass (FFM)$^{-1}$).

Creatinine concentrations in femoral blood samples showed no significant differences compared to abdominal and arterial samples, suggesting minimal contribution of

skeletal muscle drainage. In previous studies of the research group, creatinine concentrations in samples taken from a vein draining forearm (largely skeletal muscle) were approximately 20% higher than in arterial blood or in samples from a vein draining abdominal fat (149).

"Contamination" of saphenous vein samples with blood drained from muscle would also affect regional NEFA concentrations. The isoprenaline infusion study showed that NEFA concentrations in blood samples from a vein draining abdominal adipose tissue were comparable to those in samples taken from the saphenous vein (see Figure 2.6). Thus, contribution from the leg musculature seems negligible and the superficial saphenous vein and its branches drain mostly adipose tissue.

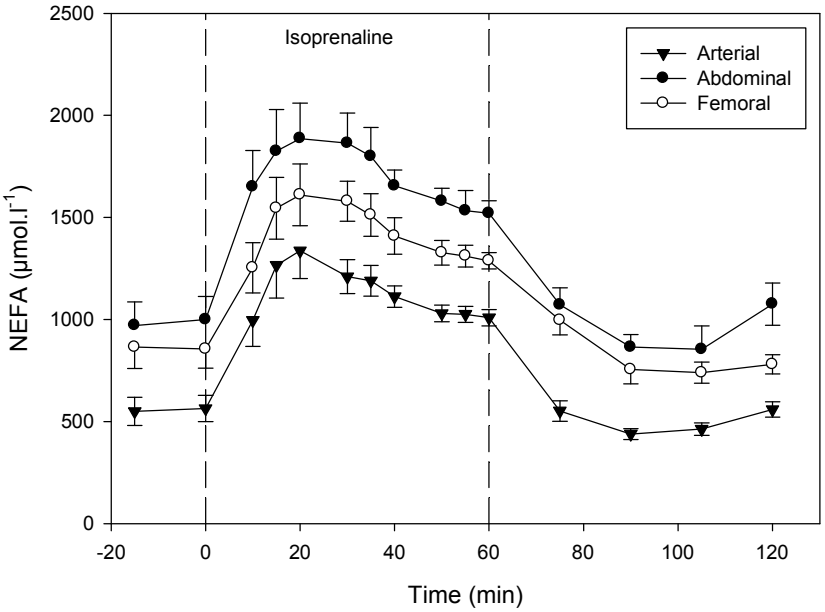

Figure 2.6: NEFA concentrations in arterial, and abdominal and femoral venous samples (n=7; isoprenaline infusion from 0 to 60 min at 20 ng.min^{-1}.kg FFM^{-1}).

2.2.5 Cannulation of the femoral artery

Arterial cannulation provides consistent blood sampling from the arterial circulation that is needed for the AV difference calculations. In my studies I used the right femoral artery for cannulation purposes given that it provides a convenient access and is a large vessel. Arterial cannulation is associated with some morbidity (152). However, the risks are insignificant when the procedure is carried out by qualified medical personnel experienced in the Seldinger technique. Risk was minimized further by the use of small-gauge catheters.

After local anaesthetic injection, I inserted a 20 gauge arterial catheter (Leadercath, Vygon, Cirencester) into the right femoral artery using the Seldinger technique. All cannulations were performed under ultrasound guidance and sterile conditions. After successful cannulation the catheter was taped in place and perfused with 0.9% NaCl solution. Blood sampling from the arterial port was performed only by medically qualified members of the group and research nurses trained in the handling of arterial lines.

2.2.6 Arterialized venous blood sampling

The principle of arterialized venous blood sampling is based on the anatomical proximity of the veins and arteries of the hand and the presence of arterio-venous shunts that open up in the hand circulation in response to heat. Accordingly, during the application of heat a faster transit time of arterial blood into the venous circulation is seen (153, 154). Thus, by cannulating a distal branch of the cephalic vein in the back of the hand in a retrograde fashion an arterialized venous blood sample can be obtained. The concentrations of many metabolites are indistinguishable in arterial and arterialized venous blood, making this technique an ideal substitute for arterial cannulations (155). To date, the technique has been validated for a number of metabolites including glucose and insulin (156, 157), 3-hydroxybutyrate (158), NEFA and NEFA tracers (159). In contrast, arterialized venous blood samples are not always suitable for the measurement of lactate, oxygen, carbon dioxide or high catecholamine concentrations (157, 160). It is essential to ensure a constant and even heating of the hand without raising total body temperature in order to obtain true arterialized samples. In the past, heating pads wrapped around the hand, or even the whole arm, were used. This is not recommended because of the resulting increase in whole body temperature (161), the uneven application of heat to the tissue with concomitant variations in shunt opening and the danger of injuries (162). Instead, the use of a box that constantly heats the air surrounding the hand is an optimal method of arterialization (155, 163). After only fifteen minutes of heating, arterialized samples can be obtained providing highly reproducible measurements (164).

I used the arterialized venous blood sampling technique in the microinfusion studies where a direct arterial cannulation was not necessary as no AV differences were measured (see Section 3.2). One hand of the volunteer was placed into a hot box that heats the air to a constant 60°C, after cannulating a superficial vein on the back of the hand in a retrograde way. Blood samples were taken at least fifteen minutes after placing the hand in the box and arterialization was frequently confirmed by

blood gas analysis (IL 628 co-oximeter, Instrumentation Laboratory Ltd, Warrington). An oxygen saturation of >94% was considered to reflect adequate arterialization of venous blood.

2.3 Systemic adrenergic agonist infusions

I used systemic isoprenaline and adrenaline infusions for assessing the effect of adrenergic stimulation on regional adipose tissue metabolism. Further, for the direct measurement of fatty acid trafficking using the AV difference technique, stable isotope tracers were infused. Here, I describe the methodological considerations related to these systemic infusions.

2.3.1 Isoprenaline infusion

Isoprenaline has β-adrenergic agonist properties that result in a significant increase of heart rate and blood pressure when infused systemically. Therefore, it was essential for my studies to find a dose that when infused into healthy volunteers would exert adipose tissue effects with minimal systemic side effects. Isoprenaline infusions have been widely used for the assessment of muscle metabolism *in vivo* (165-167). According to the literature, an infusion rate of 20 $ng.min^{-1}.kg$ fat-free mass $(FFM)^{-1}$ exerts appropriate tissue effects while heart rate increases approximately by 30% (165). It has been shown that systemic isoprenaline concentrations correlate best with FFM, resulting in comparable systemic concentrations across a wide range of BMI (130).

Isoprenaline was diluted under sterile conditions in a 0.9% NaCl solution in order to obtain a stock solution of 2 $ng.ml^{-1}$. This solution was infused using a syringe pump (Graseby 3200, Graseby Medical Ltd, Watford). The final infusion rate was calculated according to each participant's FFM, derived from dual X-ray absorptiometry (DXA) measurements, in order to achieve an infusion rate of 20 $ng.min^{-1}.kg\ FFM^{-1}$. The participants' heart rate was continuously monitored using a PowerLab system (AD Instruments, Chalgrove) and blood pressure was measured in frequent intervals. The chosen isoprenaline infusion rate resulted in significant adipose tissue effects (discussed in Chapter 3) with clinically acceptable systemic effects. Heart rate increased from a basal 62±3 bpm to a maximum of 84±4 bpm ($p<0.001$; Figure 2.7). Systolic blood pressure increased during the infusion from 118/75 mmHg to 138/71 mmHg (Figure 2.8). With the exception of one volunteer who showed muscular twitches immediately after the start of the isoprenaline infusion, no other side effects were observed.

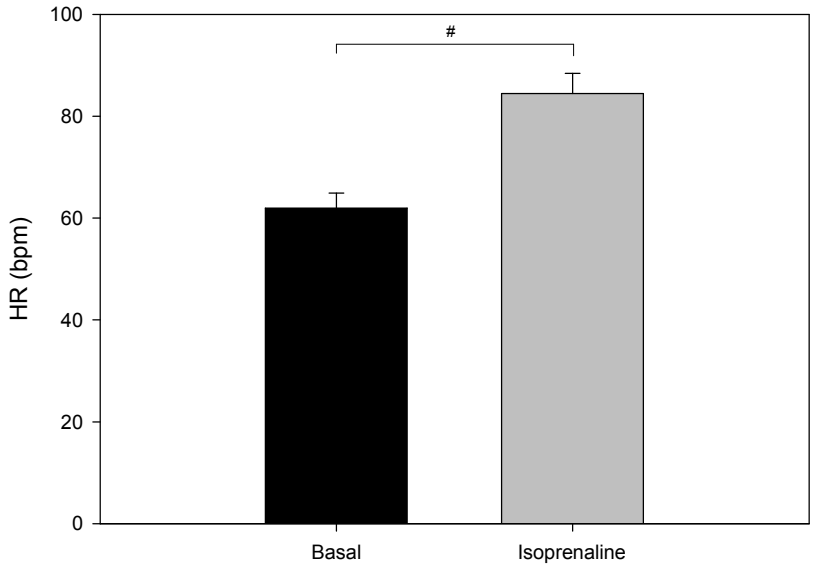

Figure 2.7: Heart rate before and after systemic isoprenaline infusion (n=7; isoprenaline for 60 min at 20 ng.min^{-1}.kg FFM^{-1}; $^{\#}$p<0.001).

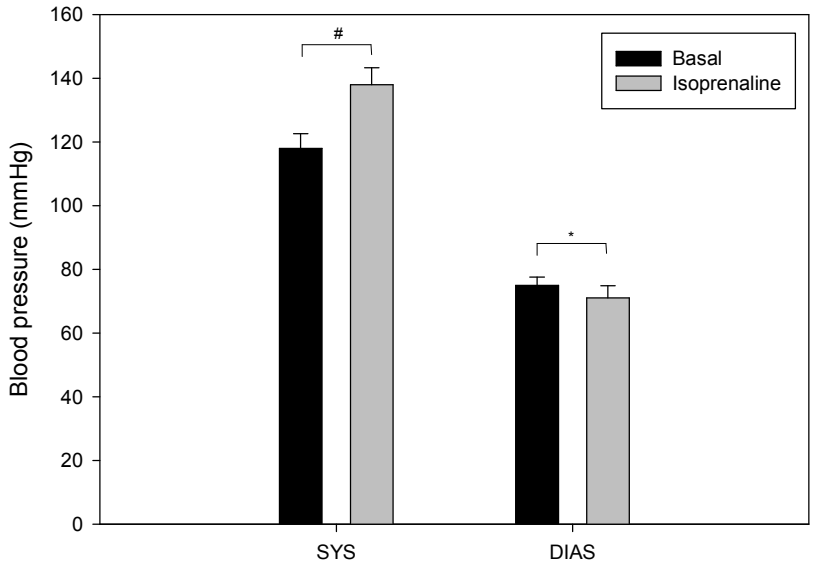

Figure 2.8: Systolic (SYS) and diastolic (DIAS) blood pressure before and after systemic isoprenaline infusion (n=7; isoprenaline for 60 min at 20 ng.min^{-1}.kg FFM^{-1}; *p<0.05, $^{\#}$p<0.001).

2.3.2 Adrenaline infusion

Adrenaline has α- and β-adrenergic properties and can cause serious haemodynamic side effects when infused in high doses. In addition, adrenaline exerts differential α- and β-effects depending on its local concentration (168). In low concentrations the α-effects prevail, whereas β-mediated effects dominate with

higher doses. Before commencing my studies it was therefore essential to decide on an appropriate infusion protocol.

Clutter et al. studied in 1980 the *in vivo* haemodynamic effects of different adrenaline doses achieved by systemic infusion rates ranging from 0.1 to 5.0 μg.min^{-1} (169). Heart rate increased significantly at plasma adrenaline concentrations of 50-100 pg.ml^{-1} (2.7-5.4 x 10^{-10} M), systolic blood pressure at 75-125 pg.ml^{-1} (4.1-6.8 x 10^{-10} M) and diastolic blood pressure at 150-200 pg.ml^{-1} (8.2 x 10^{-10} M-1.1 x 10^{-9-} M). These plasma adrenaline concentrations were achieved during infusion rates ranging from 0.1 to 1.0 μg.min^{-1}. A follow-up study of systemic lipolysis *in vivo* showed that plasma adrenaline concentrations of 75-125 pg.ml^{-1} increase glycerol and free fatty acid concentrations in plasma (170). Based on the mean weight of the study participants as provided in (169), this translates into infusion doses between 6.4 and 12.7 ng.kg body weight^{-1}.min^{-1}.

A higher dose of 25 ng.kg ideal body weight^{-1}.min^{-1} resulted after 30 minutes in a 20% increase of heart rate and a 60% increase in systemic plasma NEFA concentrations (171). However, systemic NEFA concentrations declined after the initial rise during the first 20 minutes of the infusion, probably due to tachyphylaxis. Tachyphylaxis is the process of β-adrenoceptor down-regulation after prolonged stimulation (172). Interestingly, when studying NEFA release in abdominal adipose tissue, the net efflux of NEFA remained constant during a 25 ng.kg body weight^{-1}.min^{-1} infusion of adrenaline, despite a similar decrease in systemic NEFA concentration (133). Various other infusion protocols have been used *in vivo*, whereby each research group has used its own standards (111, 113, 173-175).

In view of the literature, I decided to use a stepped adrenaline infusion (Adrenaline, non-proprietary, South Devon Healthcare, UK), with an infusion rate of 5, 15 and 25 ng.min^{-1}.kg FFM^{-1}, changing between rates every 20 min. A stepped infusion would allow studying adrenaline effects across a range of concentrations that should result in distinguishable α- and β-adrenoceptor-mediated effects. The 20 min interval of each infusion step should suffice as steady state conditions are achieved within 10 minutes (176). There have been concerns that stepped infusions of catecholamines result in potentiation of metabolic responses (177). However, in a direct comparison it was shown that potentiation effects for adrenaline are small and confined to men (178). As already discussed for isoprenaline, the use of DXA-derived FFM is a good strategy for adjusting the dose between subjects. Adrenaline is a hydrophilic

compound (179) and quantitative drug clearance of hydrophilic compounds is best described and adjusted using lean body mass (180).

A prerequisite for achieving the three steps described was to use a delivery method that allows rapid changes between infusion rates. Preparing different adrenaline solutions would have led to considerable delays during the study because of the procedure of changing infusion gear and/or reprogramming infusion pumps. I decided to use a single syringe pump and an adrenaline stock solution, so that the described infusion rates could be achieved by simply changing the rate setting on the pump. As part of the preliminary work to these studies, I tested the delivery rate change speed and overall accuracy of the syringe pump used during the studies. Using a 50 ml syringe (BD Plastipak, Franklin Lakes, NJ, USA) and a 150 cm connection line, I weighed the amount of 0.9% NaCl solution delivered per minute during three 20 minute infusion steps (0.25, 0.75 and 1.25 $ml.min^{-1}$) and used a conversion factor of 1.0046 for transforming grams saline into ml (181). As shown in Figure 2.9, the syringe pump delivery rate is adjusted within less than one minute. Table 2.2 shows that the pump is highly accurate in its delivery.

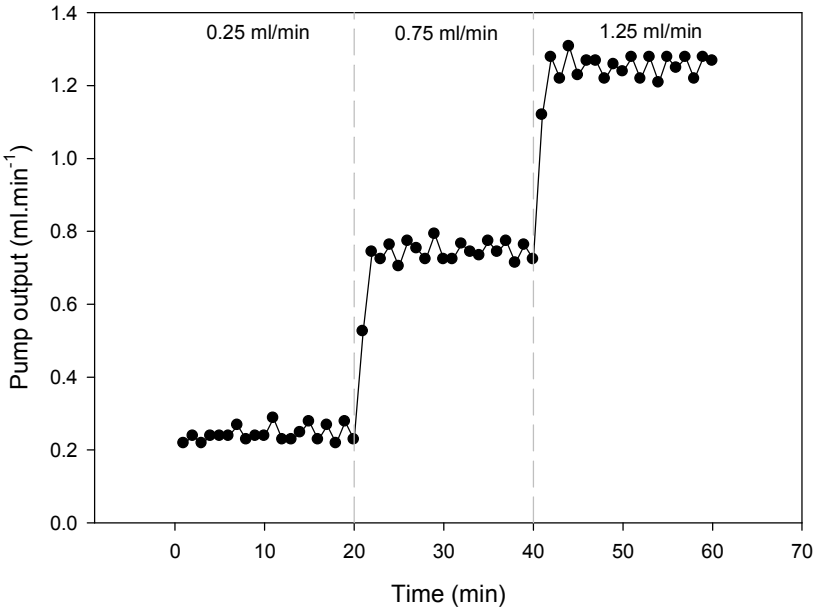

Figure 2.9: Measured delivery rates of syringe pump during a three-step infusion regime.

Table 2.2: Measured syringe pump output during a three-step infusion regime.

Set infusion rate (ml.min^{-1})	Measured output (ml.min^{-1})
0.25	0.245±0.01
0.75	0.731±0.05
1.25	1.25±0.04

Mean±standard deviation shown

In previous studies, ascorbic acid has been added to the adrenaline solution to prevent adrenaline degradation (170). In my studies, the adrenaline stock solution was prepared immediately before the infusion start. Because of the overall short duration of adrenaline infusion (total of 60 minutes) degradation of adrenaline seemed unlikely. This was confirmed by the observation of adipose tissue effects during the infusion in all studies performed.

In two pilot experiments I tested different infusion rate regimes. In the first pilot study I calculated the adrenaline infusion doses without adjusting for FFM. The infusion of 7, 21.4 and 35.7 ng.min^{-1}.kg body weight^{-1} resulted in a dose-dependent increase of abdominal ATBF and NEFA release (Figures 2.10 and 2.11). Systolic blood pressure increased by 6% and heart rate by 18% (Figure 2.12). Overall, the infusion was well tolerated.

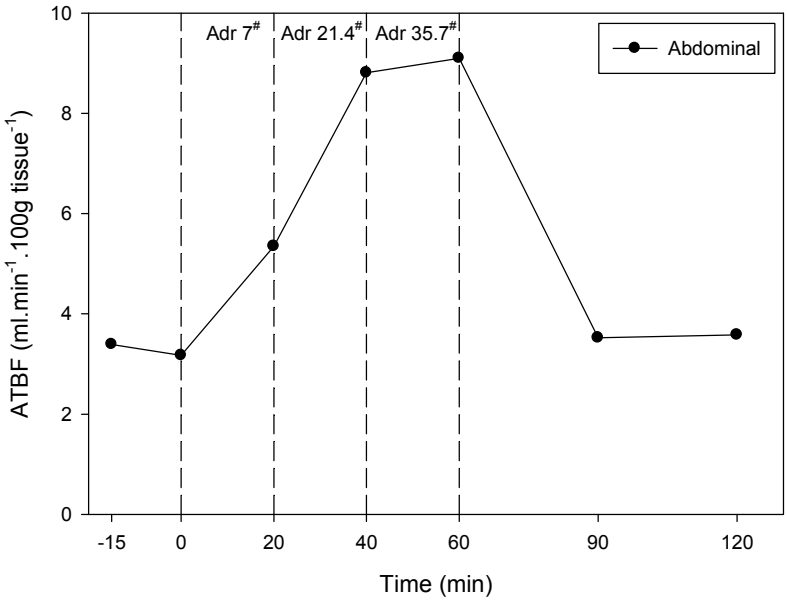

Figure 2.10: Abdominal ATBF during a pilot experiment of a systemic adrenaline infusion (#ng.min^{-1}.kg body weight^{-1}; n=1).

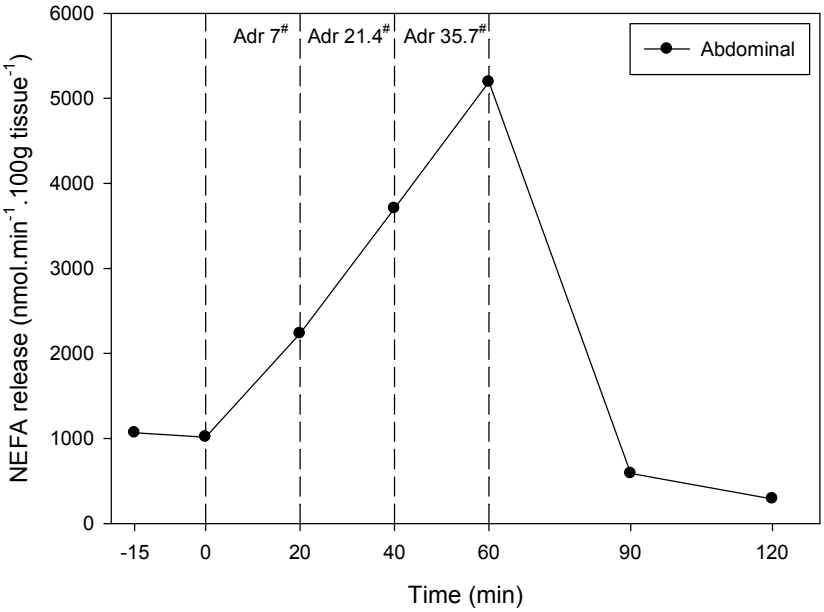

Figure 2.11: Abdominal NEFA release during a pilot experiment of a systemic adrenaline infusion (#ng.min^{-1}.kg body weight^{-1}; n=1).

In a further pilot experiment, I implemented the adrenaline dose regime adjusted for FFM (5, 15, 25 ng.min^{-1}.kg FFM^{-1}). The effects on abdominal ATBF, NEFA release and haemodynamic parameters were comparable to the initial pilot study (data not shown). I used the FFM-adjusted protocol for the studies described in Chapters 3 and 4. The rationale for using a FFM-adjusted infusion rate has been discussed in Section 2.3.1.

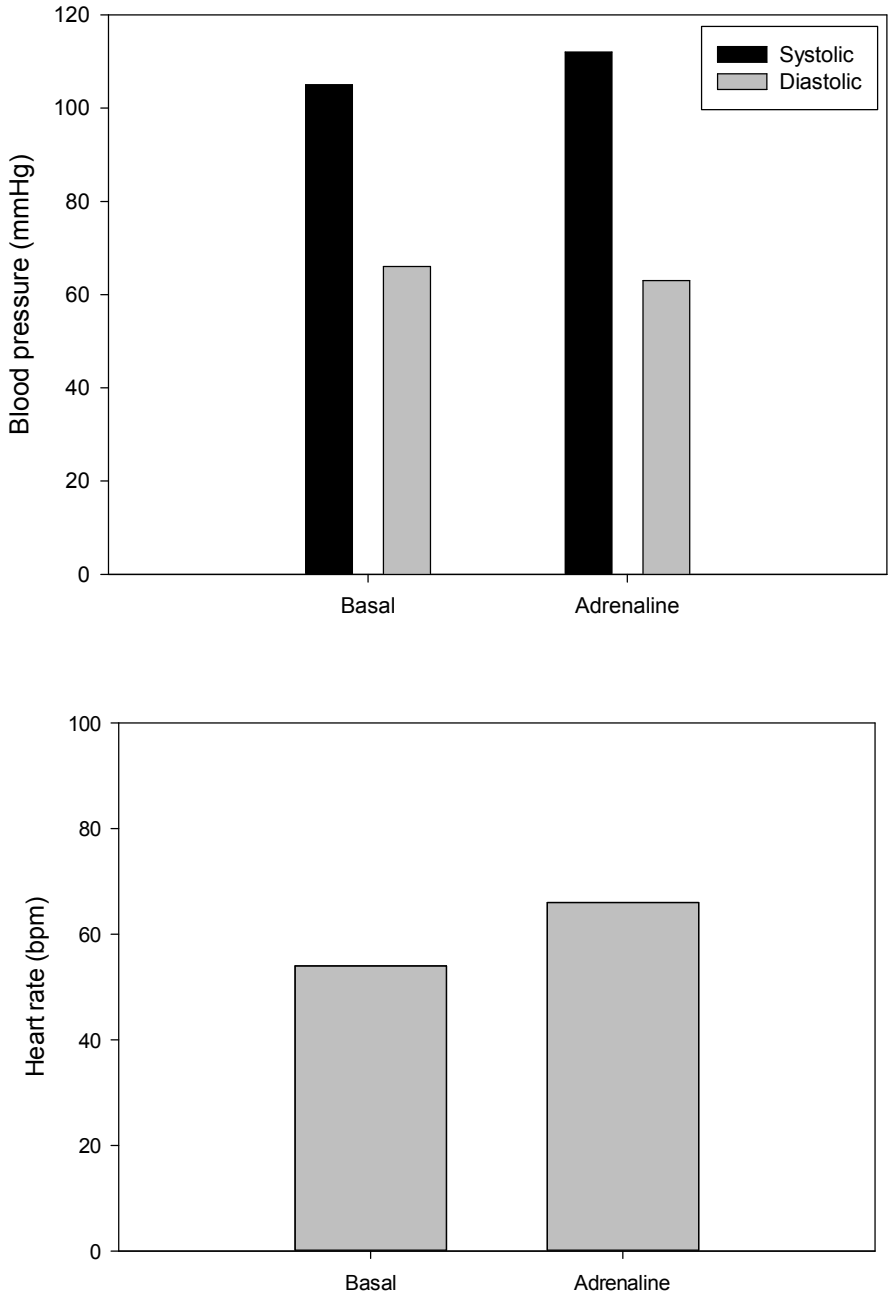

Figure 2.12: Blood pressure (upper panel) and heart rate (lower panel) before and after a 60-min systemic adrenaline infusion (n=1).

2.4 Stable isotope tracers

In nature, elements occur as chemically identical isotopes that have a different mass. In contrast to radio-isotopes, stable isotopes do not decay spontaneously. Therefore, stable isotopes can be used in the production of tracers – compounds that are chemically and functionally similar to the tracee, i.e. the compound of interest (182). These tracers can be given to study participants safely as they pose no significant

risks. Samples obtained are analysed by mass spectrometry where the measurement of the molecular mass of a sample allows for the determination of the tracer/tracee ratio (TTR). Based on the TTR, metabolic pathways, e.g. fatty acid trafficking, can be investigated. For the study of regional fatty acid trafficking, palmitic and oleic acid are most commonly labelled with stable isotope tracers. Both fatty acids are abundant in circulating NEFA and their turnover is thought to represent that of the body's NEFA pool (183).

2.4.1 Stable isotope tracer infusion

For the purpose of studying endogenous fatty acid trafficking, i.e. lipolysis-derived NEFA production and hepatic VLDL-TG production, I used a [$^{2}H_{2}$]palmitate infusion. [$^{2}H_{2}$]palmitate (isotope purity 97%, Cambridge Isotopes, Cambridge) was dissolved into human albumin (Albunorm 5%, Octapharm, Manchester), firstly to make it soluble and secondly because palmitate is physiologically transported in blood complexed to albumin. The infusion of human albumin is associated with a very low rate of morbidity, which increases only when given repeatedly or in high concentrations (184-186). For the short adrenergic response studies (see Chapters 3 and 4) I used a tracer infusion rate of 0.03 μmol.min^{-1}.kg body weight^{-1}. Based on an average body weight of 70 kg this results in an average albumin infusion volume of 400 ml. For the studies described in Chapter 7, which have an overall duration of 24 h, I used a tracer infusion rate of 0.01 μmol.min^{-1}.kg body weight^{-1}, resulting in an average infusion volume of 230 ml. Both infusion protocols have been established and validated in the group over a long period of time and achieve detectable levels of tracers in the samples of interest (2, 134). For the preparation of the infusion I followed an established protocol that is outlined in the Appendix.

2.4.2 Stable isotope tracer drink

For the study of regional fatty acid trafficking over 24 hours, there was the need for accounting for the exogenous (dietary) fatty acid trafficking pathway. In order to study chylomicron-derived fatty acid trafficking, stable isotope tracers were given orally. Moreover, in order to be able to distinguish whether the chylomicrons derive from the breakfast, lunch or dinner, three different tracer fatty acids were used. [U-^{13}C]palmitic acid (isotope purity 98%, Cambridge Isotopes, Cambridge) was given with dinner, [U-^{13}C]oleic acid (isotope purity 98%, Cambridge Isotopes, Cambridge) with lunch and [U-^{13}C]linoleic acid (isotope purity 98%, Cambridge Isotopes, Cambridge) with breakfast. The isotopes were given in form of a chocolate-flavoured fat emulsion (for details see Appendix), along with a standardised meal. The three meals were

isoenergetic and the energy was derived from set proportions of macronutrients (14% from protein, 37% from fat and 49% from carbohydrates). The meal composition used here is essentially the same used in recent studies published by the research group (106, 107). The preparation of the stable isotope drink and of the meals followed established protocols and was carried out by trained research nurses.

2.5 Metabolite analysis

Whole blood samples were collected simultaneously from the artery and the veins draining the adipose tissue depots into heparinised syringes (Saarstedt, Leicester). Plasma was immediately separated by centrifugation at 4°C and aliquoted for the measurement of metabolites and insulin. Haematocrit, haemoglobin concentration and oxygen saturation where measured in whole blood.

Plasma glucose, TG corrected for glycerol, NEFA and creatinine concentrations were measured on an ILab 600 Clinical Chemistry System (Instrumentation Laboratory, Warrington) with enzymatic methods. Insulin concentrations were measured using a radioimmunoassay (Linco Research, St. Charles, MO, USA). At specific time points during the studies, 400 µl of whole blood were added to 7% w/v perchloric acid, and 3-hydroxybutyrate (3-OHB), lactate and glycerol concentrations were determined on the ILab 600 Clinical Chemistry System using enzymatic methods.

The analysis of metabolites was performed by expert members of the research group.

2.5.1 Lipid extraction

For the purposes of specific fatty acid composition determination and for the measurement of isotopic enrichment, total lipids need to be extracted from plasma. The method is based on the chloroform/methanol extraction of lipids described by Folch *et al.* (187). This is followed by solid phase extraction using chromatography and the preparation of methyl esters of fatty acids (FAME) from the NEFA and TG fractions with methanolic sulphuric acid (188). Using gas chromatography-mass spectrometry (GC-MS), the enrichment of [$^{2}H_{2}$]palmitate in the FAME derivatives of plasma NEFA and VLDL-TG and the enrichment of [U-^{13}C]palmitate in plasma NEFA were measured (134). Lipid extraction and isotopic enrichment measurements were carried out by expert members of the research group.

2.6 Calculations

2.6.1 General biochemistry

The haematocrit was directly measured in arterial samples by centrifugation of the plasma in microhaematocrit tubes (Hawksley, Lancing). Haematocrit was used to convert plasma concentrations of glucose, NEFA and TG into whole blood values.

Whole blood glucose = [Plasma glucose] x (1-0.3 x haematocrit) (see (189))

Whole blood NEFA = [Plasma NEFA] x (1-haematocrit)

Whole blood TG = [Plasma TG] x (1-haematocrit)

AV-difference = $[Metabolite]_A - [Metabolite]_V$

VA-difference = $[Metabolite]_V - [Metabolite]_A$

A-V flux $_{(nmol.100\ g\ tissue^{-1}.min^{-1})}$ = $[Metabolite]_{A\text{-}V\ (\mu mol/L)}$ x ATBF $_{(ml.100\ g^{-1}.min^{-1})}$

Transcapillary flux $_{(nmol.100\ g^{-1}.min^{-1})}$ = $(3 \times [TG]_{A\text{-}V}) - ([NEFA]_{V\text{-}A}) \times ATBF$

2.6.2 Isotopic tracer calculations

Tracer-to-tracee ratio (TTR) for $[^2H_2]$palmitate = (M + 2) / (M + 0)

where M = mass-to-charge ratio of major ion

Tracer-to-tracee ratio (TTR) for [U-^{13}C]palmitate = (M + 16) / (M + 0)

In order to account for the relative high natural abundance of ^{13}C (1.11%) (182) the TTR of a baseline measurement (prior to the administration of the stable isotope tracer) was subtracted from each sample TTR.

Rate of appearance (Ra) of NEFA (Ra_{NEFA}) was calculated based on the rate of appearance of palmitate. The calculation of Ra_{NEFA} on whole body level has been used before (114). For the purposes of my studies an algorithm for the calculation of adipose tissue depot-specific Ra_{NEFA} was developed.

$Ra_{PALMITATE\ (\mu mol.min^{-1}.kg^{-1})}$ = infusion rate of $[^2H_2]$palmitate / TTR of plasma $[^2H_2]$palmitate-NEFA

$Ra_{NEFA\ (\mu mol.min^{-1}.kg^{-1})} = Ra_{PALMITATE}$ x (1/proportion of palmitic acid in the NEFA fraction)

Whole body $Ra_{NEFA\ (\mu mol.min^{-1})} = [Ra_{NEFA}]$ x body weight $_{(kg)}$

Regional $Ra_{NEFA\ (nmol.min^{-1}.100\ g^{-1})} = TTR_{ART\ NEFA}$ x whole blood $NEFA_{ART}$ x $(1/TTR_{VEN\ NEFA} - 1/TTR_{ART\ NEFA})$ x ATBF

Concentration of [U-^{13}C]- or $[^2H_2]$palmitate in plasma NEFA or TG =
TTR of [U-^{13}C]palmitate or $[^2H_2]$palmitate x corresponding plasma palmitate NEFA or palmitate TG concentrations

Fractional extraction of [U-^{13}C]palmitate in TG fraction $_{(\%)}$ =
[U-^{13}C]$TG_{A\text{-}V\ (\mu mol/l)}$ / [U-^{13}C]TG_{ART}, expressed in %

Fractional extraction of $[^2H_2]$palmitate in TG fraction $_{(\%)}$ =
$[^2H_2]TG_{A\text{-}V\ (\mu mol/l)}$ / $[^2H_2]TG_{ART}$, expressed in %

2.6.3 Statistical analysis

Data were analysed using PASW Statistics for Windows v18 (SPSS UK, Chertsey) and a $p<0.05$ was considered to be statistically significant. All data are presented as mean±standard error of the mean (SEM), unless otherwise stated. The area under the curve (AUC) was calculated using the trapezoid rule and is presented as a time-averaged value (AUC divided by the relevant time period). Differences between adipose tissue depots were analysed with a paired t-test, or when indicated in the relevant chapters, with repeated measures analysis of variance (ANOVA) or Wilcoxon-signed rank test.

2.7 Subject recruitment

The aim of this thesis was to investigate normal human physiology. Therefore, only healthy volunteers were recruited for my studies. Inclusion criteria were:

> Healthy young male and female participants with no medical condition or drug therapy.

Exclusion criteria were:

> Age <18 or >55 years
> Any medical condition or drug therapy
> Smoking
> Pregnancy and menopause
> Blood vessels unsuitable for cannulation, i.e. too small veins or arterial plaques

Recruitment was by poster advertisement and by using the Oxford BioBank. All studies were approved by the Milton Keynes Research Ethics Committee, for which I prepared and defended the applications.

2.7.1 The Oxford BioBank and recruitment by haplotype

The Oxford BioBank (OBB) is a databank of about 1,500 healthy individuals randomly selected from the general Oxfordshire population (190). Apart from anthropometric measurements, a full medical history and a screening blood test, these volunteers agreed to give a DNA sample for prospective genotype analysis. They also agreed to be re-approached for further studies in the future. The DNA of all participants has been analysed for specific genetic polymorphisms of interest, including those for the *ADRB2* gene (see Section 1.2.4).

With the help of the OBB, I recruited participants for the studies involving an adrenaline infusion that were stratified for their *ADRB2* haplotype. Thus, a study of haplotype effects could be carried out using small numbers of participants to achieve balanced and matched *ADRB2* haplotype carriers, as opposed to recruiting large numbers of unselected people likely to achieve imbalanced and small effects of single polymorphisms. The frequency of homozygous carriers of the three most

common haplotypes of interest in the OBB is shown in Table 2.3. The distribution of haplotypes among the study participants is discussed in the relevant Chapter (see Section 4.3.6).

Table 2.3: Frequency of homozygous ADRB2 haplotypes of interest in the OBB (total n=1478)

Haplotype	n	% frequency
2_2	305	20.6
4_4	184	12.5
6_6	49	3.3

2.7.2 Screening visit

All prospective participants attended a screening visit at least 48 hours before each study. At the screening visit the study particulars were discussed and written informed consent was obtained. Anthropometric measurements were taken, whereby all measurements were standardised and a mean of three measurements was taken.

Height was measured to the nearest cm using a wall-mounted stadiometer. Weight was measured to the nearest 0.1 kg using an electronic scale. Waist and hip circumference were measured to the nearest cm using a tape measure. Waist circumference was measured halfway between the bottom of the rib cage and the iliac crest. Hip circumference was measured as the largest circumference around the gluteal muscles. Body composition was measured using DXA (Lunar iDXA, GE Healthcare, Chalfont St Giles). In the local isoprenaline microinfusion study (see Section 3.2), total body fat mass was measured using bioelectrical impedance analysis (Bodystat 1500, Bodystat, Isle of Man).

Resting blood pressure was measured using an automatic sphygmomanometer. Two measurements taken at least 10 minutes apart were averaged. A resting ECG was taken (CP100, Welch Allyn, Aston Abbotts) and analysed to exclude any structural or functional heart disease. A fasting blood sample was taken to exclude any common organic disease.

2.8 Molecular biology methods

For the quantification of adrenoceptor expression, RNA was isolated from adipose tissue biopsies, and gene expression was measured with standard PCR techniques.

2.8.1 Adipose tissue biopsies

I obtained adipose tissue biopsies from abdominal and femoral fat from all study participants, after the end of each study. Abdominal fat biopsies were taken from the area lateral of the umbilicus, femoral fat biopsies from the front aspect of the middle third of the thigh. In both cases I took care to avoid the areas of previous cannulation and/or ^{133}Xe injection. After local infiltration with lidocaine, a small amount of subcutaneous adipose tissue was removed under suction, using a 14 gauge needle (Sterican, Braun, Sheffield) and a 50 ml syringe. The biopsies were washed with 0.9% NaCl to remove any blood residues and then immediately snap frozen in liquid nitrogen.

2.8.2 RNA extraction and real time polymerase chain reaction

RNA for gene expression analysis was extracted using a standard guanidinium thiocyanate-phenol-chloroform extraction method (191). The protocol has been established in the research group for a long time and can be found in the Appendix.

Polymerase chain reaction (PCR) is the gold standard method for the amplification of a DNA sequence and is widely used for the measurement of gene expression. The exponential amplification of DNA sequences involves a heat-stable enzyme, Taq polymerase, which acts on primers – short synthetic nucleotide sequences that target the sequence of interest. The quantification of PCR product is achieved by separation and visualization on a gel, or in real time using fluorescent probes and special apparatus (the process is then termed real-time PCR). Gene expression results in real-time PCR are expressed as the difference in the cycle number when fluorescence crosses over a threshold value between the experimental sample and a calibrator sample (termed “ddct”). When the primary extracted material is RNA (as opposed to genomic DNA), an intermediary step of DNA synthesis from RNA is needed. The product of this step is termed complementary DNA (cDNA) and is then used for the real-time PCR. Nowadays, companies provide tailored solutions for real-time PCR applications that render gene expression profiling an affordable and relatively easily applicable technology. In this thesis, the TaqMan platform (Applied Biosystems, Carlsbad, CA, USA) has been used for the measurement of adrenoceptor expression in adipose tissue. The primers used were either ready-

made or made-to-order by the manufacturer and PCR execution followed the manufacturer's protocol. Further information can be found in the Appendix. RNA extraction, cDNA synthesis and real-time PCR were performed by expert laboratory members of the group. The RNA expression of the following genes was analysed:

ADRA1A and ADRA2A

The *ADRA1A* gene is coding for the α_1-adrenoceptor, subtype 1A. There are three receptor subtypes (termed 1A, 1B and 1D) and little is known about their distribution in human adipose tissue. Animal and human data suggest that the total number of α_1-adrenoceptor binding sites in adipose tissue is low (see Section 1.2.3) and that subtype 1B plays a role in rat white adipose tissue (28). However, it is clear that subtype 1A is the most important α_1-adrenoceptor subtype involved in vascular tone regulation – mediating vasoconstriction (192, 193).

The *ADRA2A* gene is coding for the α_2-adrenoceptor, activating the main inhibitory pathway in adipocyte lipolysis (28). As discussed elsewhere, vasoconstriction is also mediated by α_2-adrenoceptors (see Sections 1.2.3 and 5.1). There are three α_2-adrenoceptor subtypes (2A/D, 2B and 2C), of which subtype 2A is the main one in adipose tissue and is coded by *ADRA2A* (28).

ADRB1 and ADRB2

The *ADRB1* gene is coding for the β_1-adrenoceptor and *ADRB2* for the β_2-adrenoceptor. Both β-adrenoceptor subtypes are expressed in adipocytes and the vasculature (see Section 1.2.3). Catecholamine-stimulated lipolysis is mediated by both β-adrenoceptor subtypes and they are equally expressed in adipocytes (109). In addition, β-adrenoceptors are important mediators of catecholamine-induced vasodilatation (see Sections 1.2.3 and 5.1). Haplotype variation of *ADRB2* and its relevance for this thesis is described in Sections 1.2.4, 2.7.1 and 4.3.6.

3 Regional fat metabolism during non-selective β-adrenoceptor stimulation with isoprenaline

3.1 Introduction

As discussed in Chapter 1, β-adrenoceptors are important determinants of fatty acid trafficking. Stimulation of β-adrenoceptors results in vasodilatation in adipose tissue by decreasing vascular smooth muscle tone, and enhances lipolysis. Studies *in vivo* have shown that whole body lipolysis is increased during isoprenaline infusion (166, 194). When studied with the microdialysis technique, isoprenaline increases glycerol appearance and adipose tissue blood flow (195). The importance of β-adrenoceptors is underlined by the variations seen in relationship to obesity: β-adrenoceptor-mediated lipolysis per unit fat mass is blunted in obese individuals compared to lean (166), probably in adaptation to the increased fat mass of the former. The *in vitro* lipolytic response to isoprenaline is reduced in adipocytes of lean individuals who have a history of obesity in first degree relatives (196). Responses to β-adrenoceptor stimuli in obese individuals are restored by diet and exercise (197, 198). Nevertheless, it should be noted that some of the differences found between lean and obese were not reproducible (199-201), probably a result of using insensitive methods such as microdialysis in some of these studies (see Section 2.1).

The response to isoprenaline infusion in different adipose tissue depots *in vivo* has been studied in women by Jensen *et al.* (112). A 3 $ng.kg^{-1}.min^{-1}$ isoprenaline infusion increased leg and splanchnic, i.e. non-subcutaneous adipose tissue, plasma flow. However, it did not increase leg or splanchnic palmitate release, despite an observed increase of whole body palmitate concentration and flux. The unexpected lack of effect of isoprenaline on leg lipolysis could be a result of the low isoprenaline dose used, which was selected to match the lipolytic response achieved with a 10 $ng.kg^{-1}.min^{-1}$ adrenaline infusion (112). As shown in Section 4.3.3, this level of adrenaline stimulation does not elicit any lipolytic effects in femoral adipose tissue. Furthermore, the results presented in the study by Jensen *et al.* might have been skewed by a technical issue. The leg catheter was placed in the iliac vein, with the tip lying above the inguinal ligament. This might have lead not only to contamination of blood samples with skeletal leg muscle blood, but also with blood drained from abdominal adipose tissue (see Section 2.2.1).

In both men and women, abdominal adipose tissue has a higher β-adrenoceptor density than femoral adipose tissue resulting in higher catecholamine-stimulated

lipolysis rates (108). Sex differences in adrenoceptor density and sensitivity *in vitro* have been described for the α_2-adrenoceptor. Women display a higher α_2-adrenoceptor density (202) and a higher anti-lipolytic α_2-adrenoceptor activity (108) in gluteal compared to abdominal adipocytes *in vitro*.

Given the importance of β-adrenoceptor-mediated adipose tissue effects and the lack of robust data with regards to regional adipose tissue responses to non-selective β-adrenoceptor stimulation, I conducted a series of experiments addressing the response of regional ATBF and lipolysis during stimulation with isoprenaline. These studies were specific to the leg adipose tissue by involving sampling of venous effluence via the saphenous vein and to abdominal adipose tissue by sampling the lower epigastric vein. The studies also addressed sex-specific differences of ATBF and lipolysis responses to isoprenaline.

3.2 Effects on ATBF during local non-selective β-adrenoceptor stimulation

3.2.1 Study design and participants

In order to study the effect on fasting and postprandial ATBF during local adipose tissue stimulation with isoprenaline, the following methods were used:

- Participant recruitment using poster advertisement
- Measurement of baseline anthropometric characteristics and total body fat mass using bioelectrical impedance analysis (see Section 2.7.2)
- Local microinfusion of isoprenaline (see Section 2.1.4)
- Measurement of ATBF with the ^{133}Xe washout technique (see Section 2.1.1)
- Measurement of systemic metabolite concentrations in arterialized venous blood samples (see Section 2.2.6)

Healthy young volunteers were recruited (n=13, 8 male; median age 25.5, range 20-56). The median BMI was 23.9 kg.m^{-2} (range 17.9-29.6 kg.m^{-2}) and the median WHR was 0.79 (range 0.72-0.95). The further participant characteristics are shown in Table 3.1.

Table 3.1: Baseline anthropometric and metabolic characteristics of subjects

	Male (n=8)	Female (n=5)
WHR	0.86 (0.77-0.95)	0.77 (0.72-0.8)*
Body fat %	16.0 (6.5-23.3)	25.0 (14.0-31.1)*
Fasting TG (µmol/l)	941 (640-1347)	552 (486-1613)
Fasting NEFA (µmol/l)	433 (269-628)	569 (495-617)
Fasting glucose (mmol/l)	4.9 (4.7-5.2)	5.0 (4.8-5.3)
Fasting insulin (mIU/l)	11.2 (5.9-16.3)	15.3 (7.3-17.2)

(*$p<0.05$ females compared to males; median and range shown)

As described in Section 2.1.4, four microinfusion probes were inserted, two in the subcutaneous adipose tissue of the abdomen, 5 cm on each side of the umbilicus, and one on the anterior aspect of each thigh, half-way between the groin and the knee. A cannula was inserted retrogradely into a vein of the dorsal hand and the hand was placed into a hot box for obtaining arterialized blood samples (see Section 2.2.6). A local isoprenaline infusion was started using one of the microinfusion catheters of each fat depot (ISO sites). As a control, a 0.9% NaCl solution was infused into the remaining catheters (SAL sites) (see Figure 3.1). Every 40 min, the concentration of isoprenaline was increased (concentration: 10^{-8} M, 10^{-6} M, 10^{-4} M, infusion rate: 2 µl.min^{-1}). Two hours after the start of microinfusion, a 75 g glucose drink was given as a positive control for endogenous regulation of ATBF. ATBF was measured with the ^{133}Xe washout technique throughout the study.

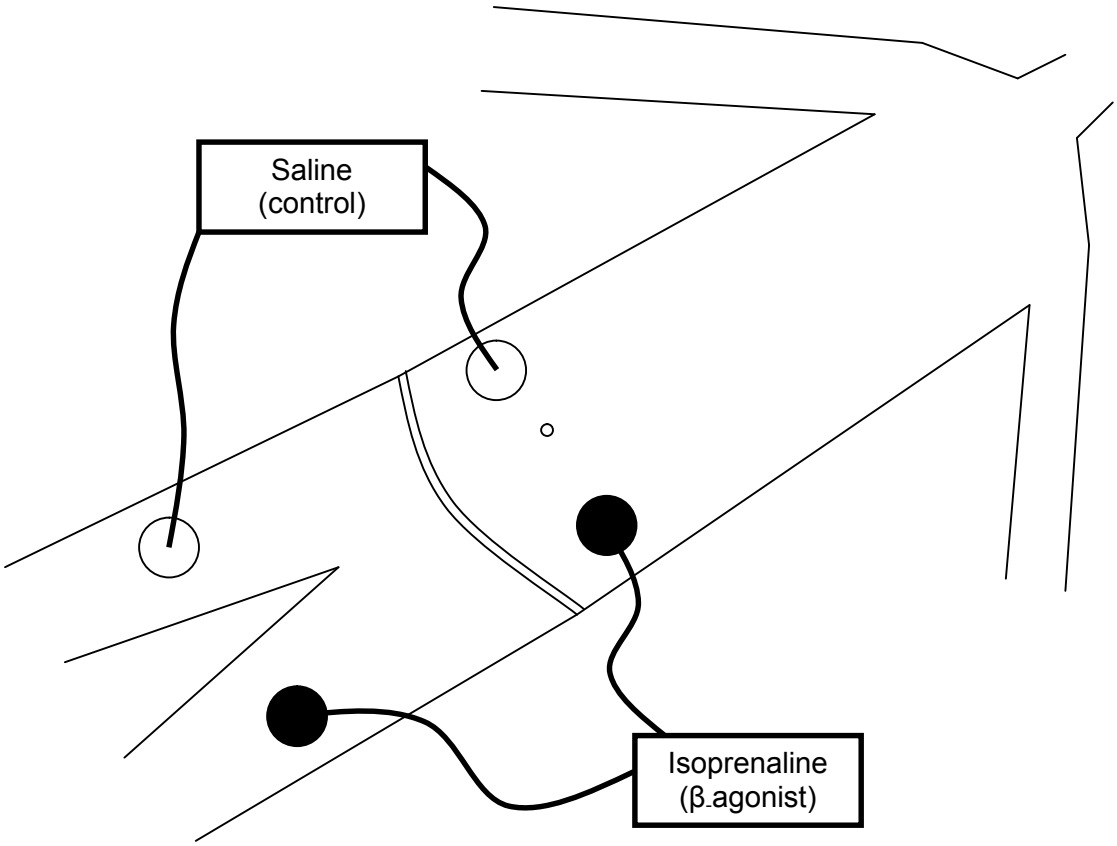

Figure 3.1: Pharmacological agents used in the microinfusion study. Isoprenaline was given in incremental doses and a 75 g glucose drink was given after 120 min of isoprenaline microinfusion.

3.2.2 Results: metabolic and haemodynamic parameters

The local microinfusion of isoprenaline for 120 min had no effects on systemic glucose, insulin, NEFA and TG concentrations (Figures 3.2-3.4). Furthermore, the basal heart rate (HR) of 63±2 bpm did not change significantly after 120 min of isoprenaline microinfusion (data not shown). This underlines the absence of any systemic effects of isoprenaline microinfusion. As expected, the ingestion of glucose had profound effects on metabolic and haemodynamic parameters (Figures 3.2-3.5). Plasma glucose doubled to a maximum of 9.5±0.4 mmol.l^{-1} at 60 min after ingestion. This was accompanied by a concomitant rise in plasma insulin (Figure 3.2). Probably as a result of the increased insulin concentration, systemic plasma NEFA concentrations were suppressed rapidly after glucose ingestion (Figure 3.3). The plasma TG concentration remained unchanged after oral glucose (Figure 3.4). Glucose ingestion resulted in a significant sustained increase in HR ($p<0.05$ for post-glucose vs. basal and for post-glucose vs. 120 min isoprenaline) (Figure 3.5).

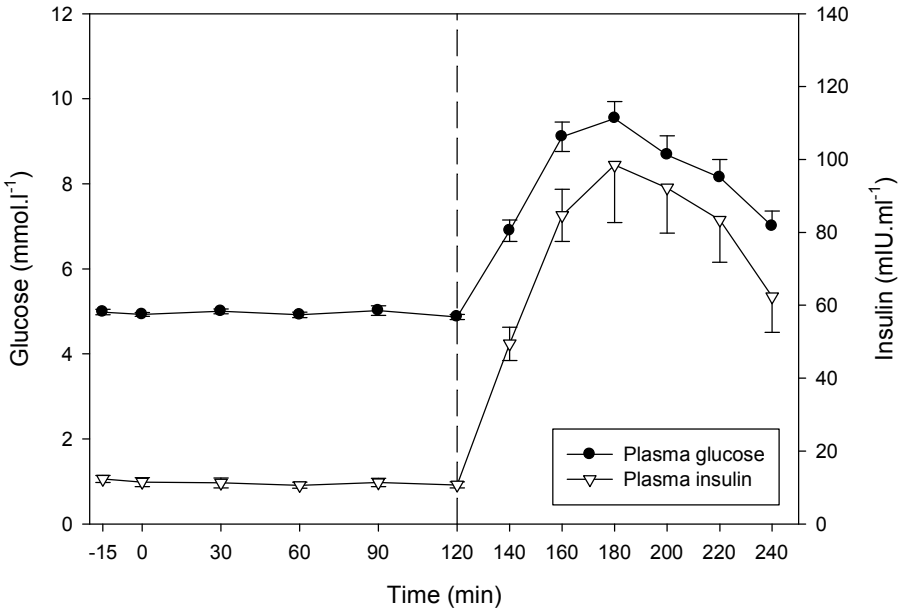

Figure 3.2: Systemic glucose and insulin responses during adipose tissue isoprenaline microinfusion (starting at 0 min). A 75 g glucose drink was given at 120 min.

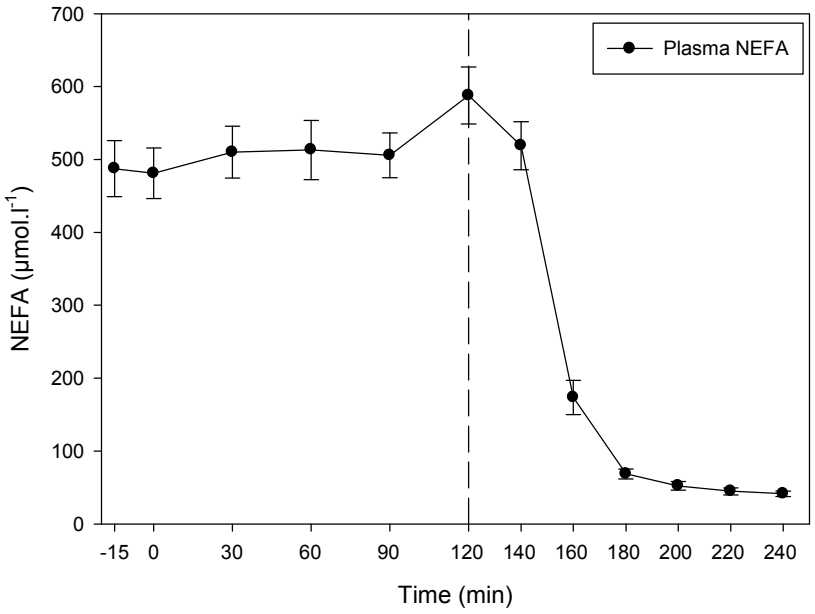

Figure 3.3: Systemic NEFA response during adipose tissue isoprenaline microinfusion (starting at 0 min). A 75 g glucose drink was given at 120 min.

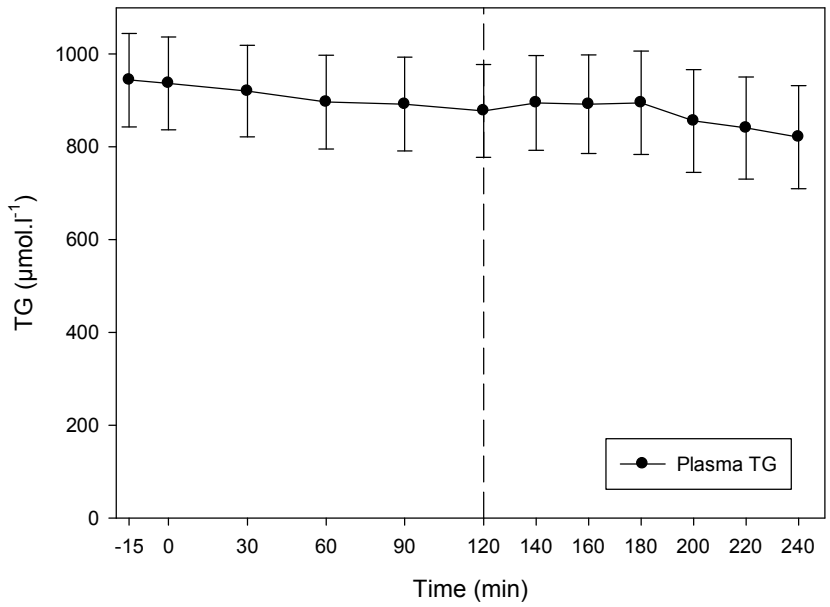

Figure 3.4: Systemic TG response during adipose tissue isoprenaline microinfusion (starting at 0 min). A 75 g glucose drink was given at 120 min.

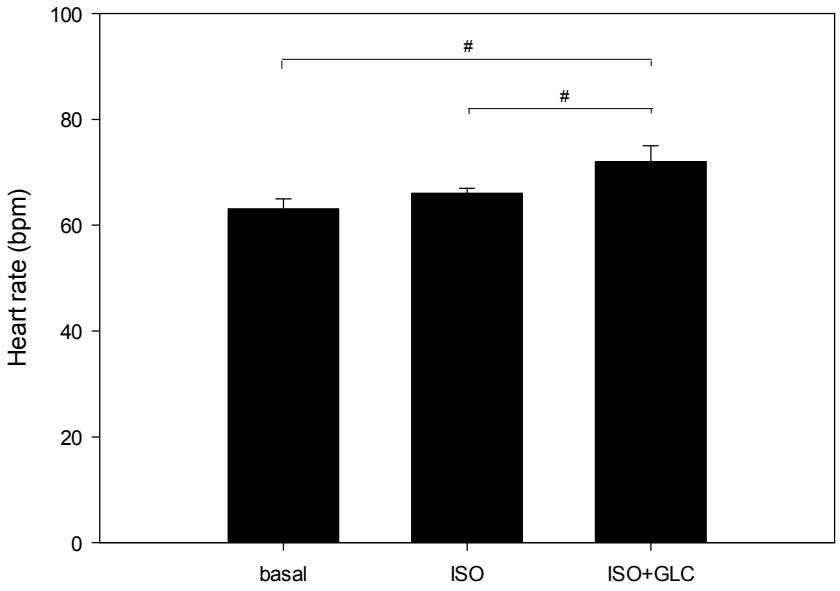

Figure 3.5: Heart rate before (basal), after 120 min of isoprenaline microinfusion (ISO) and 2h after a 75g glucose drink (ISO+GLC) ($^{\#}p<0.05$).

3.2.3 Results: Effects on ATBF

In SAL sites (Figure 3.6), fasting ATBF remained stable in abdominal and femoral adipose tissue, whereby femoral ATBF was lower than abdominal ATBF (ANOVA $p<0.05$ between fat depots). After the ingestion of glucose, ATBF increased markedly in both depots, up to a maximum 8.7±1.4 in the abdomen and 8.1±1.0 $ml.min^{-1}.100g$

tissue^{-1} in femoral adipose tissue (ANOVA $p<0.001$ for time, $p<0.05$ between fat depots, not statistically significant for time x site interaction).

Basal abdominal and femoral ATBF showed a strong negative correlation to BMI (Pearson r=-0.75 and -0.62 respectively, $p<0.05$). Abdominal basal ATBF was also negatively correlated to WHR (Pearson r=-0.56, $p<0.05$). The maximum ATBF response to glucose (at 180 min) correlated strongly between abdominal and femoral adipose tissue (Pearson r=0.63, $p<0.05$). There was a negative correlation between the maximum abdominal ATBF response to glucose and BMI and WHR (Pearson r=-0.64 and -0.58 respectively, $p<0.05$). The femoral ATBF response to glucose correlated negatively with WHR (Pearson r=-0.7, $p<0.05$). Some of these correlations were dependent on sex, as one would expect given the strong influence of sex on regional fat distribution. However, the negative relationship between basal abdominal ATBF and BMI, and the negative correlation between femoral ATBF response to glucose and WHR were independent of sex (Pearson r=-0.79 and -0.69 respectively; $p<0.05$ with sex as the controlling variable).

In ISO sites, ATBF increased dose-dependently in response to isoprenaline in both adipose tissue depots (Figure 3.7; ANOVA $p<0.001$ compared to basal). After 40 min of high-dose microinfusion of isoprenaline (10^{-4} M), femoral ATBF had increased almost four-fold from baseline, compared to abdominal ATBF which had increased a little more than two-fold. However, the actual ATBF response at the end of each isoprenaline microinfusion step was similar between the two depots (Figure 3.8). After glucose ingestion, ATBF continued to increase in both abdominal and femoral adipose tissue, before slowly declining towards lower levels. ATBF did not return to basal levels, given that the isoprenaline microinfusion continued up to the end of each study.

The maximal abdominal and femoral ATBF during isoprenaline microinfusion (at 120 min) correlated positively (Pearson r=0.59, $p<0.05$). There was a strong negative correlation between BMI and the maximal abdominal and femoral ATBF during isoprenaline (Pearson r=-0.76 and -0.59 respectively; $p<0.05$). The negative relationship between abdominal ATBF and BMI remained after controlling for sex (Pearson r=-0.74, $p<0.05$).

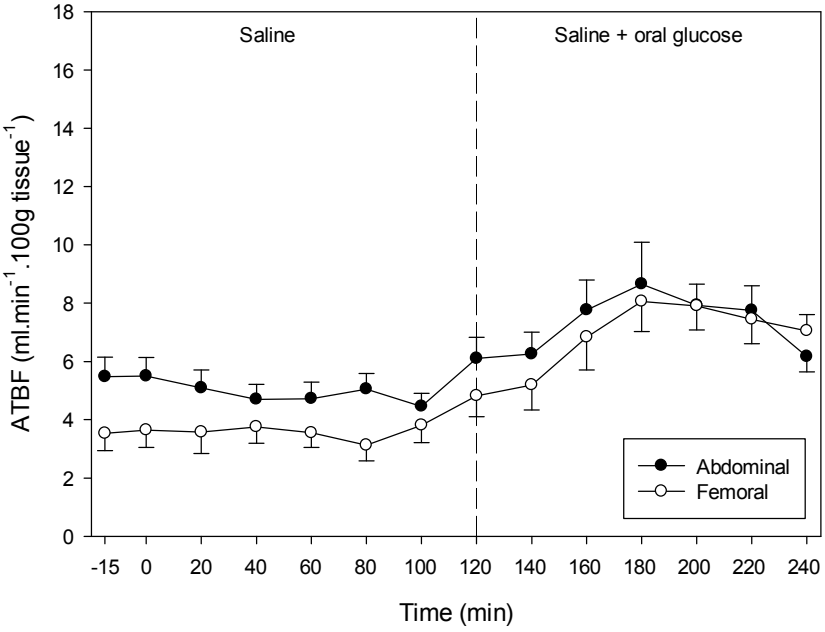

Figure 3.6: Abdominal and femoral ATBF during microinfusion of saline. A 75 g glucose drink was given at 120 min.

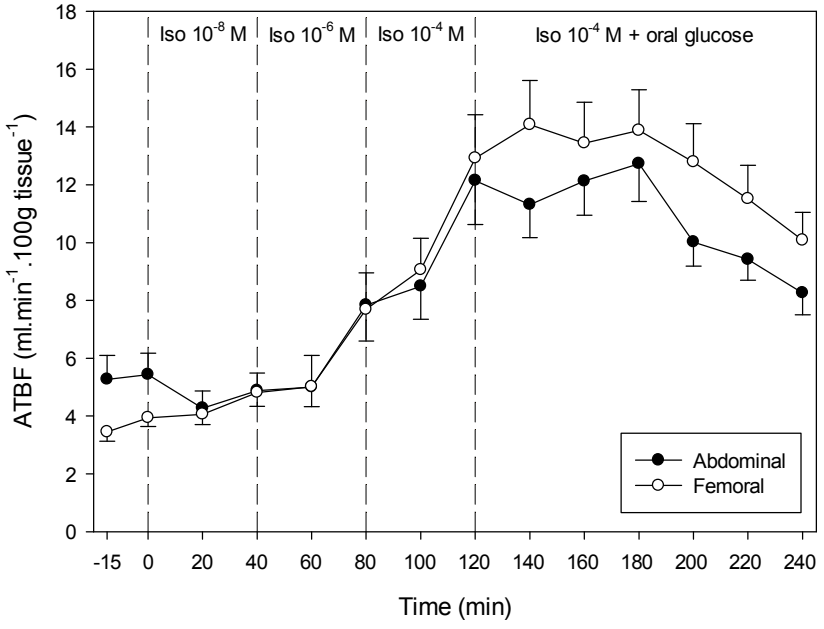

Figure 3.7: Abdominal and femoral ATBF during incremental microinfusion of isoprenaline. A 75 g glucose drink was given at 120 min and microinfusion was continued with isoprenaline 10^{-4} M.

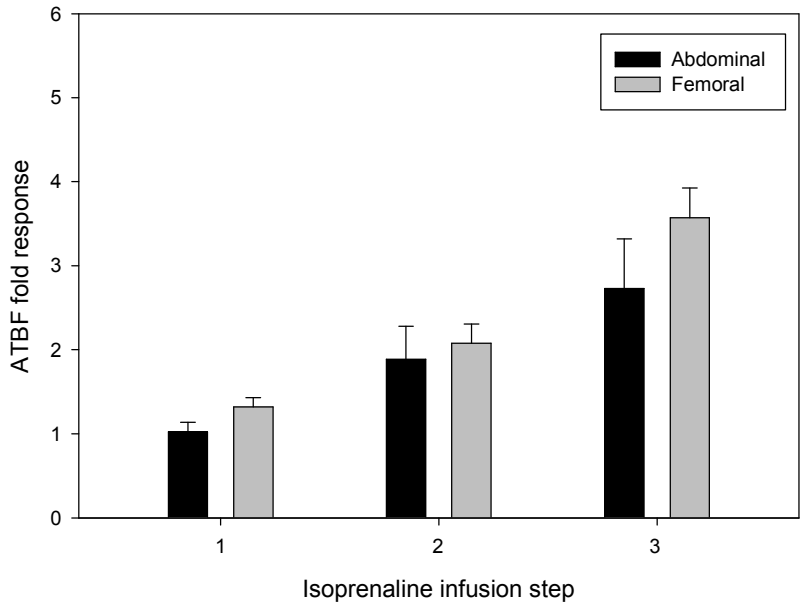

Figure 3.8: Abdominal and femoral ATBF response (expressed as fold change from basal) during incremental microinfusion of isoprenaline (Infusion steps 1=10^{-8} M, 2=10^{-6} M, 3=10^{-4} M).

3.3 Effects on ATBF and lipolysis during systemic non-selective β-adrenoceptor stimulation

3.3.1 Study design and participants

In the previous study I established that local non-selective β-adrenoceptor stimulation resulted in a similar ATBF response in abdominal and femoral adipose tissue. The microinfusion study did not allow for the study of lipolysis and I therefore investigated the effect of a systemic isoprenaline infusion with the AV difference technique. The following methods were used:

- Recruitment of participants using the OBB (see Section 2.7.1)
- Measurement of baseline anthropometric characteristics, including total body and regional fat mass with DXA (see Section 2.7.2)
- Systemic infusion of isoprenaline (see Section 2.3.1)
- Measurement of ATBF with the ^{133}Xe washout technique (see Section 2.1.1)
- Measurement of fatty acid trafficking with the AV difference technique (see Section 2.2)
- Infusion of a stable isotope tracer for measurement of regional NEFA release (see Section 2.4.1)

Healthy young volunteers (n=7, 5 male; median age 39.0, range 24-43) were recruited. The median BMI was 25.7 $kg.m^{-2}$ (range 21.2-27.0 $kg.m^{-2}$) and the median WHR was 0.95 (range 0.72-1.00). Further details of the participants are shown in Table 3.2.

The participants arrived after an overnight fast and four cannulas were inserted as described before (see Section 2.2). In brief, an arterial catheter was inserted into the femoral artery and two venous catheters were placed in the superficial epigastric and the saphenous vein respectively to obtain drainage from subcutaneous abdominal and femoral adipose tissue. An additional cannula was inserted in an antecubital vein for infusion purposes. After taking a basal blood sample for background enrichment, a [$^2H_2$]-palmitate infusion was started at an infusion rate of 0.03 $\mu mol.min^{-1}.kg$ body $weight^{-1}$. ^{133}Xe was injected in abdominal and femoral adipose tissue and ATBF was measured throughout the study. After 60 min of equilibration, a one-step systemic infusion of isoprenaline was started for 60 min (infusion rate 25 $ng.min^{-1}.kg\ FFM^{-1}$). Blood samples were taken simultaneously from all three sites at frequent intervals. After termination of the isoprenaline infusion, blood samples were taken for further 60 min.

Table 3.2: Baseline anthropometric and metabolic characteristics of subjects

	Male (n=5)	Female (n=2)
WHR	0.96 (0.92-1.0)	0.75 (0.72-0.79)[§]
Body fat %	24.7 (22.8-29.3)	33.6 (29.9-37.4)*
Fasting TG (µmol/l)	919 (442-1284)	488 (375-601)
Fasting NEFA (µmol/l)	461 (377-836)	661 (659-664)
Fasting glucose (mmol/l)	5.4 (5.3-5.9)	5.3 (5.3-5.3)
Fasting insulin (mIU/l)	11.6 (9.0-14.6)	21.1 (14.9-27.3)*

([§]p=0.001 and *p<0.05 females compared to males; median and range shown)

3.3.2 Results: metabolic and haemodynamic parameters

Isolated non-selective β-adrenoceptor stimulation is known to stimulate pancreatic insulin secretion (203). In the present study, basal insulin concentration was 14.4±2.3 $mIU.l^{-1}$ and increased to a maximum of 24.8±3.1 $mIU.l^{-1}$ at 30 min of infusion before returning to basal levels after the end of the isoprenaline infusion (Figure 3.9).

Isoprenaline infusion showed no effect on plasma glucose concentrations, which remained stable around a basal plasma glucose concentration of 5.5±0.1 mmol.l^{-1}.

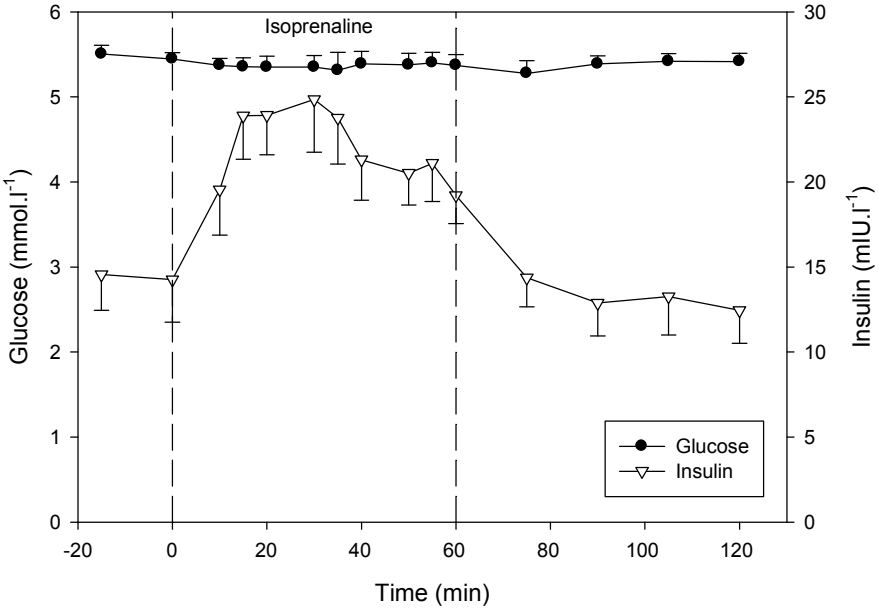

Figure 3.9: Plasma glucose and insulin responses during systemic isoprenaline infusion (20 ng.min^{-1}.kg FFM^{-1}; from 0 to 60 min).

Systemic plasma NEFA concentrations rose markedly in the first 20 min of isoprenaline infusion ($p<0.001$ compared to basal), in line with the expected increase in whole-body lipolysis (Figure 3.10). Systemic plasma NEFA declined slowly after their peak at 20 min, most likely because of desensitization, and reached basal concentrations rapidly after the end of infusion.

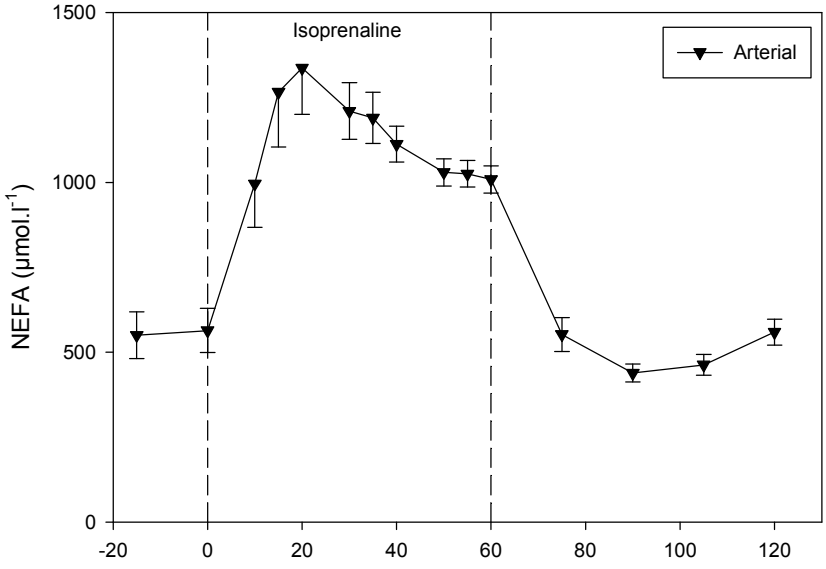

Figure 3.10: Arterial plasma NEFA response during systemic isoprenaline infusion (20 ng.min^{-1}.kg FFM^{-1}; from 0 to 60 min).

Systemic TG concentrations did not change during the isoprenaline infusion and remained stable around a basal mean of 784±128 µmol/l (Figure 3.11). AV differences for abdominal and femoral TG were small and inconsistent throughout the study (not shown).

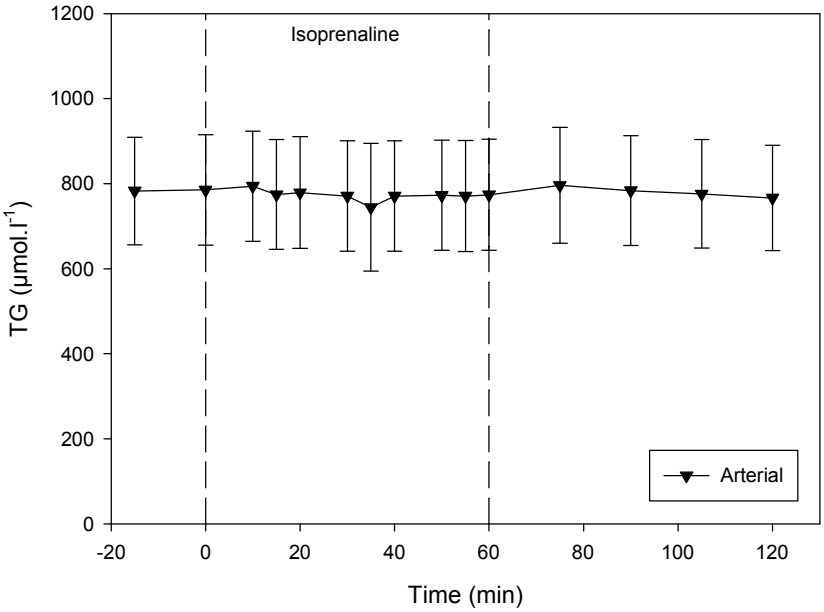

Figure 3.11: Arterial TG concentrations during systemic isoprenaline infusion (20 ng.min^{-1}.kg FFM^{-1}; from 0 to 60 min).

The participants' HR increased during the isoprenaline infusion by about 22 bpm ($p<0.001$ compared to basal; Figure 3.12). Systolic blood pressure rose by about 20 mmHg ($p<0.01$ compared to basal) and diastolic blood pressure decreased slightly by about 4 mmHg ($p=0.05$ compared to basal; Figure 3.13).

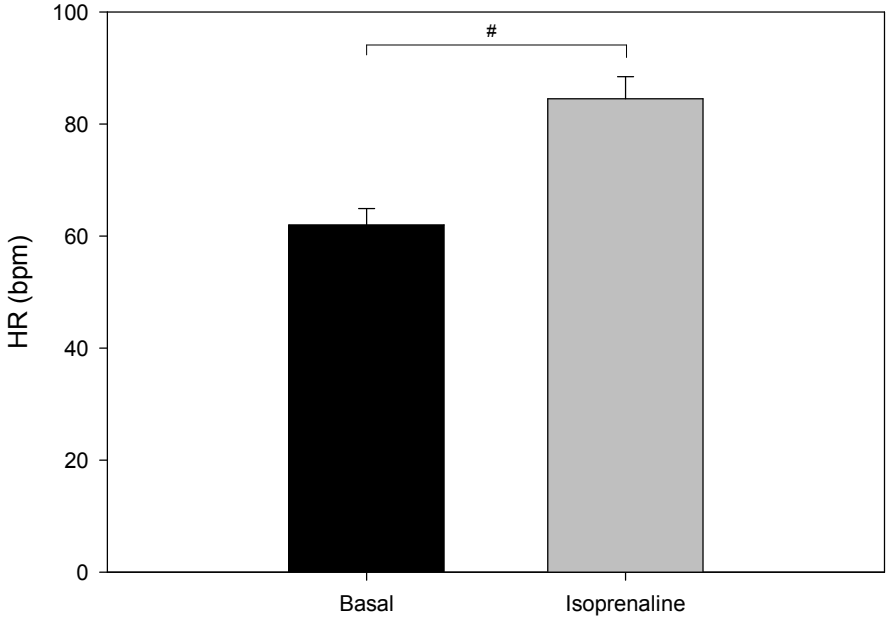

Figure 3.12: Heart rate before and after 60 min of isoprenaline infusion (#p<0.001).

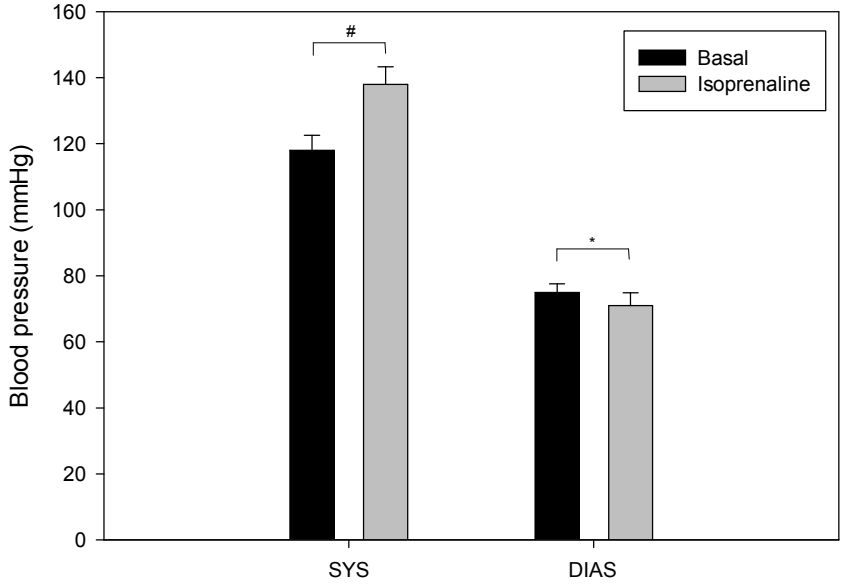

Figure 3.13: Systolic (SYS) and diastolic (DIAS) blood pressure before and after 60 min of isoprenaline infusion (*p=0.05, #p<0.001).

3.3.3 Results: Regional ATBF response

As shown by local microinfusion, non-selective β-adrenoceptor stimulation with isoprenaline results in a similar dose-response in both abdominal and femoral ATBF (see Section 3.2.3). Systemic isoprenaline infusion had similar effects on regional ATBF (ANOVA p<0.001 for time effect, no site interaction; see Figure 3.14). Within

20 min after the start of the infusion, abdominal ATBF increased almost 4-fold from basal. Similarly, femoral ATBF increased 3.5-fold from baseline. After the first 20 min, abdominal ATBF started declining – most likely due to desensitization. In contrast, femoral ATBF remained elevated between 4- and 3.5-fold from baseline ($p<0.05$ for response comparison between sites at 40 min; see Figure 3.15). Over the 60 min period of the infusion, abdominal and femoral ATBF responses were comparable (AUC abdominal ATBF 10.1±2.1 $ml.min^{-1}.100g\ tissue^{-1}$ vs. femoral ATBF 11.3±2.2 $ml.min^{-1}.100g\ tissue^{-1}$). After the end of isoprenaline infusion, abdominal and femoral ATBF returned rapidly to baseline.

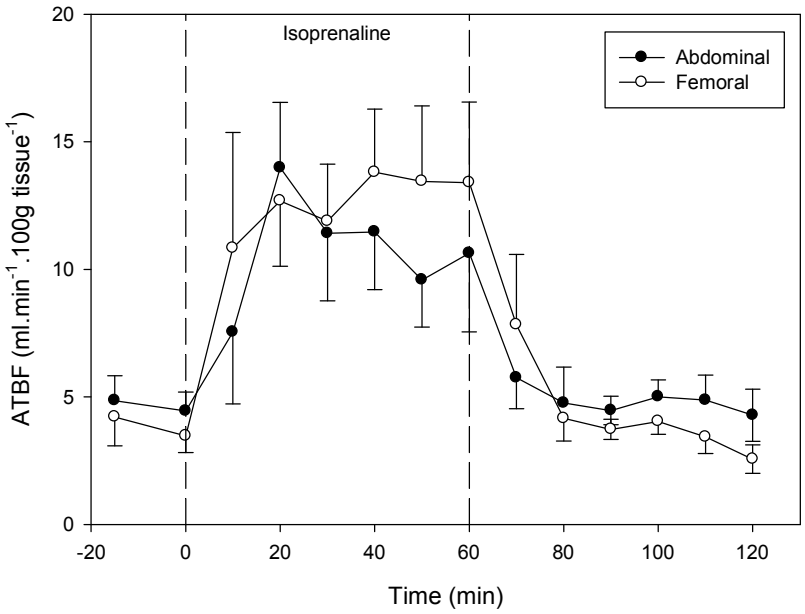

Figure 3.14: Abdominal and femoral ATBF during systemic isoprenaline infusion (20 $ng.min^{-1}.kg\ FFM^{-1}$; from 0 to 60 min).

Basal abdominal and femoral ATBF were positively correlated (Pearson r=0.8, $p<0.05$). The maximal ATBF response to isoprenaline (at 20 min), as well as the total response to isoprenaline (calculated as AUC) did not correlate between abdominal and femoral adipose tissue. There was a strong negative correlation between femoral response to isoprenaline (both absolute ATBF at 20 min and AUC for the total infusion period), BMI and WHR (Pearson r=-0.9 and -0.95, $p<0.05$ and $p=0.001$ respectively). However, this association was not independent of sex – most likely due to the sex-specific effects on fat distribution as discussed above.

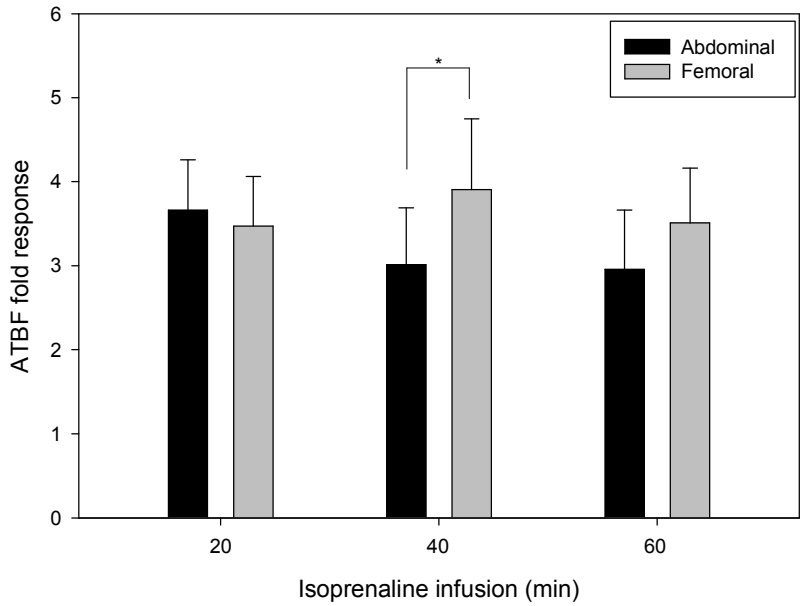

Figure 3.15: Abdominal and femoral ATBF responses (expressed as fold change from baseline) during systemic isoprenaline infusion (20 ng.min^{-1}.kg FFM^{-1}) (*p<0.05).

3.3.4 Results: Regional fatty acid trafficking

Systemic β-adrenoceptor stimulation with isoprenaline resulted in a significant increase in whole body NEFA concentrations, indicating increased lipolysis. Both abdominal and femoral adipose tissue contributed to the systemic NEFA concentrations by significantly increasing NEFA release during isoprenaline stimulation (ANOVA p<0.001 for time effect; Figure 3.16). There were differences in the dynamics of the responses between abdominal and femoral adipose tissue (ANOVA p<0.05 for site difference). Femoral adipose tissue displayed a lower basal lipolytic rate per unit tissue compared to abdominal adipose tissue (Wilcoxon p<0.05). The femoral adipose tissue response to isoprenaline stimulation was lower and seemed somewhat delayed compared with abdominal adipose tissue (ANOVA p<0.05 for time x site effect). However, when the femoral lipolysis response was expressed as a change from baseline, it was comparable to the abdominal adipose tissue response (Figure 3.17).

Abdominal and femoral NEFA release were not correlated with each other and basal NEFA release was not correlated to BMI or WHR. Femoral NEFA release response (AUC) correlated with hip circumference (Pearson r=0.755, p=0.05). This correlation disappeared when controlled for sex. Overall, correlations were weak given the small number of participants and the skewed distribution between sexes.

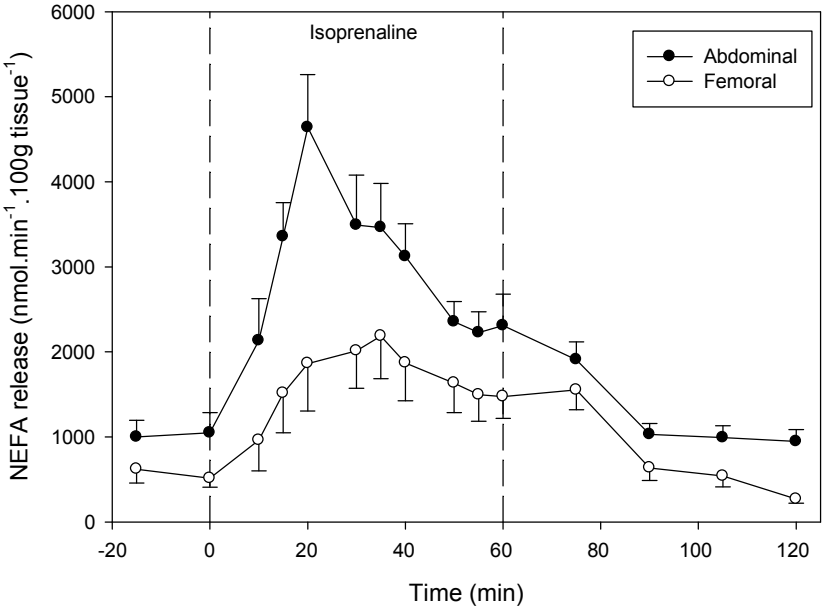

Figure 3.16: Abdominal and femoral NEFA release during systemic isoprenaline infusion (20 ng.min^{-1}.kg FFM^{-1}; from 0 to 60 min).

Extraction of plasma-TG and uptake of glucose across abdominal and femoral adipose tissue were not significant (data not shown), given the constant concentration shown in Figure 3.11.

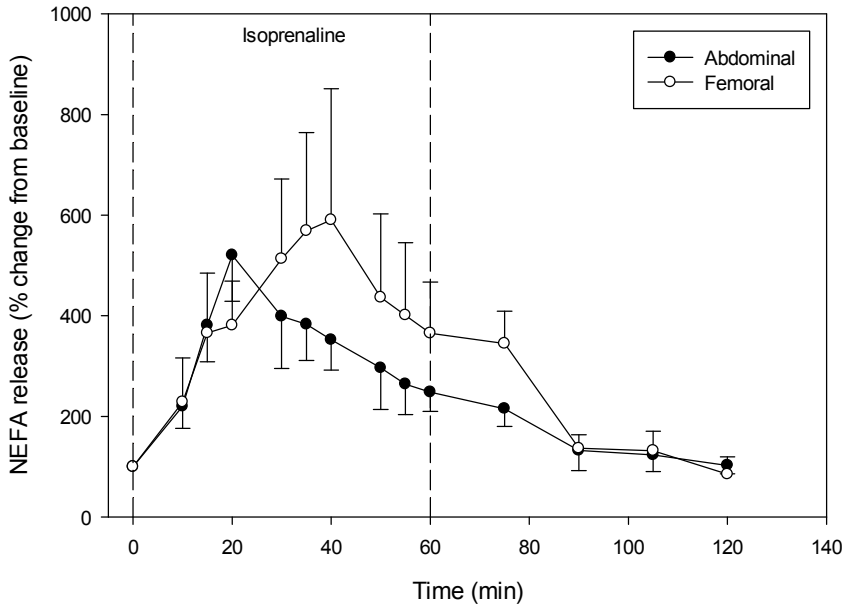

Figure 3.17: Abdominal and femoral NEFA release expressed as % change from baseline in response to systemic isoprenaline infusion (20 ng.min^{-1}.kg FFM^{-1}; from 0 to 60 min).

3.3.5 Results: Regional metabolic isotope data

By applying the stable isotope tracer technique it is possible to calculate the rate of appearance of NEFA (Ra_{NEFA}) on a whole-body level, as well as regionally (abdominal/femoral adipose tissue Ra_{NEFA}) (see Section 2.6.2). The isotopic data reflect the increase in whole-body lipolysis during systemic β-adrenoceptor stimulation (Figure 3.18). Basal Ra_{NEFA} doubled within 20 min after the start of isoprenaline infusion ($p=0.001$ for comparison to basal). From there, Ra_{NEFA} decreased steadily during the remaining duration of the infusion, and returned to basal levels after the end of infusion. Abdominal and femoral Ra_{NEFA} increased similarly during isoprenaline infusion but showed a difference in the magnitude of the response. Basal abdominal Ra_{NEFA} increased four-fold within 20 minutes after the start of infusion (Figure 3.19). Femoral Ra_{NEFA} increased two-fold in the same time period (ANOVA $p<0.05$ for time effect, statistically not significant for difference between sites). In both depots, signs of desensitization were seen. Abdominal Ra_{NEFA} decreased steadily and femoral Ra_{NEFA} levelled out during the remainder of the infusion. Note the difference in the level of magnitude between whole-body and regional Ra_{NEFA}, and that regional Ra_{NEFA} were normalised per unit of tissue.

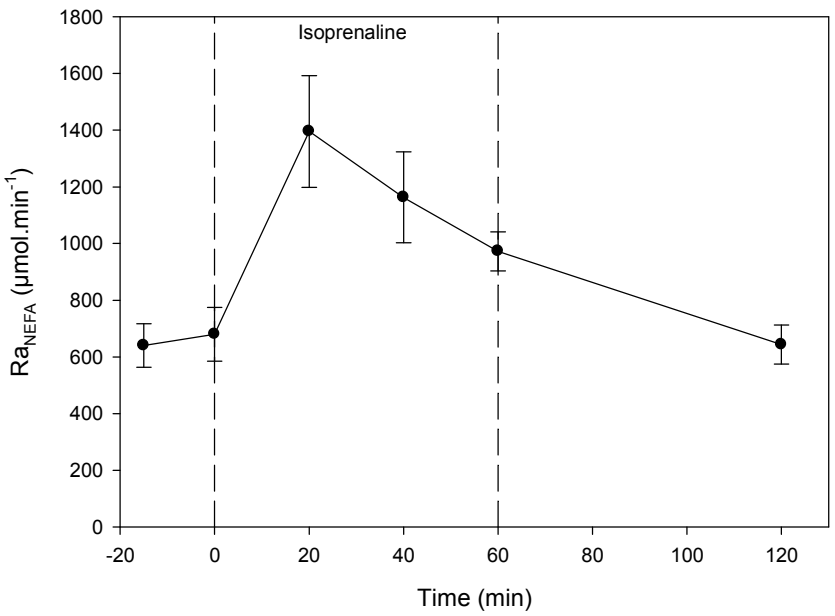

Figure 3.18: Whole-body Ra_{NEFA} during systemic isoprenaline infusion (20 ng.min^{-1}.kg FFM^{-1}; from 0 to 60 min).

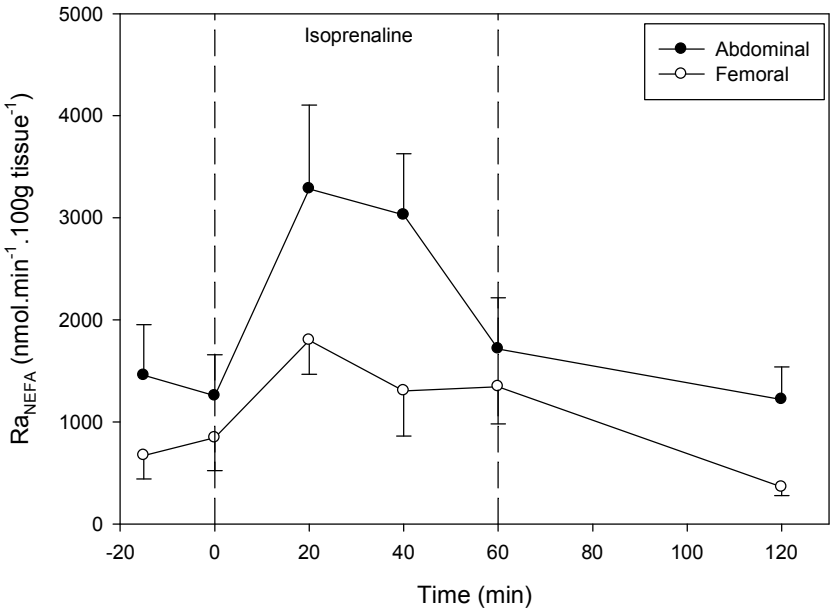

Figure 3.19: Regional Ra_{NEFA} during systemic isoprenaline infusion (20 ng.min^{-1}.kg FFM^{1}; from 0 to 60 min).

3.4 Results: sex differences

I compared the basal, glucose- and isoprenaline-dependent ATBF-response in the microinfusion study. Abdominal ATBF responses did not differ between sexes and conditions, and the femoral ATBF response to glucose was similar in men and women (data not shown). However, women showed a higher increase in ATBF during local non-selective β-adrenoceptor stimulation with isoprenaline (ANOVA $p<0.05$) (Figure 3.20). This was confirmed in the systemic isoprenaline infusion study, although the results have to be interpreted with caution, given the small subgroups (women n=2) (Figure 3.21). There were no sex differences between regional NEFA release rates during isoprenaline infusion (data not shown).

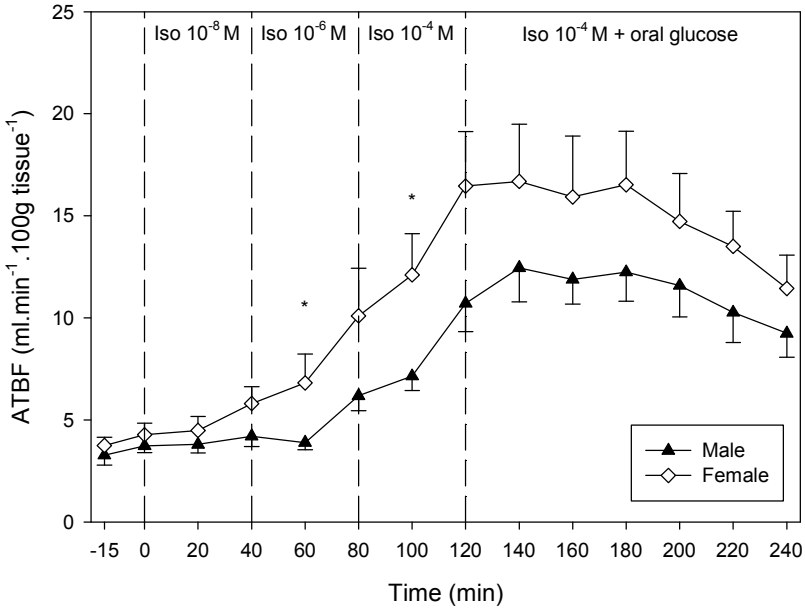

Figure 3.20: Femoral ATBF response in men and women during local isoprenaline microinfusion (*p<0.05). A 75 g glucose drink was given at 120 min.

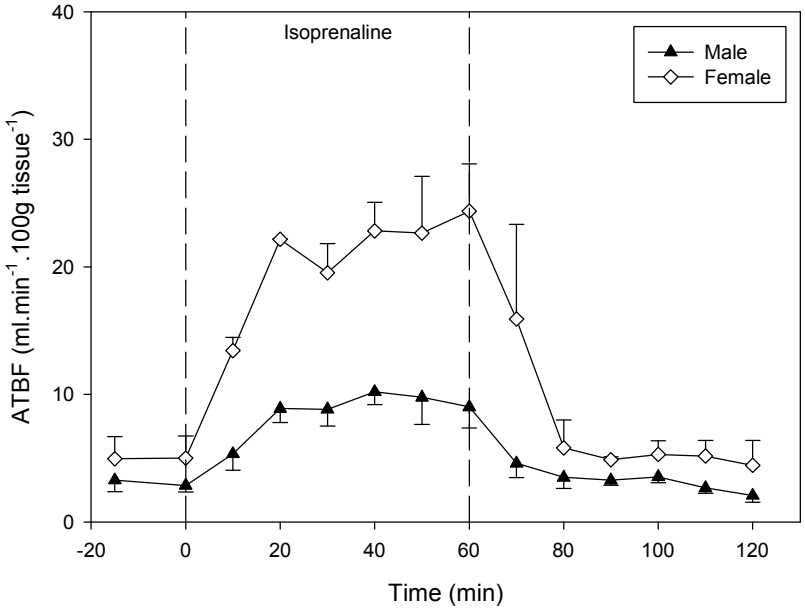

Figure 3.21: Femoral ATBF response in men and women during systemic isoprenaline infusion (20 ng.min^{-1}.kg FFM^{-1}; from 0 to 60 min).

3.5 Discussion

In this Chapter I confirmed some basic concepts about regional adipose tissue metabolism. Basal femoral ATBF is lower than abdominal ATBF (see Figure 3.6), as is the basal femoral lipolytic rate (see Figure 3.16). This confirms a recent report that

showed a lower femoral adipose tissue metabolic activity (106). Strong inverse relationships were found between measures of regional adiposity and local ATBF and lipolysis responses to β-adrenoceptor stimulation. Increased body fat mass, expressed in a raised BMI, and abdominal obesity, expressed in a high WHR, were negatively correlated both to basal and β-adrenoceptor-dependent adipose tissue metabolic activity. This is much in line with the current hypothesis of down-regulation of adipose tissue fatty acid trafficking in obesity reported recently (114). Given the health implications of a raised BMI and WHR, decreased β-adrenoceptor-dependent fatty acid trafficking could be a determinant of metabolic disease.

In this Chapter I provide evidence that non-selective β-adrenoceptor stimulation is an important factor in regional lipolysis *in vivo*. Furthermore, ATBF and lipolytic responses to β-adrenoceptor stimulation were similar in abdominal and femoral adipose tissue.

The ATBF response to local and systemic stimulation with isoprenaline showed no differences between abdominal and femoral adipose tissue. The femoral ATBF response during systemic isoprenaline infusion suggested in fact that there is some increased femoral responsiveness compared to abdominal adipose ATBF (see Figure 3.15). It is interesting to note that the ATBF response seen during systemic isoprenaline infusion was similar to that seen during local microinfusion with 10^{-4} M of isoprenaline (see Figures 3.7 and 3.14). ATBF is partly determined by the vasodilatating effect of β-adrenoceptors (18). Despite the difference in the mode of isoprenaline delivery (local microinfusion vs. systemic infusion), it appears that maximal β-adrenoceptor stimulation was reached in both cases and was the limiting factor in ATBF response. This is supported by the desensitization effects seen. Desensitization is known to occur when adrenoceptors are maximally stimulated over prolonged periods of time (204).

The addition of a sympathetic stimulus, in form of a glucose drink, during the microinfusion studies did not lead to a further increase of ATBF (Figure 3.7). As above, this probably reflects maximal β-adrenoceptor stimulation during the final stage of local isoprenaline microinfusion, before the glucose drink. Sympathetic activation includes also an α-adrenergic effect, which should result in a reduction of ATBF. Indeed, the slow decline in ATBF observed after glucose ingestion (Figures 3.6 and 3.7) could be a sign of the α-adrenoceptor stimulation as part of the postprandial sympathetic activation. The fact that this was seen in both the SAL and

ISO sites starting at 180 min into the experiment supports that this is an α-adrenergic effect rather than desensitization.

The effects of glucose on the sympathetic nervous system are also seen in the cardiovascular data gathered during the microinfusion study (Figure 3.5). The observed sustained increase in HR is recognised as a direct insulin effect on the sympathetic nervous system (205).

Interestingly, plasma TG concentration remained unchanged after glucose ingestion (Figure 3.4). The TG measured in the fasting state are contained mostly in liver-derived VLDL particles. Hepatic VLDL production has been shown to decrease when the liver is exposed to insulin only (206), but to remain unaffected when a glucose stimulus triggers the insulin response (207).

With regards to lipolysis, both abdominal and femoral adipose tissue responded to β-adrenoceptor stimulation with an increase in lipolytic rate. Per unit fat mass, femoral lipolysis remained lower than abdominal. However, lipolytic responses in both adipose tissue depots were comparable in terms of change from baseline (see Figure 3.17). The fact that the femoral and abdominal ATBF responses per unit fat mass were similar suggests a differential distribution of β-adrenoceptors between adipose tissue vasculature and adipocytes.

My data are in contrast to the data of Jensen *et al.*, who did not find any lipolytic response in leg fat during isoprenaline stimulation in women (112). As already discussed in the introduction of this Chapter, this might be a result of the low isoprenaline dose used and the relatively crude measurement of regional lipolysis as opposed to the very specific AV difference technique used here.

Lipolysis studies *in vitro* suggest a negative relationship between obesity and regional adipocyte lipolysis (166, 196-198). My data suggest a positive relationship between gluteofemoral fat mass and β-adrenoceptor-dependent lipolysis. Increased metabolic activity of femoral adipose tissue could therefore be a determinant of metabolic health. However, my studies were not designed to compare responses between lean and obese, and the small number of participants covered only a narrow range of adiposity. It is suspected that the relationships discussed in this Chapter

would be much stronger if studied in large participant numbers and in the extreme ends of the fat distribution spectrum.

My data show an increased ATBF response to β-adrenoceptor stimulation in femoral adipose tissue in women (Figures 3.20 and 3.21). This finding suggests that female femoral adipose tissue displays a higher sensitivity to non-selective β-adrenoceptor stimulation compared to males. Studies on isolated adipocytes showed similar β-adrenoceptor density between men and women, but a higher α_2-adrenoceptor density/activity in female adipocytes (108, 202). The differences in β-adrenoceptor response shown here could suggest a compensatory mechanism for the higher α_2-adrenoceptor density/activity described. Interestingly, differential responsiveness to β-adrenoceptor stimulation appears to be confined to the femoral vascular bed, given that no differences were seen between men and women with regards to lipolysis.

The data in this Chapter confirm that β-adrenoceptors are important determinants of regional ATBF and lipolysis *in vivo*. However, selective stimulation of β-adrenoceptors does not occur in the human body. A comparison of responses to non-selective adrenergic stimulation with adrenaline (which is the physiological stimulus *in vivo*) between adipose tissue depots and the effect of genetic β-adrenoceptor haplotypes are described in the next Chapter.

4 Regional fat metabolism during non-selective adrenergic stimulation with adrenaline

4.1 Introduction

In the previous Chapter I described the adipose tissue effects of non-selective β-adrenoceptor stimulation with isoprenaline, and established that β-adrenergic stimulation is an important determinant of ATBF and lipolysis. However, under physiological conditions isolated β-adrenoceptor stimulation does not occur in the human body. In contrast, catecholamines bind to both α- and β-adrenoceptors, and tissue effects depend on the balance between adrenoceptor subtypes (see Section 1.2.3). With regards to adipose tissue, adrenoceptors and catecholamine effects on adipose tissue physiology have been studied extensively in the past. As discussed in Section 3.1, abdominal adipocytes were found to have a higher β-adrenoceptor density than gluteal adipocytes, resulting in higher lipolytic rates during adrenaline stimulation *in vitro* (108). When studied *in vivo*, a systemic adrenaline infusion increased abdominal ATBF and NEFA release (133). Comparing men and women, adrenaline increased NEFA release from abdominal adipose tissue in both, but leg NEFA release only in men (113). When lean and obese women were compared using the microdialysis technique, adrenaline increased abdominal and femoral ATBF in both, although the abdominal ATBF response was blunted in the obese group (111). The same study found that adrenaline resulted in an increase of whole body Ra_{NEFA} and abdominal and femoral glycerol release, as measured by microdialysis. Again, the glycerol release response in abdominal adipose tissue was blunted in obesity.

To date, there are suggestions from *in vitro* studies that abdominal and femoral adipose tissue respond differently to catecholamines, but it is less clear whether these regional differences persist *in vivo*. Furthermore, it is unclear whether differences in the responses to adrenergic stimulation are a determinant of the metabolic health effects associated with femoral adipose tissue. With the exception of Jensen *et al.* (113), no physiological studies comparing the two adipose tissue depots have been reported. As discussed in Section 3.1, the methodology used by Jensen is less specific than the highly selective AV difference technique. The aim of the current study was to measure abdominal and femoral ATBF and lipolysis in response to non-selective adrenergic stimulation with adrenaline in men and women.

I also aimed to study the effects of haplotypic variation of the *ADRB2* gene *in vivo*. As discussed in Section 1.2.4, different *ADRB2* haplotypes are known to affect β_2-adrenergic sensitivity of adipocytes *in vitro* (45), but no studies of *in vivo* effects exist to date. Finally, sex-specific differences in regional ATBF and lipolysis rates which may contribute to the male/female pattern of fat distribution were investigated.

4.2 Study design and participants

The following methods were used in this study:

- Participant recruitment using the OBB and a recruitment-by-genotype approach (see Section 2.7.1)
- Measurement of baseline anthropometrics, including total body and regional fat mass with DXA (see Section 2.7.2)
- Systemic infusion of adrenaline (see Section 2.3.2)
- Measurement of ATBF with the ^{133}Xe washout technique (see Section 2.1.1)
- Measurement of fatty acid trafficking with the AV difference technique (see Section 2.2)
- Infusion of a stable isotope tracer for measurement of whole body and regional NEFA release (see Section 2.4.1)
- Collection of abdominal and femoral adipose tissue biopsies for RNA extraction and adrenoceptor expression analysis (see Section 2.8.1)

Recruitment aimed to recruit carriers of the three most common *ADRB2* haplotypes, in order to study haplotype effects *in vivo* (this is discussed in more detail in Section 4.3.6). For the purposes of the study of regional fatty acid trafficking during adrenaline stimulation, all participants were studied in one group. The team members carrying out the studies, including myself, were blinded as to the participants' genotype until all data analysis was completed.

A total n=28 was recruited (14 male, median age 45.5, range 30-59). The median BMI was 24.1 kg.m^{-2}, range 21.5-39.3 kg.m^{-2}, and the median WHR was 0.92, range 0.78-1.05. Further details of the participants are shown in Table 4.1.

Table 4.1: Baseline anthropometric and metabolic characteristics of subjects

	Male (n=14)	Female (n=14)
WHR	0.94 (0.85-1.05)	0.90 (0.78-0.99)*
Body fat %	26.6 (17.3-33.3)	35.6 (20.7-50.4)§
Fasting TG (μmol/l)	1001 (403-1588)	731 (215-1334)
Fasting NEFA (μmol/l)	514 (348-1084)	672 (417-1012)
Fasting glucose (mmol/l)	5.2 (4.8-6.6)	5.0 (4.4-5.6)*
Fasting insulin (mIU/l)	11.8 (7.1-20.8)	10.0 (3.8-16.8)

(§p=0.001 and *p<0.05 females compared to males; median and range shown)

The participants arrived after an overnight fast and remained fasting throughout the study. As described in Section 2.2, an arterial catheter was inserted into the femoral artery and two venous catheters were placed in the superficial epigastric and the saphenous vein respectively to obtain drainage from subcutaneous abdominal and femoral adipose tissue. A further cannula was inserted into an antecubital vein for intravenous infusion purposes. After taking a basal blood sample for background enrichment, a [$^2H_2$]-palmitate infusion was started at a rate of 0.03 μmol.min^{-1}.kg body weight. ^{133}Xe was injected in abdominal and femoral adipose tissue and ATBF was measured throughout the study. After 60 min of equilibration, a three-step incremental systemic infusion of adrenaline was started for 60 min (step1: 5, step 2: 15, step 3: 25 ng.min^{-1}.kg FFM^{-1}; rate change every 20 minutes). Blood samples were taken simultaneously from all three sites at frequent intervals. After termination of the adrenaline infusion, blood sampling was continued for a further 60 min. After the end of the study, biopsies were taken from abdominal and femoral subcutaneous adipose tissue.

4.3 Results

4.3.1 Metabolic and haemodynamic parameters

Systemic adrenaline infusion resulted in a rise of plasma glucose concentrations to a maximum of 15% from baseline, from 5.2±0.1 mmol.l^{-1} to 5.9±0.1 mmol.l^{-1} ($p<0.001$; Figure 4.1). This well-known effect of adrenaline is due to direct adrenergic effects on liver and pancreas. Hepatic glycogenolysis and gluconeogenesis increase following adrenergic stimulation (208). At the same time, adrenergic stimulation of pancreatic

α-cells leads to glucagon secretion (208, 209). Accordingly, plasma glucagon concentrations (measured in a subgroup of participants, n=15) increased during the adrenaline infusion (p=0.001) (Figure 4.2). The stimulation of pancreatic α-cells by catecholamines results also in the inhibition of insulin secretion (210, 211). I found a small but significant increase in plasma insulin concentration during adrenaline infusion (p<0.001 for comparison baseline vs. 60 min; Figure 4.1). However, the insulin response appeared inappropriately blunted, much in line with the well described adrenaline-dependent inhibition of the acute insulin response to glucose (212). There were two indications to support that. Firstly, insulin concentrations rose sharply after the end of adrenaline infusion, despite falling plasma glucose concentrations (p=0.002 for comparison 60 min vs. 75 min; Figure 4.1). Secondly, the insulin response appeared disconnected from the rising plasma glucose concentrations during adrenaline infusion. The physiological plasma glucose threshold for insulin secretion has been established to be around 5.5 mmol.l^{-1} (213). When I compared the insulin responses during adrenaline infusion between participants whose plasma glucose rose above 5.5 mmol.l^{-1} (n=22, 13 male) and those who remained below this threshold (n=6, 1 male), insulin responses were essentially identical (Figure 4.3). This was despite the significant difference in glucose concentrations between the two groups throughout the study (ANOVA p<0.05 to p=0.001; Figure 4.3). Of note, the uneven sex distribution between the groups did not contribute to the glucose difference (Linear Regression with sex as coefficient not significant).

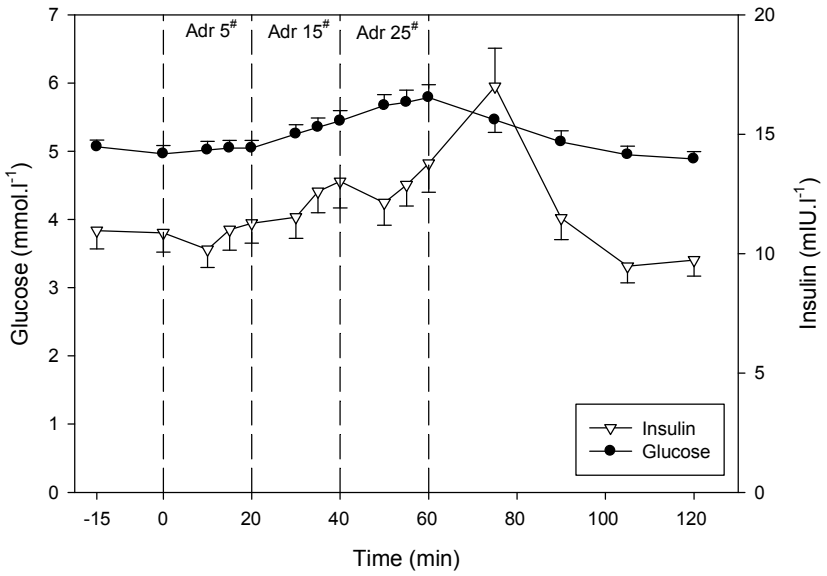

Figure 4.1: Plasma glucose and insulin concentrations during an incremental systemic adrenaline infusion (from 0 to 60 min, #ng.min^{-1}.kg FFM^{-1}).

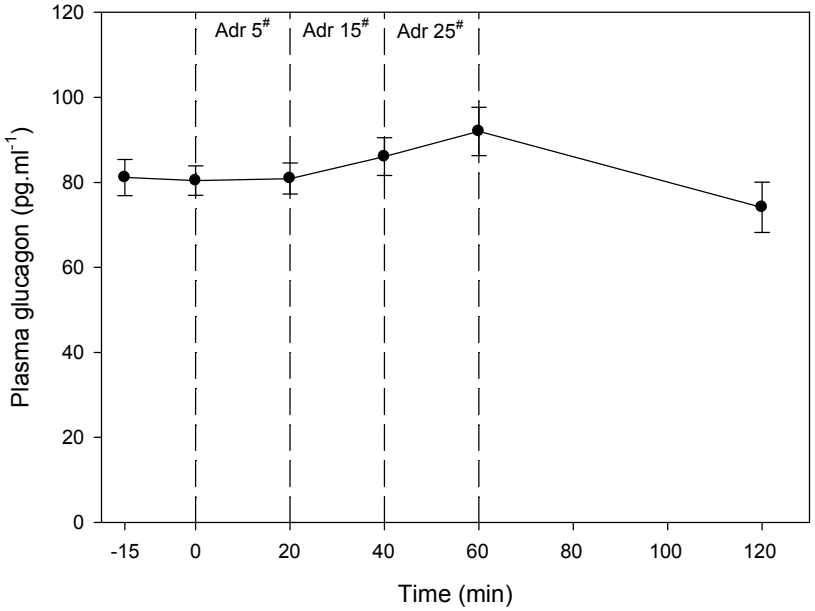

Figure 4.2: Plasma glucagon concentrations during and after an incremental systemic adrenaline infusion (from 0 to 60 min, #ng.min-1.kg FFM-1).

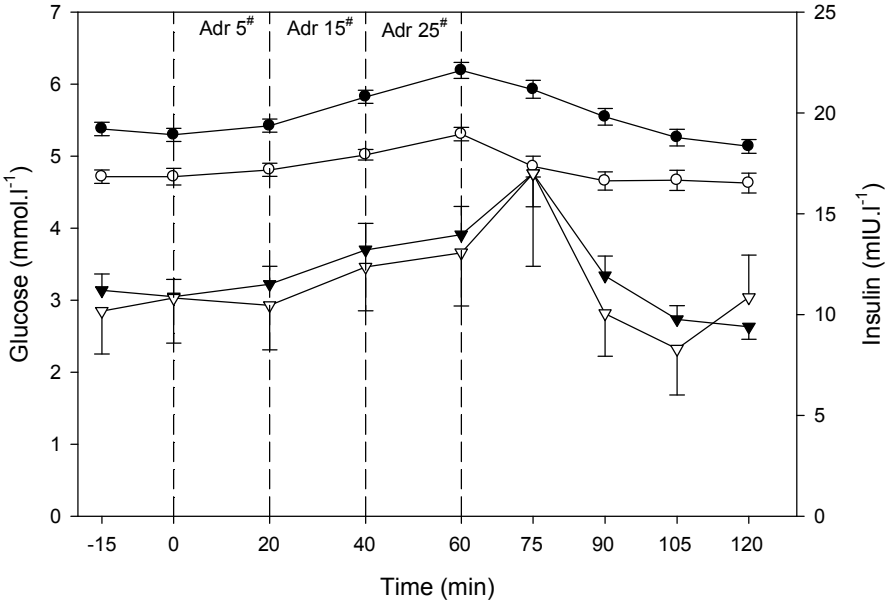

Figure 4.3: Plasma glucose (circles) and insulin (triangles) concentrations, above (black) and below (white) a plasma glucose threshold of 5.5 mmol/l, during and after an incremental systemic adrenaline infusion (from 0 to 60 min, #ng.min-1.kg FFM-1).

The plasma NEFA concentration increased during adrenaline infusion (Figure 4.4). Arterial NEFA concentrations rose by almost 50% from basal at 40 min after the start of infusion ($p<0.001$) and thereafter reached a plateau until the end of the adrenaline

infusion (60 min). After stopping the adrenaline infusion, the plasma NEFA concentration declined rapidly.

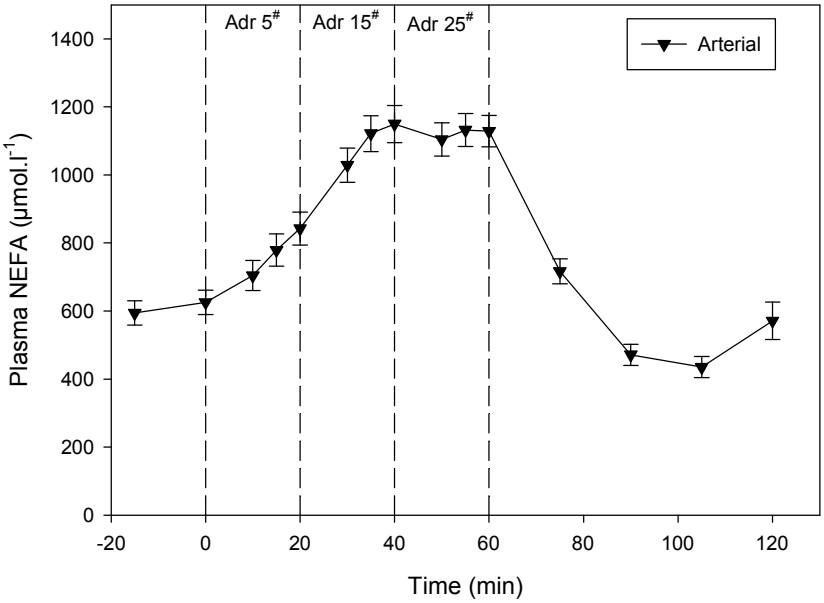

Figure 4.4: Plasma NEFA concentration during an incremental systemic adrenaline infusion (from 0 to 60 min, #ng.min-1.kg FFM-1).

Systemic plasma TG levels remained stable during the study irrespective of the presence of adrenaline in the circulation (Figure 4.5). This is much in line with the finding of a previous study, where adrenaline had no effect on arterialized venous TG concentrations (133).

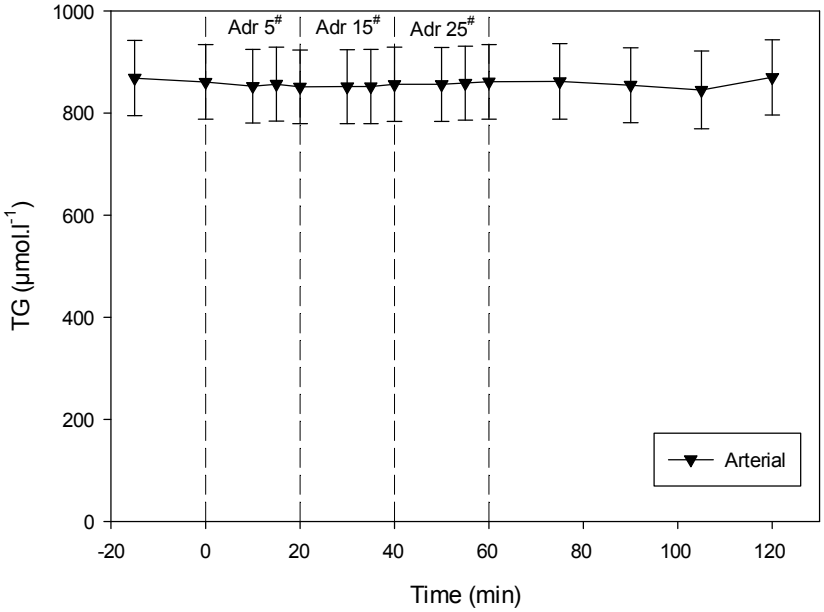

Figure 4.5: Arterial plasma TG response during an incremental systemic adrenaline infusion (from 0 to 60 min, #ng.min-1.kg FFM-1).

The participants' heart rate increased in a dose-dependent manner during the adrenaline infusion (Figure 4.6). Basal HR was 63±2 bpm and increased to 65±2 bpm, 68±2 bpm and 71±2 bpm at the end of each infusion step ($p<0.001$). The adrenergic effect on HR was sustained, since at the end of the study, 60 min after the end of the adrenaline infusion, mean HR was 67±1.7 bpm ($p<0.05$ compared to baseline). This sustained adrenaline effect on HR has been described earlier (214). Possible explanations include the pre-synaptic stimulation of β-adrenoceptors by adrenaline with consecutive sustained noradrenaline release (215), and adrenaline-mediated hypermetabolism resulting in sustained stimulation of cardiac β-adrenoceptors (214).

Basal systolic blood pressure was 117±2 mmHg and did not change significantly throughout the study. Basal diastolic blood pressure was 76±2 mmHg and decreased significantly during the adrenaline infusion to a minimum of 69±1 mmHg at 60 min ($p<0.05$) (Figure 4.7).

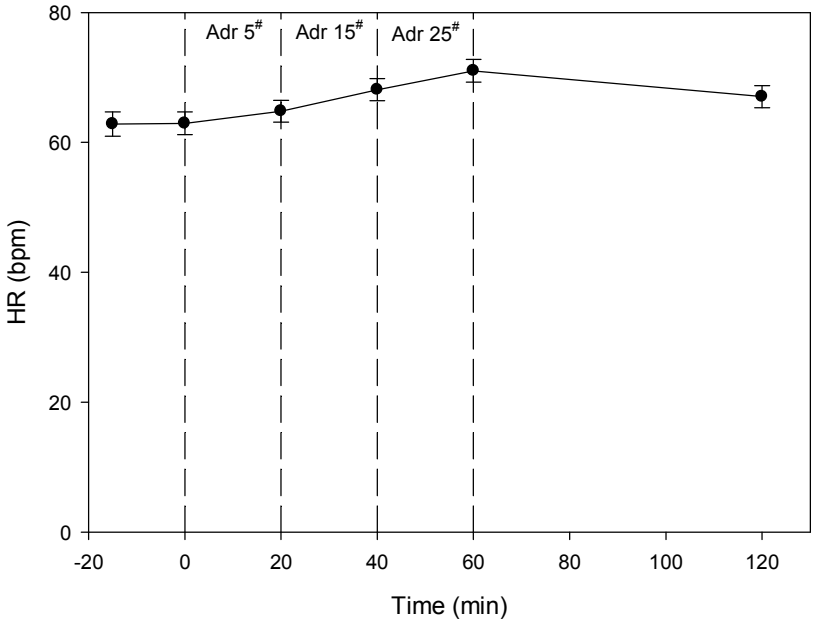

Figure 4.6: Heart rate response during an incremental systemic adrenaline infusion (from 0 to 60 min, $^{\#}ng.min^{-1}.kg\ FFM^{-1}$).

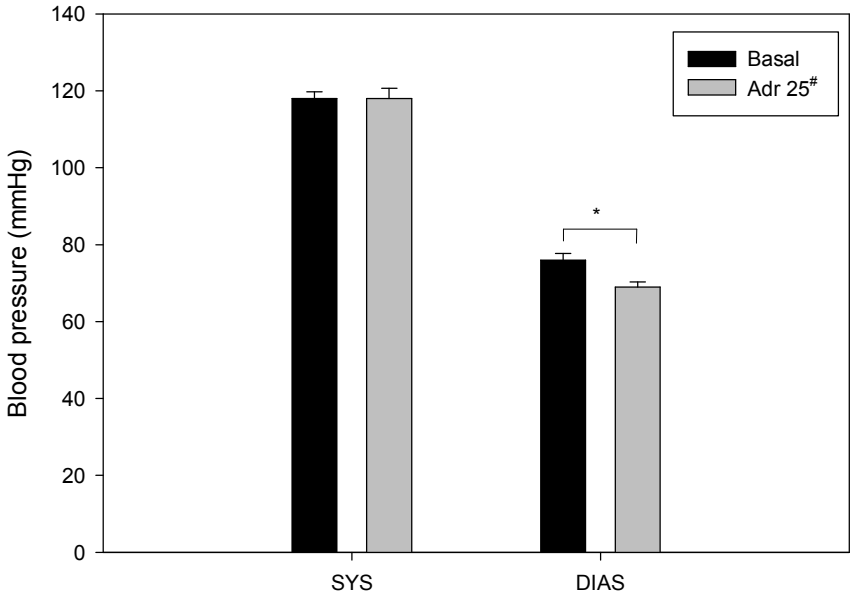

Figure 4.7: Systolic (SYS) and diastolic (DIAS) blood pressure before and after 60 min of adrenaline infusion (*p<0.05, #ng.min^{-1}.kg FFM^{-1}).

The lowering of diastolic blood pressure during adrenaline infusion could be a direct effect of muscle vascular β_2-adrenoceptors and an effect of central α_2-adrenoceptor stimulation which results in a decrease in sympathetic tone. Again, this is in line with previous findings, where a low-dose adrenaline infusion resulted in a decrease of diastolic blood pressure, but had no effect on systolic blood pressure (214). It has been suggested that different plasma thresholds exist for systolic and diastolic blood pressure effects of adrenaline (214, 216).

4.3.2 Regional ATBF response

Adrenaline had a profound dose-dependent effect on ATBF, whereby clear regional differences became apparent (Figure 4.8). Abdominal ATBF increased more than two-fold within the first 40 min of infusion from basal (ANOVA $p<0.001$ for time effect). Thereafter, abdominal ATBF did not increase any further but remained stable until the end of infusion (60 min). Abdominal ATBF declined back to basal levels after the end of adrenaline infusion. Femoral ATBF increased also during the infusion but the response was less pronounced compared to abdominal ATBF (ANOVA $p<0.001$ for time x site interaction). Femoral ATBF increased only up to 1.8-fold at the end of infusion (ANOVA $p<0.001$ for time effect). This is in contrast to the findings during isoprenaline infusion (Figure 3.14) which resulted in almost identical blood flow responses in the two depots. During adrenaline infusion, femoral ATBF, in contrast to abdominal ATBF, showed no plateau and continued to rise for 15 min after the end of

infusion before declining to baseline. The overall femoral ATBF response to adrenaline was lower compared to abdominal ($p<0.001$ for AUC comparison – data not shown).

Basal abdominal and femoral ATBF correlated in a positive fashion (Pearson $r=0.37$, $p<0.05$). However, this somewhat weak association was not independent of BMI, WHR or gender. Adrenaline-stimulated ATBF correlated strongly between abdominal and femoral adipose tissue (Pearson $r=0.73$, $p<0.001$). In contrast to basal ATBF, this correlation was independent of BMI, WHR and sex (Pearson $r=0.73$, $p<0.001$ with BMI, WHR and sex as controlling variables).

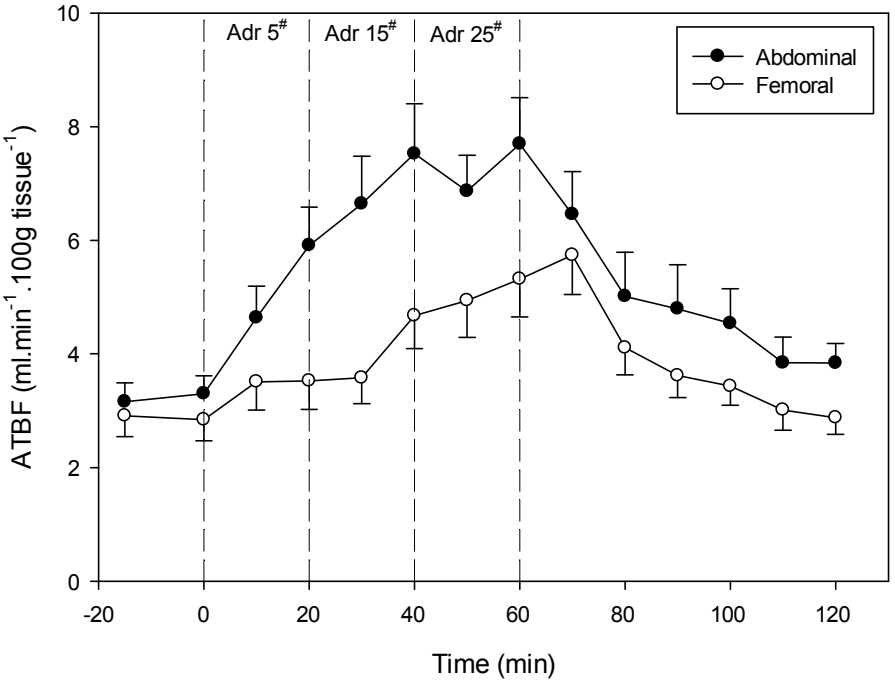

Figure 4.8: Abdominal and femoral ATBF during an incremental systemic adrenaline infusion (from 0 to 60 min, #ng.min^{-1}.kg FFM^{-1}).

4.3.3 Regional fatty acid trafficking

It was not possible to measure fatty acid trafficking in two studies due to technical difficulties, i.e. unsuccessful attempts to place the venous catheters. Therefore, all data presented on fatty acid trafficking are in n=26 (male n=13).

Abdominal NEFA release showed a clear dose-dependent response to adrenaline (Figure 4.9). Compared to basal, it increased 2-fold after 20 min, 3-fold after 40 min and 3.5-fold at 60 min of adrenaline infusion (ANOVA $p<0.001$ for time effect).

Abdominal NEFA release remained stable and did not increase further from 40 to 60 min. After infusion end, abdominal NEFA release declined rapidly. This is in line with the abdominal ATBF response described above (see Figure 4.8) and implies adrenoceptor desensitization. In contrast to abdominal NEFA release, the femoral NEFA release response was much lower. Compared to basal, the maximum increase was just above 1.5-fold at 40 min ($p<0.001$ for difference between sites; Figure 4.9). It was interesting to note that despite the presence of a femoral ATBF response to adrenaline infusion (see Figure 4.8), femoral lipolysis appeared to be largely unresponsive to adrenergic stimulation. This is in contrast to the findings during isoprenaline infusion, where abdominal and femoral lipolysis showed a similar increase from baseline (Figure 3.17). These data suggest that abdominal tissue lipolysis significantly contributes to the observed increase in plasma NEFA concentrations during adrenaline infusion (see Figure 4.4), while femoral adipose does not.

There was a strong positive correlation between abdominal and femoral NEFA release response at the end of adrenaline infusion (60 min), which was independent of BMI and sex (Pearson $r=0.67$, $p=0.006$). However, there was no correlation between basal abdominal and femoral NEFA release. Abdominal adrenaline-stimulated lipolysis showed a negative relationship to measures of abdominal fat mass. The overall abdominal NEFA response to adrenaline, expressed as AUC, was negatively correlated to waist circumference (Pearson $r=-0.61$, $p<0.05$) and WHR (Pearson $r=-0.68$, $p=0.005$). These correlations were independent of BMI and sex. Interestingly, femoral NEFA release AUC did not correlate significantly with any measure of fat mass. In contrast, femoral NEFA release per 100 g tissue at 60 min was negatively associated with waist circumference (Pearson $r=-0.64$, $p=0.01$) and WHR (Pearson $r=-0.65$, $p=0.008$). Again, these relationships were independent of BMI and sex.

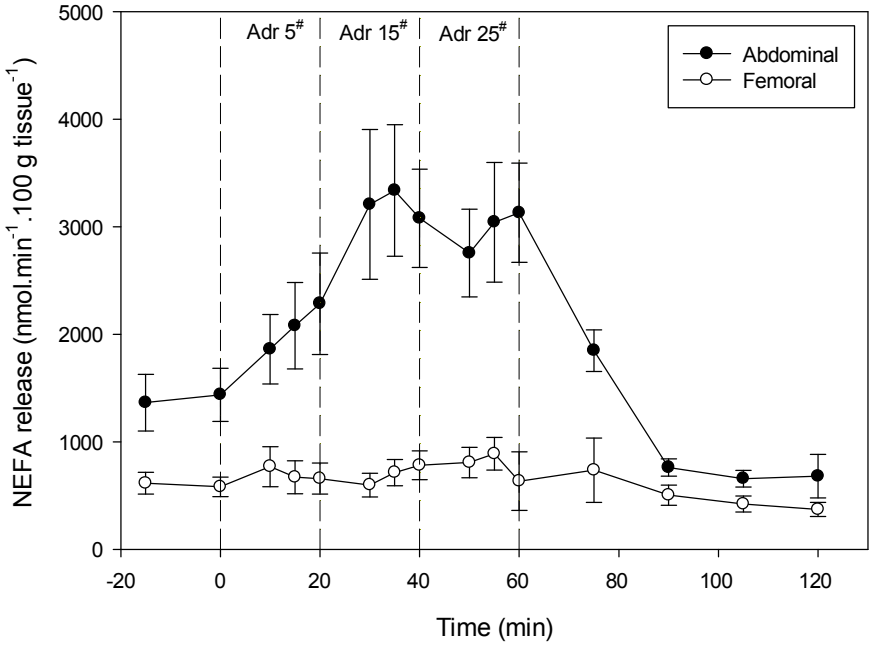

Figure 4.9: Abdominal and femoral NEFA release during an incremental systemic adrenaline infusion (from 0 to 60 min, #ng.min^{-1}.kg FFM^{-1}).

4.3.4 Regional fatty acid trafficking: Isotope data

Adrenaline infusion resulted in a dose-dependent increase in whole body Ra_{NEFA} (Figure 4.10). Whole body Ra_{NEFA} almost doubled during adrenaline infusion ($p<0.001$ for AUC increment). The increase was most pronounced during the second step of the infusion and appeared attenuated during the last 20 min of infusion. As seen with all the metabolic data at this time point so far, this attenuation could be due to adrenoceptor desensitization. Whole body Ra_{NEFA} declined towards the baseline after the end of the infusion. There was no correlation between whole body Ra_{NEFA} and any measures of whole body or regional fat mass.

Regional Ra_{NEFA} responses during adrenaline stimulation showed distinct differences (Figure 4.11). Abdominal Ra_{NEFA} increased throughout the first 40 min ($p<0.001$ for AUC increment), but then declined slightly during the last 20 min of adrenaline infusion. Once more, this is most likely the effect of desensitization. After the end of infusion abdominal Ra_{NEFA} declined further towards baseline levels.

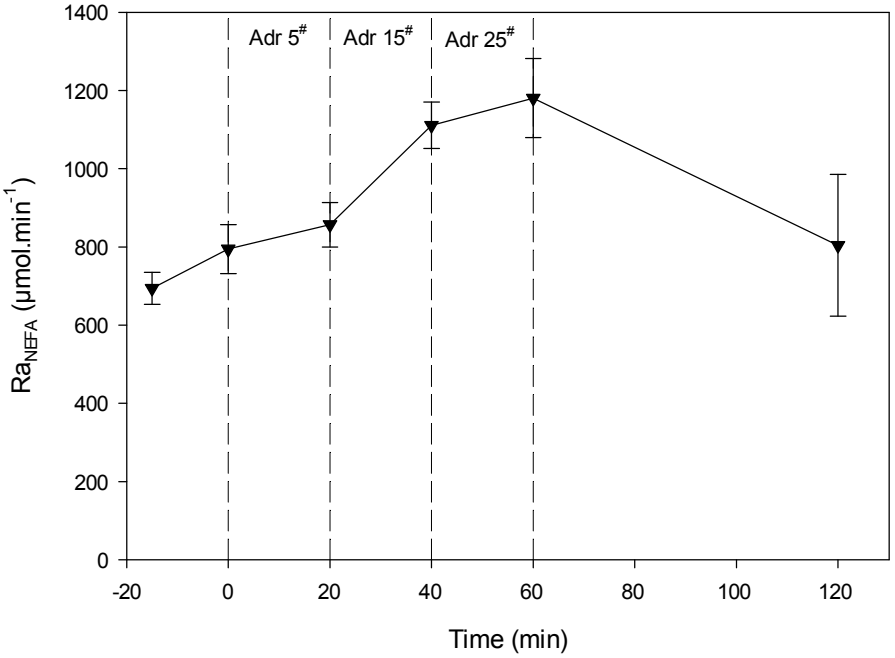

Figure 4.10: Whole body Ra_{NEFA} during an incremental systemic adrenaline infusion (#ng.min^{-1}kg FFM^{-1}).

In contrast, femoral Ra_{NEFA} showed no response during the adrenaline infusion (Figure 4.11). Baseline femoral Ra_{NEFA} was 762±179 nmol.min^{-1}.100g tissue^{-1} and did not change, irrespective of the infused adrenaline concentration (all subsequent time points not statistically significantly different from baseline).

There was no correlation between abdominal and femoral Ra_{NEFA}. Abdominal Ra_{NEFA} during maximum adrenaline stimulation (60 min) showed a negative correlation to WHR (Pearson r=-0.8, p<0.001). This association was independent of BMI and sex. Femoral Ra_{NEFA} showed no association to measures of regional fat mass.

In summary, the isotope data support that a major contributor of NEFA during adrenaline stimulation is abdominal adipose tissue, while femoral adipose tissue is unresponsive to the lipolytic stimulus of adrenaline.

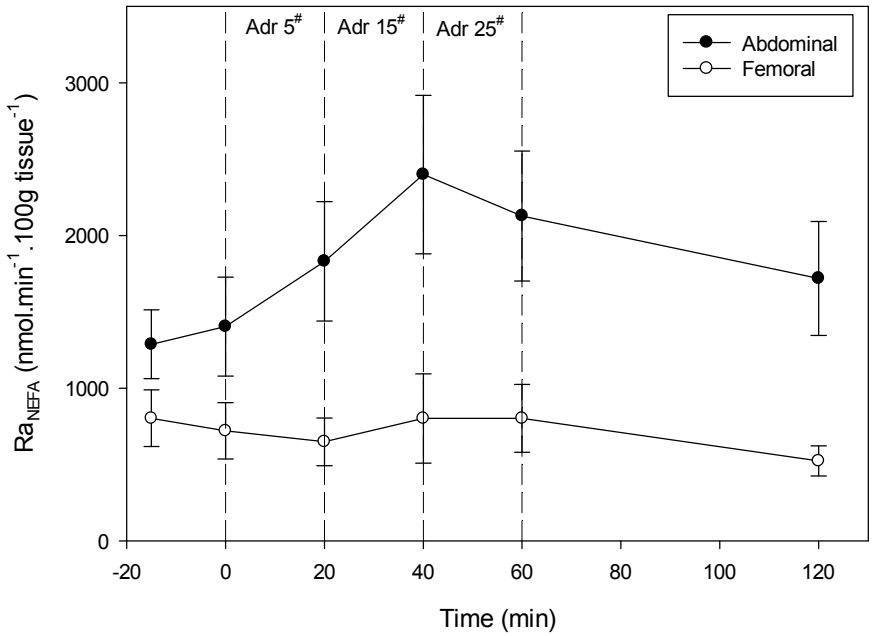

Figure 4.11: Regional R_a NEFA during an incremental systemic adrenaline infusion ($^{\#}$ng.min^{-1}.kg FFM^{-1}).

4.3.5 Sex differences

There are clear sex differences in fat distribution patterns and metabolic properties of adipose tissue (discussed in Sections 1.4 and 3.1). The differential fat distribution between sexes in my study participants is shown in Table 4.2.

Table 4.2: Fat distribution characteristics of subjects

	Male (n=14)	Female (n=14)
WHR	0.94 (0.85-1.05)	0.90 (0.78-0.99)*
WC (cm)	90 (76-107)	81 (70-112)
HC (cm)	95 (88-108)	95 (83-128)
Abdominal fat mass (kg)	9.7 (0.6-17.0)	11.1 (0.4-25.5)
Gluteofemoral fat mass (kg)	6.0 (3.5-8.7)	7.6 (6.0-15.3)*

(*p<0.05 females compared to males; median and range shown)

Abdominal and gluteofemoral fat mass were measured using DXA. Men and women had a comparable abdominal fat mass, although the median was skewed in women because of the presence of two overweight individuals (as apparent from the range

shown in Table 4.2). Nevertheless, women had a larger gluteofemoral fat mass, as one would expect ($p<0.05$; Table 4.2).

Differences in regional lipolysis *in vivo* could explain the gluteofemoral accumulation of adipose tissue in women. I have therefore compared ATBF responses and lipolysis rates between abdominal and femoral adipose tissue during adrenaline infusion in men and women. Given that the maximum response to adrenaline was seen at 40 min (see Sections 4.3.2 and 4.3.3), I compared responses both at 40 min and at the end of adrenaline infusion (60 min). In order to calculate whole-depot lipolysis, the rate derived from AV difference and ATBF (measured in $ml.min^{-1}.100g\ tissue^{-1}$; see Section 2.6.1) was multiplied by the fat mass of each respective depot (measured by DXA).

Abdominal and femoral basal and adrenaline-stimulated ATBF (at 40 and 60 min of adrenaline infusion) did not differ between men and women (Figure 4.12, data at 60 min shown). In both sexes, there was a dose-dependent increase in abdominal and femoral ATBF during adrenaline infusion. As seen before, femoral basal and adrenaline-stimulated ATBF were lower than abdominal ATBF.

With regards to lipolysis, it is clear that the dominant source of adrenaline-stimulated NEFA release is the abdominal depot in both sexes (Figure 4.13). Basal and adrenaline-stimulated abdominal lipolysis per unit fat mass was comparable between men and women (not shown). This was also the case when comparing whole-depot abdominal lipolysis, although it must be noted that when involving abdominal DXA measurements of fat mass, visceral adipose tissue cannot be distinguished from subcutaneous adipose tissue. However, there were differences in femoral lipolysis. Women had a higher basal lipolytic rate, both per unit fat mass, as well as per whole-depot ($p=0.007$ compared to men for both; whole-depot data shown in Figure 4.13). They also showed a higher adrenaline-stimulated femoral NEFA release rate than men, both at 40 and 60 min of adrenaline infusion. This difference in femoral lipolysis was true per unit fat mass ($p=0.006$ at 40 min, $p=0.051$ at 60 min), as well as per whole-depot ($p<0.001$ for both 40 and 60 min; whole-depot data at 60 min shown in Figure 4.13).

The basal and stimulated difference in femoral NEFA release rate is a true sex difference independent of femoral fat mass (ANCOVA $p<0.05$ for sex with femoral fat mass as covariate).

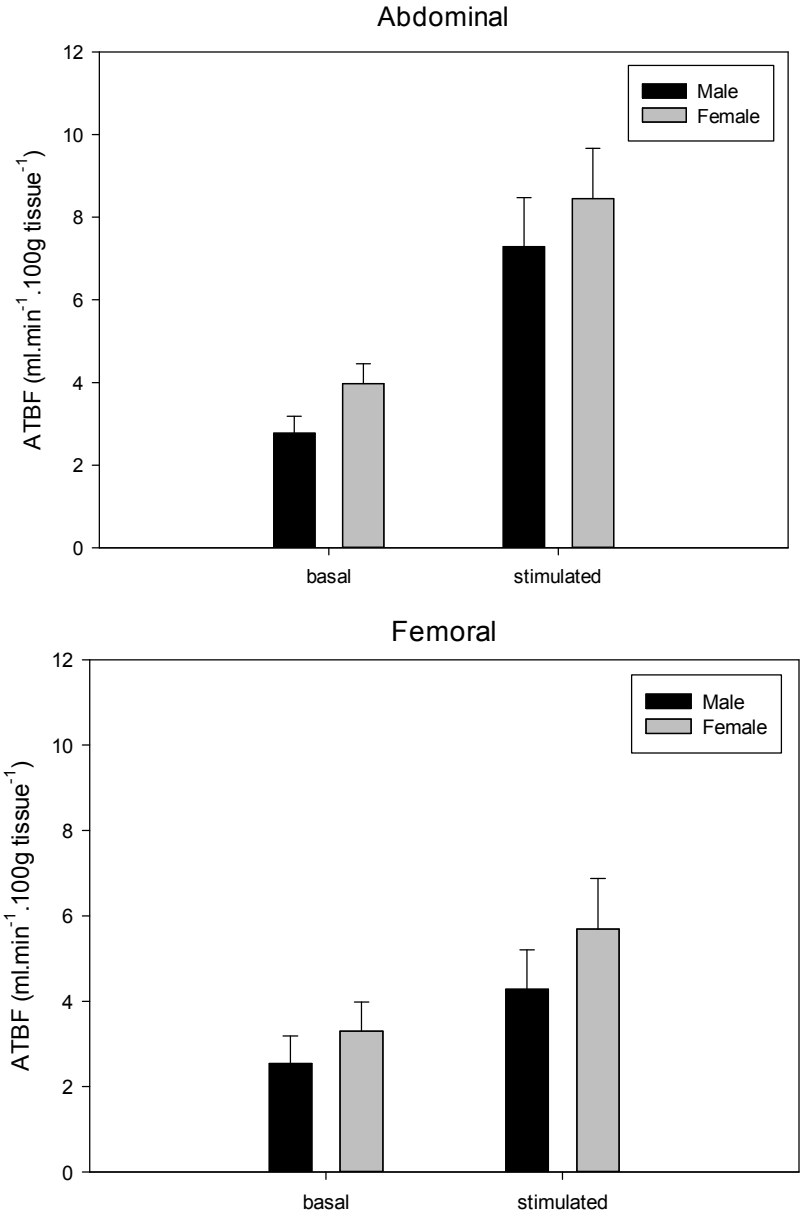

Figure 4.12: Male/female differences in abdominal (upper panel) and femoral (lower panel) ATBF response to a systemic adrenaline infusion.

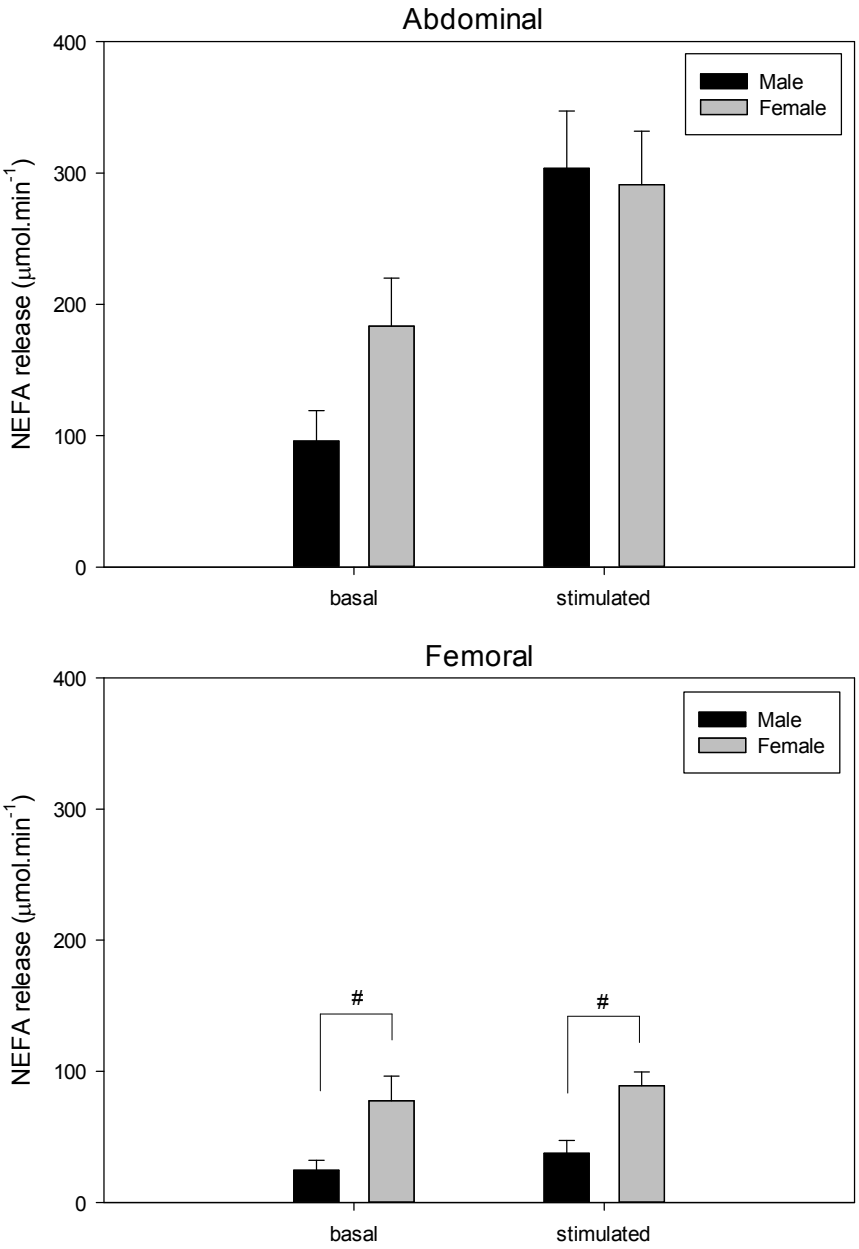

Figure 4.13: Male/female differences in abdominal (upper panel) and femoral (lower panel) lipolysis response to a systemic adrenaline infusion ($^{\#}p<0.001$).

4.3.6 *ADRB2* haplotypes

As discussed in Section 1.2.4, several haplotypes of the *ADRB2* gene that encodes the β_2-adrenoceptor have been described. The commonest three haplotypes in Caucasians, termed *2*, *4*, and *6*, have been found to influence β_2-adrenoceptor-mediated lipolysis *in vitro* (45). Thus, one of the aims of this thesis was to determine whether this finding could be replicated *in vivo*.

The search strategy for recruitment employed the OBB which allows a recruitment-by-genotype approach (see Section 2.7.1). All OBB entries of volunteers

homozygous for one of the haplotypes of interest were identified (n for *2_2* = 305, *4_4* = 184, *6_6* = 49; see also Table 2.3). All volunteers meeting the inclusion criteria were invited by mailing (n for *2_2* = 66, *4_4* = 96, *6_6* = 32). While it was unproblematic to recruit participants of the *2_2* haplotype, response numbers were low for the other two haplotype groups. In order to achieve satisfactory participant numbers in these groups, the inclusion criterion of age was extended to 59 years (n=1) and peri-/postmenopausal women were also included (n=2). The final participant numbers after screening and characteristics per haplotype group are shown in Table 4.3.

Table 4.3: Baseline characteristics of subjects according to ADRB2 haplotype

	2_2 (n=13)	*4_4* (n=11)	*6_6* (n=4)
Male/female (n)	6/7	7/4	1/3
BMI	23.8 (21.5-39.3)	25.3 (21.8-34.2)	25.0 (23.4-30.6)
WHR	0.90 (0.79-0.99)	0.94 (0.78-0.98)	0.94 (0.90-1.05)
Body fat %	28.2 (17.3-50.4)	29.0 (19.1-50.3)	33.4 (30.2-42.0)
Fasting TG (µmol/l)	683 (214-1351)	1067 (780-1588)*	652 (613-997)
Fasting NEFA (µmol/l)	616 (348-793)	563 (355-1084)	556 (411-810)
Fasting glucose (mmol/l)	5.0 (4.4-5.7)	5.2 (4.8-5.6)	5.3 (4.9-6.6)
Fasting insulin (mIU/l)	10.5 (3.8-20.8)	12.9 (5.9-16.4)	8.5 (4.7-14.1)

(*p<0.05 *4_4* compared to *2_2* and *6_6*; median and range shown)

Abdominal and femoral ATBF before and after 60 min of adrenaline infusion is shown in Figure 4.14. Overall, there were no significant differences between basal and adrenaline-stimulated regional ATBF responses between haplotype groups.

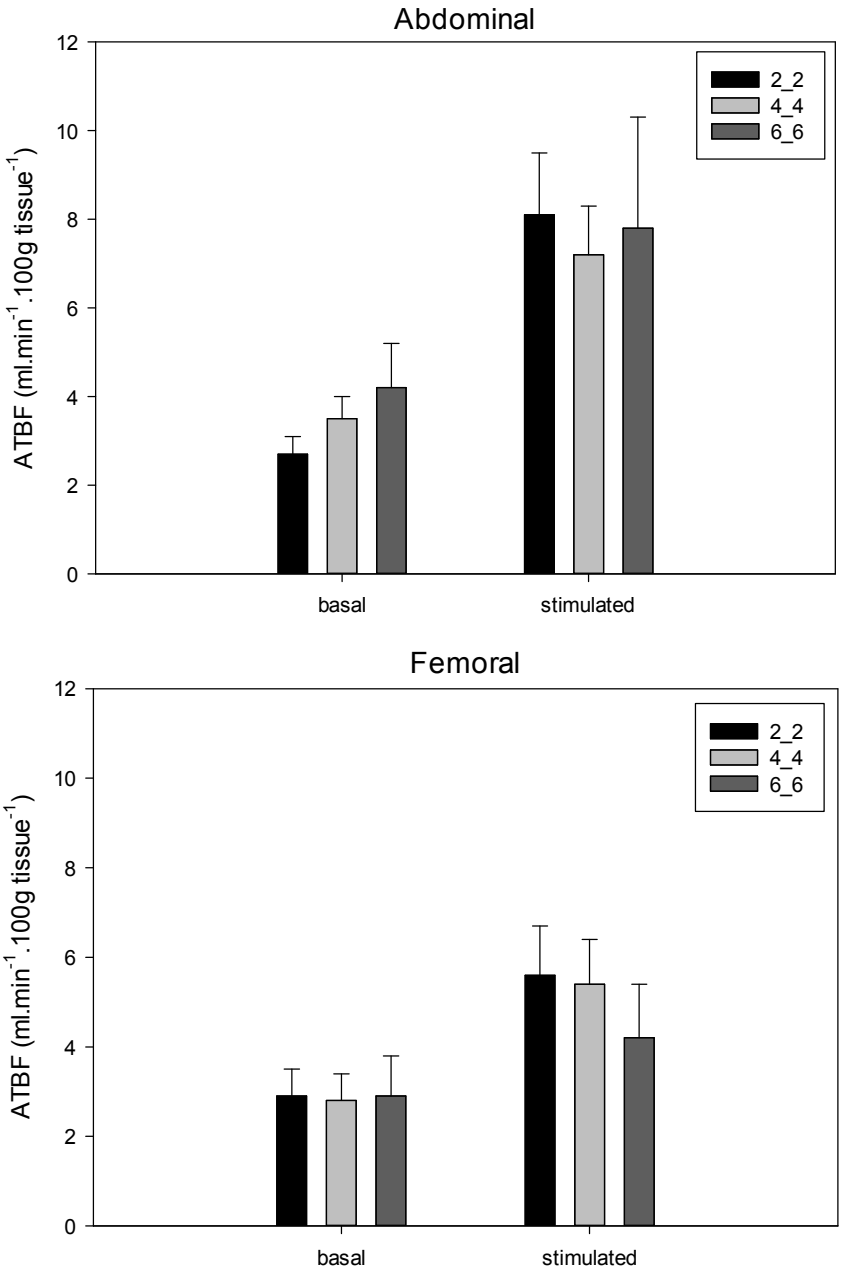

Figure 4.14: ADRB2 haplotype differences in abdominal (upper panel) and femoral (lower panel) ATBF response to a systemic adrenaline infusion.

Figure 4.15 shows basal NEFA release rates and the response to adrenaline expressed as AUC for each haplotype group. No differences between haplotypes were seen in regional NEFA release rates.

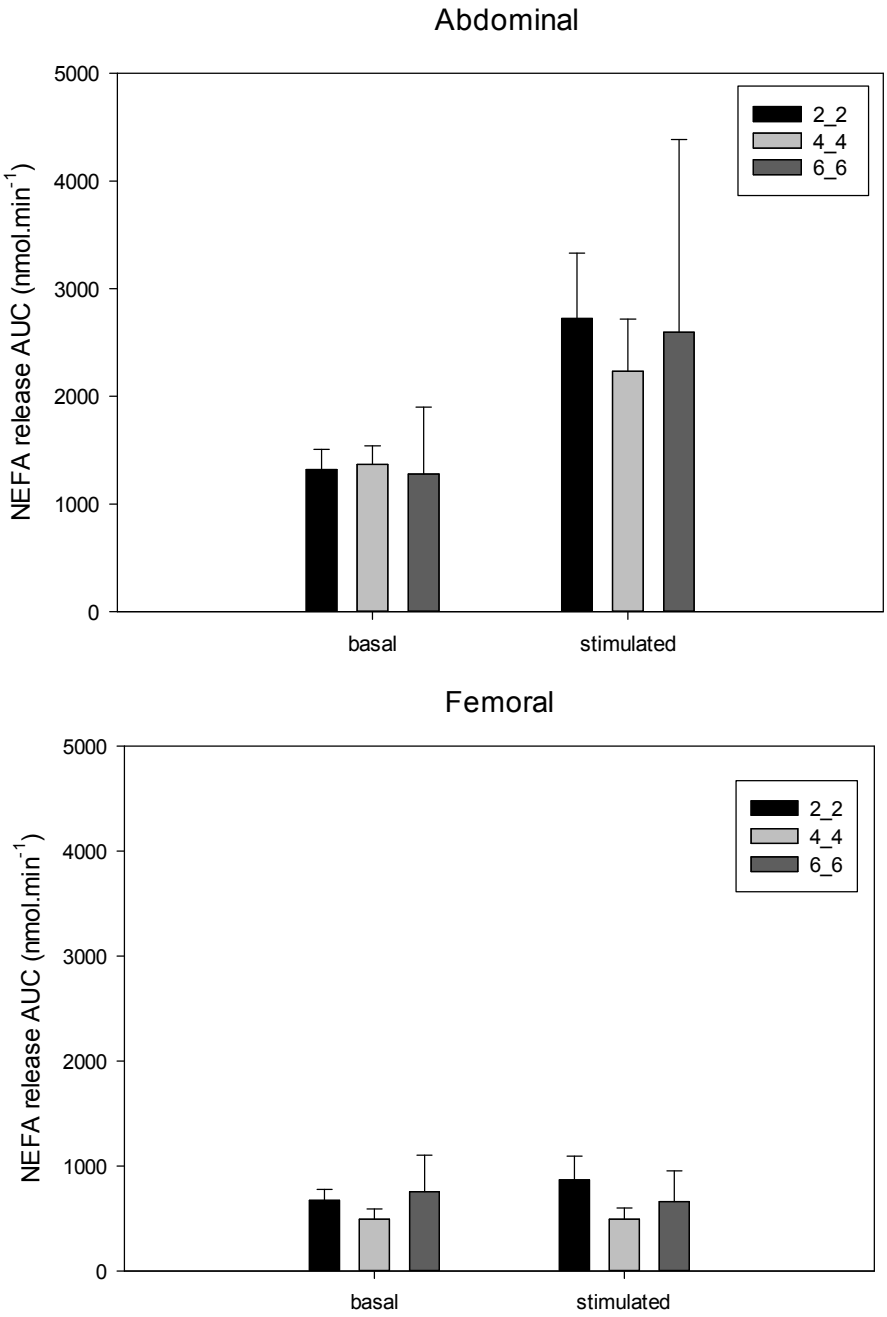

Figure 4.15: ADRB2 haplotype differences in abdominal (upper panel) and femoral (lower panel) NEFA release response to a systemic adrenaline infusion.

Furthermore, no differences were found in regional R_{aNEFA}, in blood pressure and HR or in any other metabolic parameters (data not shown). Overall, a significant effect of *ADRB2* haplotypes on adipose tissue or cardiovascular function could not be demonstrated *in vivo* either in the basal state or during adrenaline infusion.

4.4 Discussion

In this chapter I showed that adrenaline is a major stimulus for whole-body lipolysis, and that abdominal and femoral adipose tissue responded quite differently to

stimulation. The main finding is that abdominal adipose tissue responded to adrenaline infusion with an increase in ATBF and lipolysis rate, while femoral adipose tissue remained largely unresponsive (Figures 4.8 and 4.9). The prolonged stimulation with adrenaline resulted in desensitization effects, whereby no further increase in abdominal ATBF and lipolysis rate was seen during the final step of the infusion. This effect is well known and in fact appears more pronounced when adrenaline is given as an incremental stepped infusion (178). I chose the incremental infusion protocol as I was more interested in the dose-dependent interactions between adrenaline and adipose tissue function, accepting that possibly some desensitization will be present. Abdominal ATBF and NEFA release responded to adrenaline with a clear dose-dependent increase.

Femoral ATBF showed a delayed and blunted response compared to abdominal ATBF (see Figure 4.8), while femoral lipolysis essentially remained unchanged compared to baseline (Figure 4.9). This is even more surprising given the fact that ATBF is a component in the calculation of NEFA release (see Section 2.6.1). This implies a differential distribution of adrenoceptors between femoral adipose tissue vasculature and adipocytes. Most functional *in vitro* studies have been carried out on isolated adipocytes or whole adipose tissue, and to the best of my knowledge there are no studies investigating the differential adrenoceptor distribution between adipocytes and the stromavascular fraction.

The results in this Chapter provide further evidence that gluteofemoral adipose tissue is an independent fat depot *in vivo.* Tan *et al.* showed first that ATBF and fasting NEFA release is lower in gluteal adipose tissue (102). McQuaid *et al.* confirmed that basal and postprandial NEFA release are lower in femoral adipose tissue (106). The only other relevant *in vivo* study investigating leg adipose tissue responses during adrenaline stimulation is by Jensen *et al.* (113). They found adrenaline to increase both abdominal and leg plasma flow, and femoral NEFA release in men, but not in women. However, the findings are not comparable to those shown here because of the big methodological differences between the two studies. They used a relatively small dose of adrenaline (10 $ng.min^{-1}.kg$ body $weight^{-1}$) which was given continuously over 120 min and where regional measurements were taken from 60 to 120 min of the infusion, assuming that a steady-state had been achieved. As shown here and by others, prolonged adrenaline infusion results in signs of tachyphylaxis and this effect increases over time, which makes the findings of Jensen's study likely to be confounded. Furthermore, while femoral plasma flow and NEFA release were

measured by AV difference, abdominal measurements were calculated from the difference between the measured AV differences in leg and splanchnic fat and systemic concentrations (58). Thus, the data are not comparable to the direct measurement achieved here by the highly specific cannulation technique of veins draining adipose tissue. The less specific measurement methods and the low adrenaline concentration used by Jensen *et al.* might explain the lack of demonstration of a response in leg lipolysis in women.

The data in this Chapter demonstrate also relationships between regional adipose tissue function and fat mass. Basal abdominal and femoral ATBF correlated only weakly and not independently of BMI, WHR or sex. Moreover, abdominal and femoral lipolysis did not correlate with each other. In contrast, both ATBF and lipolysis were strongly correlated between abdominal and femoral adipose tissue during adrenaline stimulation. These findings are in line with the study of McQuaid *et al.* (106), where fasting ATBF did not correlate between adipose tissue depots, but postprandial ATBF did. This implies that the overall adrenoceptor-mediated response between abdominal and femoral adipose tissue is coordinated and a direct function of adrenoceptor density. In contrast, basal (i.e. fasting/postabsorptive) adipose tissue function is determined by other physiological mechanisms. This is confirmed by the finding that basal ATBF is determined by local NO production (18), a process that is independent of actual regional receptor density. With regards to the relationship to fat mass, both abdominal and femoral lipolytic responses to adrenaline showed a negative correlation to measures of regional fat. This supports the finding of adipose tissue function adapting to an increase in fat mass by decreasing the metabolic activity per unit fat mass (106, 114).

With regards to the differences between men and women, it has long been known that, between sexes, adipocytes show differential adrenoceptor expression and/or sensitivity *in vitro*. Women have been found to have a higher α_2-adrenoceptor expression in gluteal adipocytes (202) and a decreased α_2-adrenoceptor sensitivity to catecholamines in abdominal adipocytes (108). The only relevant *in vivo* study is again that of Jensen *et al*. (113), whose limitations have been discussed above. The data in this Chapter show that, compared to femoral, abdominal adipose tissue is more lipolytically active during basal conditions and adrenaline stimulation in both men and women. However, when compared to men, femoral basal and adrenaline-stimulated lipolysis was higher in women. This might be interpreted as an indication that the female femoral adipose tissue depot is more metabolically active that male

femoral fat. It does not support the idea of gluteofemoral fat mass accumulation in women being a result of decreased lipolytic responsiveness, as widely claimed (217). This is not surprising, given that nowadays it is appreciated that regional fat depot formation is the result of a complex interplay of hormonal, humoral and genetic factors – rather than the result of simple variation of a single adrenoceptor subtype (51). Therefore, studies that compare gluteofemoral adipose tissue turnover between sexes are warranted.

The lack of any *in vivo* effect of the *ADRB2* haplotypes on regional adipose tissue function was surprising, given the data available from previous studies. Firstly, isolated *ADRB2* SNPs (namely Arg16Gly, Glu27Gln and Ile164Thr) have been associated with significant differences in β2-adrenoceptor function *in vivo* (218, 219). Furthermore, when SNPs were arranged as haplotypes, which allows for the study of physiological interaction between SNPs, there was a clear difference in β_2-adrenoceptor-mediated bronchodilatation in patients with asthma (44). This haplotype effect was also found in relation to the *in vitro* lipolytic response of isolated adipocytes to terbutaline, a selective β_2-agonist (45). Clearly, the findings of increased β_2-adrenoceptor sensitivity described for haplotype *6_6*, and decreased responsiveness of haplotype *4_4* compared to haplotype *2_2*, could not be replicated in my studies. Furthermore, I could not find any haplotype effect on other catecholamine-mediated parameters, i.e. HR and blood pressure. One possible weakness of the study in this respect could be the use of adrenaline as a stimulus. The non-selective stimulation of α- and β-adrenoceptors could mask a haplotype effect that is highly selective for β_2-adrenoceptors. However, while selective β_2-agonism is an important *in vivo* pharmacological pathway in clinical medicine (e.g. in the treatment of asthma), it plays essentially no role in adipose tissue physiology *in vivo*. In contrast, it appears that haplotype-mediated differences in β_2-adrenoceptor sensitivity are counter-balanced by other physiological mechanisms. These could be a differential expression of α-adrenoceptors or adaptation of desensitization mechanisms.

In summary, in this Chapter I provide evidence for differential fatty-acid trafficking, in terms of lipolysis, between abdominal and femoral adipose tissue *in vivo*. As shown in Chapter 3, β-adrenoceptor stimulation with isoprenaline resulted in an increase of ATBF and lipolysis in both adipose tissue depots. This, in conjunction with the findings of the current Chapter, leads to the question as to the possible physiological mechanism responsible for the regional differences described here. A plausible

mechanism would be differential expression and/or sensitivity of α-adrenoceptors in femoral adipose tissue. This is supported by the finding that femoral adipose tissue responses are only seen during the final stages of adrenaline infusion, because it is known that adrenaline in low concentrations has a higher affinity for α-adrenoceptors which is only overcome when adrenaline is infused in higher doses. The hypothesis of an α-adrenoceptor dominance in the response to adrenaline in femoral adipose tissue is explored further in an *in vivo* approach described in the next Chapter. Furthermore, in the next Chapter I present supporting molecular data obtained from adipose tissue biopsies from the current study. The intriguing question as to whether differential fatty-acid trafficking between abdominal and femoral adipose tissue also applies to postprandial fatty acid uptake is then explored in Chapter 6.

5 Differential α- and β-adrenoceptor balance in regional adipose tissue function *in vivo*

5.1 Introduction

In the two previous chapters I have shown that abdominal and femoral adipose tissue respond differently to adrenergic stimulation *in vivo* depending on the agonist used. Non-selective stimulation of β-adrenoceptors with isoprenaline resulted in a similar increase of ATBF in both adipose tissue depots. Lipolytic rate was lower in femoral adipose tissue during isoprenaline infusion, but was comparable to abdominal adipose tissue in terms of response from baseline (see Section 3.3.4). In contrast, non-selective stimulation of α-/β-adrenoceptors with adrenaline resulted in a dose-dependent response of both lipolysis and ATBF in abdominal adipose tissue, but not in femoral adipose tissue (see Section 4.3). This implies a role for α-adrenoceptors in femoral adipose tissue, since inhibition of lipolysis and vasoconstriction are α-adrenoceptor mediated effects (see Section 1.2.3).

It has been long known that differential expression and/or sensitivity patterns of adrenoceptors exist between human adipose tissue depots *in vitro* (108, 109, 220). Interestingly, it appears that the regional variation in adrenoceptor density is not innate, but is acquired during adolescence, driven by hormonal changes (221). Abdominal and femoral adipocytes express α_2- and β-adrenoceptors in a ratio of 3:2 (168). Adrenaline in low concentrations has a higher affinity to α-adrenoceptors and under such conditions it exerts anti-lipolytic effects *in vitro* (222). At higher concentrations it elicits lipolytic effects in abdominal, but not in femoral adipocytes (168). The same response pattern was seen in abdominal and gluteal adipocytes stimulated with noradrenaline (220). Therefore, it has been suggested that α-adrenoceptors are important physiological regulators of regional adipose tissue function (110). Gluteal adipocytes from female donors were found to have higher numbers of α_2-adrenoceptors than men (202). In postmenopausal women, gluteal adipocytes have a lower α_2-adrenoceptor density than abdominal adipocytes, but a similar β-adrenoceptor density (223). The basal postabsorptive lipolysis rate is determined, at least partly, by α-adrenoceptor stimulation (224). In obesity, it appears that down-regulation of β-adrenoceptors rather than changes in α-adrenoceptor density is responsible for the observed resistance to lipolytic adrenergic stimuli (225). Most studies agree that the differential sensitivity observed, results from variation at the adrenergic receptor level, rather than post-receptor changes (108, 223, 226).

The study of abdominal ATBF regulation *in vivo* has shown that β-adrenoceptor mediated vasodilatation is important for the postprandial ATBF increase (18). Using the microdialysis technique, it has been suggested that vascular overexpression of α_2-adrenoceptors is responsible for the lower lipolytic rates seen in gluteal adipose tissue, as vasoconstriction suppresses the efflux of fatty acids out of the tissue bed (116).

So far, there are no studies that investigate the role of α-adrenoceptors in adrenaline-mediated regional adipose tissue function *in vivo* using integrative physiology techniques. The studies described in this chapter aim to confirm the hypothesis that α-adrenoceptor predominance in femoral adipose tissue is the responsible mechanism for the differential response to adrenaline-stimulation as seen *in vitro* and during my previous studies *in vivo*. These data are complemented by RNA expression studies of paired abdominal and femoral adipose tissue biopsies, obtained from the studies described in Chapter 4.

5.2 Study design and participants

The study design comprised a systemic incremental infusion of adrenaline with local microinfusion of vasoactive agents in order to unmask specific adrenoceptor subtype effects on ATBF. The following methods were used:

- Recruitment of participants using the Oxford BioBank and poster advertising (see Section 2.7)
- Local microinfusion of propranolol, phentolamine and saline (see Section 2.1.4)
- Systemic infusion of adrenaline (see Section 2.3.2)
- Measurement of ATBF with the ^{133}Xe washout technique (see Section 2.1.1)
- Measurement of systemic metabolites using arterialized venous samples (see Section 2.2.6)

The majority of participants were drawn from the pool of participants of the adrenaline infusion study described in Chapter 4, who initially had been recruited using the Oxford BioBank. Two participants were recruited by poster advertising. A total n=13 was recruited (7 male, median age 47, range 36-60). The median BMI was 26.5 kg.m^{-2}, range 22.2-39.3 kg.m^{-2}, and the median WHR was 0.93, range 0.85-1.05. The further participant characteristics are shown in Table 5.1.

Table 5.1: Baseline anthropometric and metabolic characteristics of subjects

	Male (n=7)	Female (n=6)
BMI	26.2 (22.8-30.6)	26.8 (22.2-39.3)
WHR	0.95 (0.85-1.05)	0.90 (0.88-0.99)
Body fat %	29.0 (19.1-33.3)	33.8 (28.2-50.4)*
Fasting TG (μmol/l)	1200 (900-1500)	500 (400-1000)*
Fasting NEFA (μmol/l)	410 (330-520)	580 (350-840)
Fasting glucose (mmol/l)	5.2 (4.8-6.2)	4.7 (4.3-4.9)*
Fasting insulin (mIU/l)	11.8 (9.3-18.5)	7.6 (2.4-27.5)

(*$p<0.05$ females compared to males; median and range shown)

The participants arrived after an overnight fast and remained fasting throughout the study. Three microinfusion probes were placed into the abdominal and one into the femoral adipose tissue of each thigh (Figure 5.1). The abdominal probes were used for the local infusion of propranolol (β-blocker, concentration 10^{-4} M at 2 $\mu l.min^{-1}$), phentolamine (α-blocker, concentration 10^{-4} M at 2 $\mu l.min^{-1}$) and saline (control). The femoral probes were used for infusing phentolamine (concentration 10^{-4} M at 2 $\mu l.min^{-1}$) and saline. After allowing 60 min for equilibration and for the locally-infused agents to reach an effective concentration, a three-step incremental systemic infusion of adrenaline was started for 60 min (as described in Section 4.2; step 1: 5, step 2: 15 and step 3: 25 $ng.min^{-1}.kg\ FFM^{-1}$ adrenaline; rate change every 20 min). After the end of the adrenaline infusion, ATBF was measured for a further 60 min. Because of the local character of any pharmacological effects of propranolol and phentolamine, no regional samples were taken for AV difference calculations. Instead, arterialized venous samples (using a “hot box”, see Section 2.2.6) were obtained at frequent time intervals.

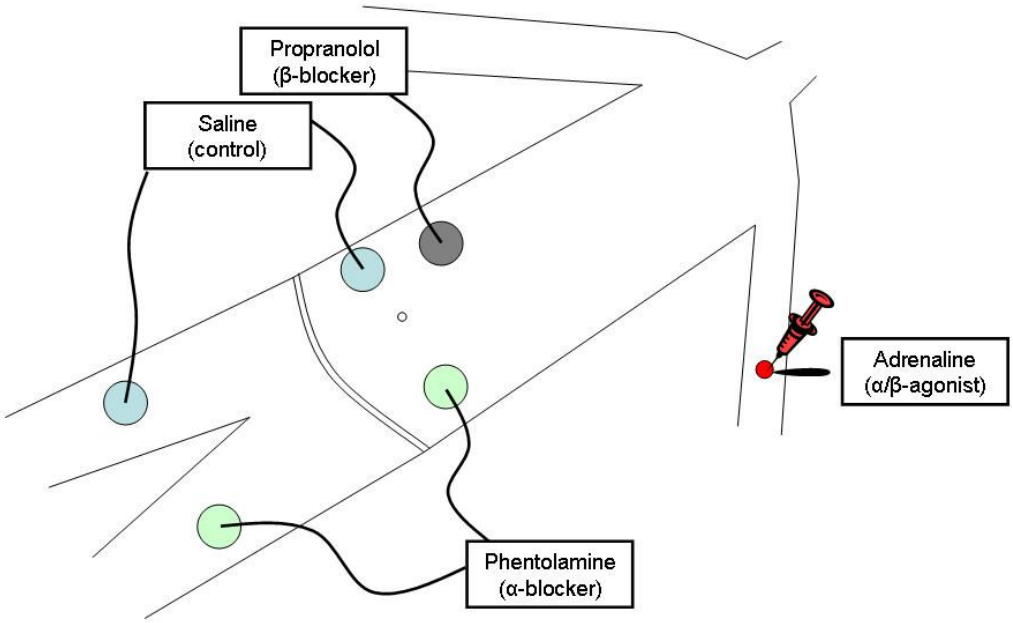

Figure 5.1: Pharmacological agents infused locally with microinfusion. Adrenaline was given systemically in incremental doses for 60 min.

Adipose tissue biopsies for the purposes of RNA extraction and expression analysis of specific genes were obtained from the participants of the study described in Chapter 4 (for participant characteristics see Table 4.1). The following methods were used:

- Obtaining biopsies of abdominal and femoral adipose tissue (see Section 2.8.1)
- RNA extraction, cDNA generation and PCR of selected gene sequences (see Section 2.8.2)
- Statistical analysis of gene expression data and correlation with metabolic parameters obtained from the studies described in Chapter 4

5.3 Results

5.3.1 Metabolic and haemodynamic parameters

As observed in the studies described in Chapter 4, systemic adrenaline infusion led to a moderate increase in plasma glucose concentrations (to a maximum of 14% from baseline), while insulin concentrations were suppressed during the initial steps of the infusion (Figure 5.2). Since no blood samples were taken between 60 and 120 min of the study, the previously described peak of insulin after the end of adrenaline infusion was not seen here. Adrenaline resulted in a profound increase of systemic

plasma NEFA concentrations up to 140% from baseline (Figure 5.3). As found in my previous studies, plasma TG did not change significantly during the study (data not shown).

Basal systolic blood pressure was 116±4 mmHg and basal diastolic blood pressure was 70±2 mmHg. Systolic blood pressure did not change significantly during the study, while diastolic blood pressure dropped to 65±2 mmHg at the end of adrenaline infusion ($p<0.05$ compared to basal), as seen before. The participants' HR increased from basal 57±3 bpm to 67±4 bpm at 60 min of adrenaline infusion ($p<0.001$). As described in Chapter 4, the adrenaline-induced HR elevation was sustained after the end of the infusion (HR at 120 min: 63 bpm±4; $p<0.05$ compared to basal).

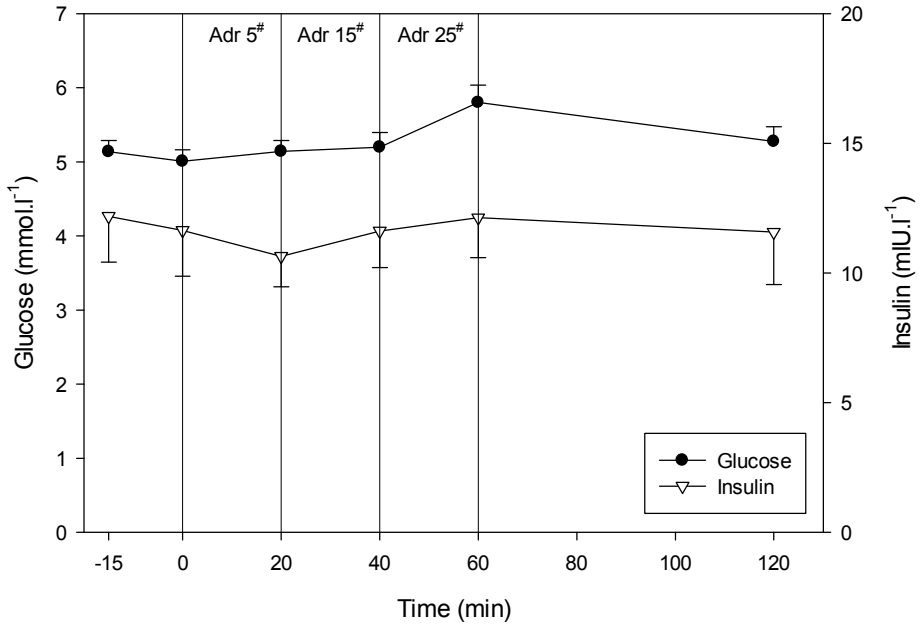

Figure 5.2: Plasma glucose and insulin concentrations during incremental systemic adrenaline infusion (from 0 to 60 min, $^{\#}ng.min^{-1}.kg\ FFM^{1}$) and local microinfusion of vasoactive agents (throughout the study).

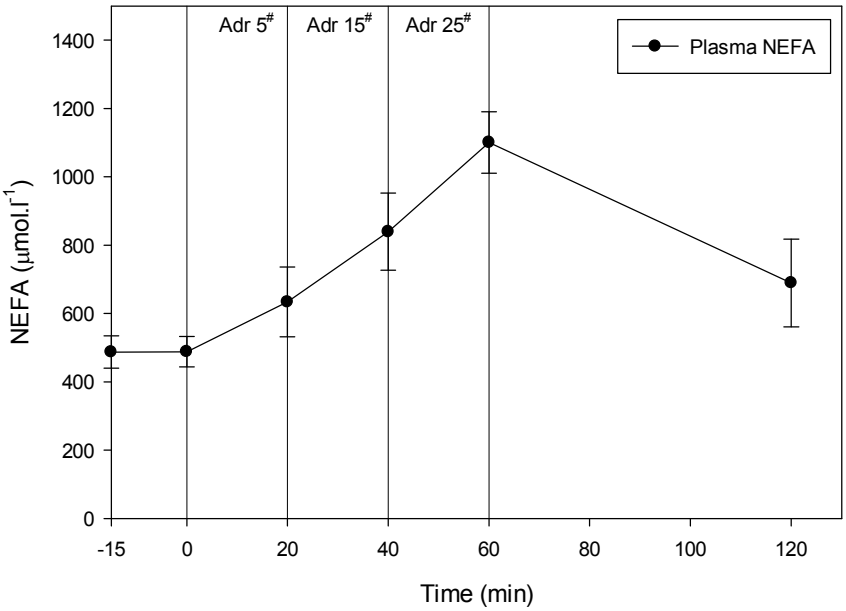

Figure 5.3: Plasma NEFA concentrations during incremental systemic adrenaline infusion (from 0 to 60 min, #ng.min-1.kg FFM-1) and local microinfusion of vasoactive agents (throughout the study).

5.3.2 Effects of local microinfusion on the abdominal ATBF response to adrenaline

Phentolamine and propranolol were infused locally into abdominal adipose tissue. The effect of α-adrenoceptor blockade with phentolamine was the primary effect I wanted to study. I used propranolol as a "negative control" to exclude any specific α-adrenergic effect on abdominal adipose tissue. The effects of local phentolamine and propranolol microinfusion on abdominal ATBF are shown in Figure 5.4. Basal ATBF did not differ significantly between the three microinfusion sites. Local α-adrenergic blockade with phentolamine did not affect the ATBF response to adrenaline, and the response pattern was similar to that of the control site (saline). ATBF increased both under phentolamine and saline during low dose adrenaline infusion and doubled from baseline during the last two infusion steps of adrenaline ($p<0.05$ compared to basal for both phentolamine and control sites; no significant difference between sites). Propranolol microinfusion blunted the abdominal ATBF response to adrenaline, which reached only 39% of basal after 60 min of adrenaline infusion (Figure 5.4, $p<0.05$ for difference to saline/phentolamine sites).

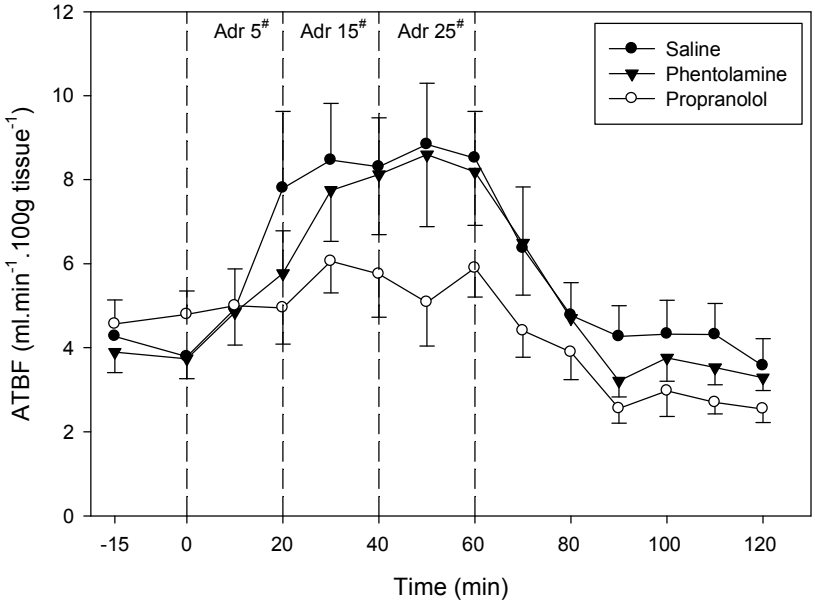

Figure 5.4: Abdominal ATBF response during incremental systemic adrenaline infusion (from 0 to 60 min, $^{\#}$ng.min^{-1}.kg FFM^{-1}) and local microinfusion of vasoactive agents (throughout the study).

5.3.3 Effects of local microinfusion on the femoral ATBF response to adrenaline

In femoral adipose tissue, only phentolamine was infused locally. The ATBF response was compared to the contralateral site which was infused with saline as a control (Figure 5.1). On the control site the femoral ATBF response to adrenaline was similar to that observed in the studies described in Chapter 4 (see Section 4.3.2). There was a slow response to adrenergic stimulation with ATBF, doubling from basal only during the last step of the adrenaline infusion (Figure 5.5; $p<0.001$ for time effect). This has to be compared to the respective abdominal ATBF increase under saline shown in Figure 5.4, where abdominal ATBF rose dose-dependently immediately after the start of infusion and peaked at 40 min of infusion. As before, the overall femoral ATBF response to adrenaline was lower than in abdominal adipose tissue ($p<0.05$ for difference between sites at 60 min). Local α-adrenergic blockade with phentolamine resulted in the "disinhibition" of the femoral ATBF response to adrenaline (Figure 5.5). Femoral ATBF increased now dose-dependently and more sharply during the incremental adrenaline infusion ($p<0.001$ for phentolamine effect compared to femoral control site).

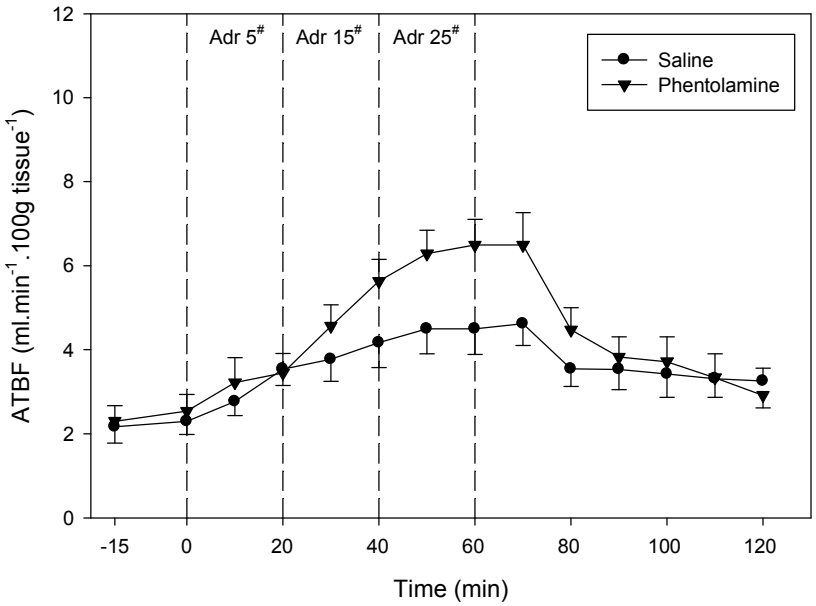

Figure 5.5: Femoral ATBF response during incremental systemic adrenaline infusion (from 0 to 60 min, #ng.min-1.kg FFM-1) and local microinfusion of phentolamine or saline (throughout the study).

5.3.4 Sex differences

When comparing the abdominal ATBF response to α- and β-adrenoceptor blockade between men and women, no difference in responses was found. In both men and women, propranolol resulted in a blunted ATBF response, while ATBF increased similarly in phentolamine and saline microinfusion sites as shown above (see Figure 5.4; data not shown).

Similarly, the femoral ATBF response to adrenaline on the control microinfusion site (saline) did not differ significantly between sexes (Figure 5.6). Both men and women showed a slow femoral ATBF increase during adrenaline infusion that peaked at 4.1±0.9 ml.min^{-1}.100g tissue^{-1} and 5.0±0.7 ml.min^{-1}.100g tissue^{-1} respectively during the last step of the infusion (difference not statistically significant).

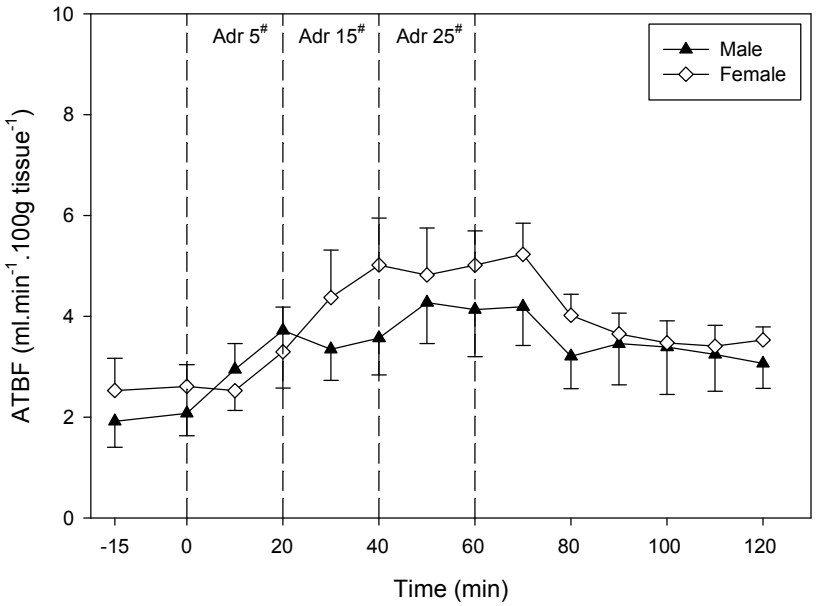

Figure 5.6: Femoral ATBF response in men and women during incremental systemic adrenaline infusion (from 0 to 60 min, $^{\#}$ng.min^{-1}.kg FFM^{1}) and local microinfusion of saline (throughout the study).

Basal femoral ATBF did not differ significantly between men and women. However, when comparing the femoral ATBF response to adrenaline during α-adrenoceptor blockade with phentolamine, clear sex-specific differences were seen (Figure 5.7). The overall ATBF response to adrenaline appeared shifted towards a higher level in women. Women showed a higher increase of femoral ATBF from baseline during adrenaline stimulation than men, which peaked at 70 min, after the end of adrenaline infusion (ANOVA $p<0.05$ for sex difference). This difference remained significant even 60 min after the end of infusion ($p<0.05$ at 120 min).

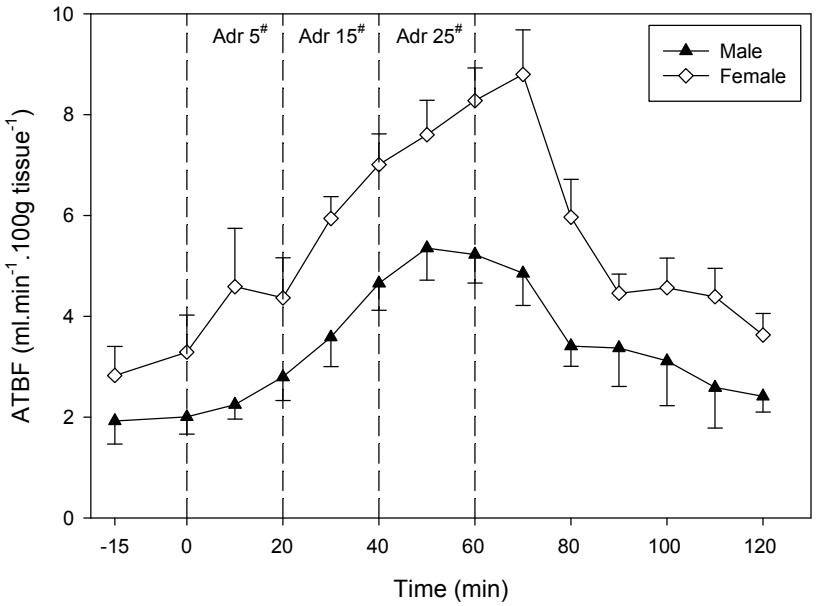

Figure 5.7: Femoral ATBF response in men and women during incremental systemic adrenaline infusion (from 0 to 60 min, $^{\#}$ng.min^{-1}.kg FFM^{1}) and local microinfusion of phentolamine (throughout the study).

5.3.5 *ADRB2* haplotypes

With the exception of two participants, all other participants were recruited from the adrenaline study described in Chapter 4 (see Section 4.2). As described above, the initial recruiting implemented the Oxford BioBank in a recruitment-by-haplotype approach. Therefore, it was possible to analyse the results of the current study also stratified for the *ADRB2* haplotypes described above (see Sections 1.2.4 and 4.3.6). Given the overall small total number of participants in this current study, inevitably this resulted in very small subgroups (see Table 5.2). Overall, no significant differences were seen in the abdominal and femoral response to adrenaline during local microinfusion of propranolol and phentolamine (data not shown). The differences seen in basal regional ATBF between haplotype groups (see Table 5.2) were small and due to the small subgroups not significant.

Table 5.2: Baseline characteristics of subjects according to ADRB2 haplotype

	2_2 (n=5)	*4_4* (n=3)	*6_6* (n=3)
BMI	27.3 (22.2-39.3)	26.0 (25.8-27.6)	23.7 (23.4-30.6)
WHR	0.95 (0.88-0.99)	0.94 (0.88-0.98)	0.95 (0.90-1.05)
Body fat %	30.4 (27.1-50.4)	29.0 (19.1-33.3)	31.7 (30.2-35.0)
Fasting TG (µmol/l)	1000 (500-1500)	1100 (1000-1400)	1000 (500-1500)
Fasting NEFA (µmol/l)	360 (330-630)	460 (400-520)	450 (410-500)
Fasting glucose (mmol/l)	4.7 (4.6-5.2)	5.4 (5.0-5.7)	5.6 (4.9-6.2)
Fasting insulin (mIU/l)	11.9 (6.5-27.5)	11.8 (11.7-18.5)	8.2 (2.4-15.2)
Basal abdominal ATBF*	5.3±0.8	1.3±0.2	4.6±0.3
Basal femoral ATBF*	1.4±0.2	1.7±0.6	3.1±0.6

(median and range shown); *in $ml.min^{-1}.100g\ tissue^{-1}$ (mean±SE)

5.3.6 Regional RNA expression of adrenoceptors

Distinct differences between abdominal and femoral adipose tissue were found with regards to the mRNA expression of *ADRA1A, ADRA2A, ADRB1* and *ADRB2* in biopsies of whole adipose tissue (see Figure 5.8). Both β-adrenoceptor subtypes were more highly expressed in abdominal adipose tissue ($p<0.001$ for *ADRB1* and $p=0.008$ for *ADRB2*). While there was no difference in regional α_1-adrenoceptor expression, a higher mRNA expression of α_2-adrenoceptors was found in femoral adipose tissue ($p<0.001$ for *ADR2A*). There was no correlation between BMI or WHR and regional adrenoceptor mRNA expression.

The regional expression of adrenoceptor subtypes varied significantly between sexes. Women had a higher expression of abdominal β_1-adrenoceptors and a lower abdominal and femoral α_1-adrenoceptor expression compared to men (see Figures 5.9 and 5.10). The difference between abdominal and femoral α_1-adrenoceptor expression in men and women was independent of BMI and fat distribution (ANCOVA $p<0.05$ for abdominal *ADRA1A* expression; ANCOVA $p=0.001$ for femoral *ADRA1A* expression; both with BMI and WHR as covariates).

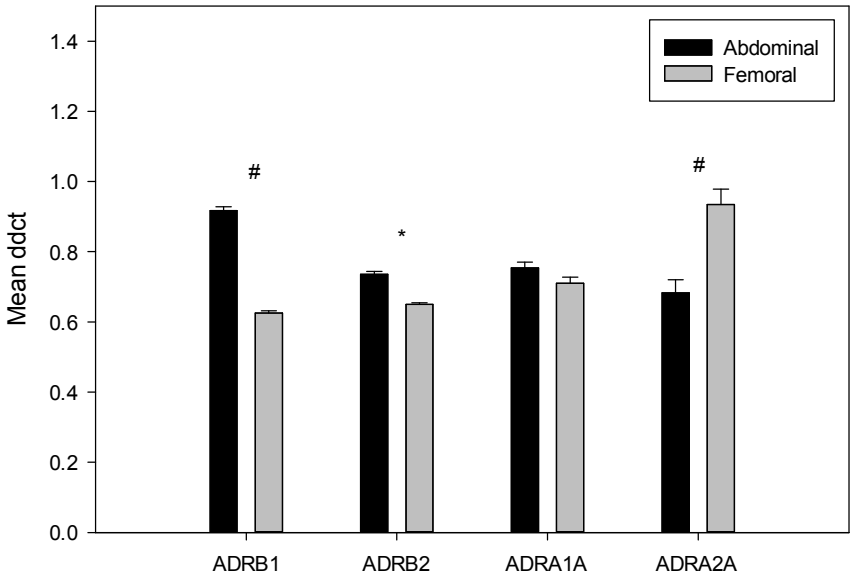

Figure 5.8: Abdominal and femoral RNA expression of adrenoceptor genes (n=28; *p<0.05, #p<0.001).

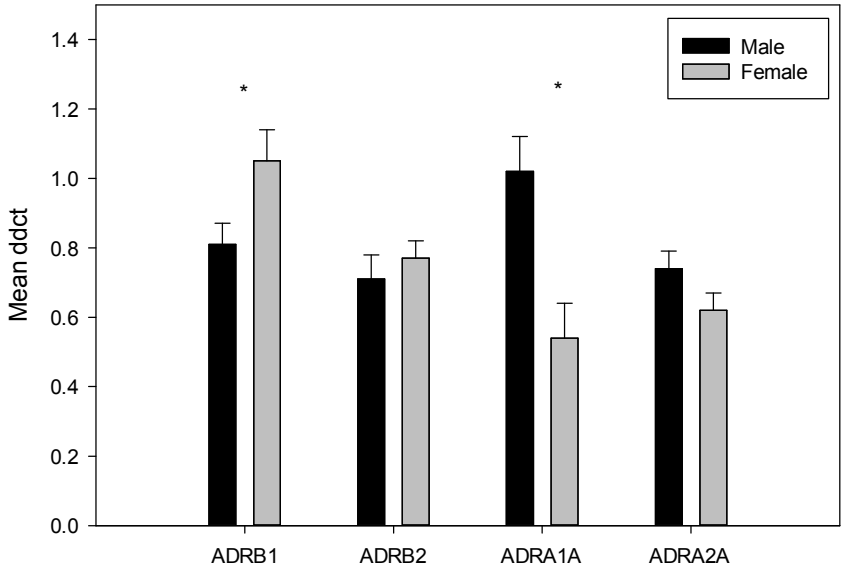

Figure 5.9: Abdominal RNA expression of adrenoceptor genes in men and women (n=28, 14 male; *p<0.05).

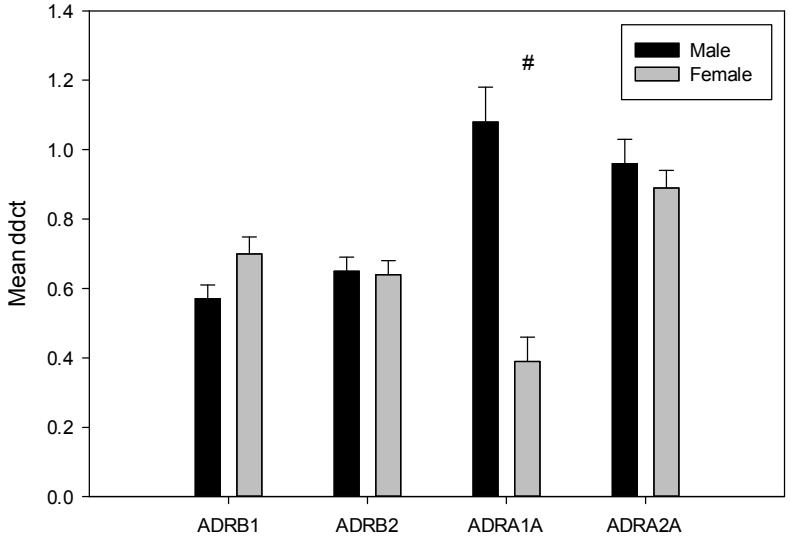

Figure 5.10: Femoral RNA expression of adrenoceptor genes in men and women ($^{\#}p<0.001$).

5.4 Discussion

The combination of local microinfusion with a systemic adrenaline infusion allowed testing the regional effect of α-adrenergic blockade on ATBF *in vivo*. The methodology used has the limitation that only ATBF effects can be studied, since the local microinfusion does not exert any large tissue effects that could be measured by the AV difference technique. It is possible to extrapolate the ATBF findings to whole tissue metabolism and to assume that the observed greater α-adrenoceptor responsiveness in femoral adipose tissue, compared with abdominal adipose tissue, is the primary mechanism for the blunted femoral lipolytic response to adrenaline described in Section 4.3.3. However, the differences seen between femoral ATBF response and lipolysis rate during adrenaline infusion suggest that regional adrenoceptor distribution might differ between adipose tissue vasculature and adipocytes (see discussion in Section 4.4). To date, no technique exists for measuring directly regional lipolysis during selective adrenoceptor blockade for a specific adipose tissue depot *in vivo*.

The observed systemic adrenaline effects on haemodynamic parameters and lipolysis in this study were comparable to those described in Chapter 4 (see section 4.3.1). This suggests that there was no overspill of the locally-infused propranolol/phentolamine into the systemic circulation. The clear differences in ATBF effect found between microinfusion sites also suggest that there was no “cross-

contamination" between microinfusion catheters, especially in abdominal adipose tissue where the probes were placed in relatively close proximity to each other (see Figure 5.1). The clear differences seen between saline and propranolol microinfusion sites also make the possibility of "cross-contamination" with ^{133}Xe between sites unlikely.

The study of α- and β-adrenoceptor blockade in abdominal adipose tissue confirms that the main stimulus for the ATBF increase during lipolysis is mediated by β-adrenoceptors. The importance of β-adrenoceptors in abdominal adipose tissue is underlined by the finding of a greater expression of β-adrenoceptors on mRNA level in this adipose tissue depot compared with the femoral depot. An interesting finding was the lack of difference in basal ATBF between the three microinfusion sites, despite the fact that a 60 min period of continuous α- and β-adrenoceptor blockade had preceded the start of the adrenaline infusion. This provides further evidence for the hypothesis that basal (postabsorptive) ATBF tone is not regulated by catecholamines, but by other vasoactive mediators, e.g. nitric oxide (18).

The major finding of this study was that the observed blunted response of femoral ATBF to adrenaline is due to a greater local responsiveness of α-adrenoceptors compared with abdominal adipose tissue. The mRNA expression studies confirmed a greater expression of α2-adrenoceptors in femoral adipose tissue compared with the abdominal depot, in line with the findings of the physiological studies *in vivo*. Once the α-adrenoceptors were blocked, the femoral ATBF response was comparable to abdominal adipose tissue. So far only indirect evidence supporting local vascular α-adrenoceptor activity in lower-body adipose tissue has been published (116). The study described in this Chapter provides direct evidence using a quantitative measurement of ATBF during local α-adrenoceptor blockade. The hypothesis of a local *in vivo* effect of α-adrenoceptors on femoral lipolysis remains to be tested directly, although the data in this thesis point strongly towards it.

Based on the findings discussed in Chapter 4 (see Section 4.3.6) it could have been hypothesized that *ADRB2* haplotype-dependent variation in β2-adrenoceptor function could lead to adaptation in α- and/or β-adrenoceptor expression and/or sensitivity. The current study design would allow for such differences to become apparent, at least at vascular adrenoceptor level. However, stratification for the *ADRB2* haplotypes showed no significant effect of the β2-adrenoceptor-specific ATBF response to adrenaline during α- and β-adrenoceptor blockade. Although it is

possible that a haplotype effect was not detected because of the very small subgroups, it is more likely that other adaptational mechanisms play a role. This is not surprising, given that ATBF is regulated by the complex interplay of several mediators (23).

The comparison of the femoral ATBF response during α-adrenoceptor blockade in men and women provided compelling evidence for a greater responsiveness of vascular α-adrenoceptors in women compared with men. It also is in line with the findings in Chapter 3, where selective β-adrenoceptor stimulation with isoprenaline resulted in a higher femoral ATBF response in women (see Figures 3.18 and 3.19). However, analysis of adrenoceptor expression on RNA level was not in line with these physiological findings (possible reasons for this are discussed further below). Men showed a greater femoral adipose tissue expression of α1-adrenoceptors compared to women. This finding is also in contrast to the physiological findings of Chapter 4, where adrenaline infusion (without any α-adrenoceptor blockade) resulted in similar ATBF responses between men and women (see Figure 4.14). A similar leg plasma flow response during adrenaline infusion between men and women was also found by Jensen *et al.* (113), while microinfusion studies did not show any significant differences in femoral blood flow during local stimulation with isoprenaline, adrenaline or noradrenaline (227). Overall, male-female differences in regional ATBF regulation and in fatty-acid trafficking need further investigation. This is evident from the fact that when I compared femoral lipolysis in men and women, women had a higher basal and adrenaline-stimulated lipolysis rate (see Section 4.3.5). Again, this would be in contrast to the finding of greater α-adrenergic responsiveness in femoral adipose tissue of women. It is most certainly so that other factors, beyond simple differences in adrenoceptor density and/or sensitivity, are involved in differential regional adipose tissue function in men and women.

The apparently conflicting findings of regional adrenoceptor mRNA expression in men and women highlight a methodological problem with the technique of RNA extraction from crude adipose tissue biopsies. It is not clear which proportion of the RNA is derived from adipocytes and which from the stromavascular fraction. Moreover, adrenoceptor function depends upon a complex post-receptor regulation that determines receptor function *in vivo*. Therefore, the only approach for studying adipose tissue adrenoceptor function *in vitro* that may deliver reliable data is that of adrenoceptor binding studies on isolated adipocyte membranes (personal

communication M. Lafontan and D. Langin, INSERM, Toulouse, France; see also (228)).

In summary, with this study I confirmed that the observed regional differences in ATBF response and lipolysis to non-selective adrenergic stimulation are based on greater α-adrenoceptor responsiveness in femoral adipose tissue compared with abdominal adipose tissue. The overall lower responsiveness of femoral adipose tissue to catecholamine-mediated lipolysis suggests that the femoral adipose tissue depot is not participating in short-term trafficking of fatty acids but represents a long-term buffer. In the next Chapter I explore this hypothesis further by investigating femoral fatty-acid trafficking over a 24 h period.

6 Regional fatty acid trafficking over a 24h period

6.1 Introduction

So far, my work has concentrated on the differential aspects of catecholamine-induced lipolysis in abdominal and femoral adipose tissue. Catecholamine-induced lipolysis is important for the release of fatty acids during exercise and during periods of fasting and starvation (197, 229). In previous chapters I have shown that femoral adipose tissue is less responsive to the physiological adrenergic stimulus of adrenaline in terms of ATBF response and lipolytic rate *in vivo*. This suggests that the femoral adipose tissue depot is less responsive to high-demand lipolysis and could serve as a metabolic sink for dietary fatty acids, protecting other tissues from ectopic fat deposition by long-term storage of fatty acids. However, lipolysis is only one aspect of adipose tissue metabolism and in order to support this hypothesis, fatty acid uptake into abdominal and femoral adipose tissue has to be investigated.

Postprandial fatty acid uptake in adipose tissue is largely driven by the hydrolysis of chylomicron-derived TG by LPL, a process under the control of insulin (see Section 1.2.1). In addition, adipose tissue takes up NEFA from the circulating pool – a process termed “direct NEFA uptake” (134). The physiology of fatty acid trafficking in abdominal adipose tissue has been studied extensively *in vivo*. Uptake of dietary fatty acids into abdominal adipose tissue occurs for up to 5 hours postprandially (230, 231). Using stable isotope tracers and the AV difference technique, it was found that abdominal adipose tissue preferentially takes up fatty acids released by LPL from chylomicrons in comparison to circulating NEFA (134). Furthermore, over a 24h period, abdominal adipose tissue adapted and increased its ability to absorb chylomicron-derived fatty acids with each meal given (2). In contrast, the postprandial abdominal fatty acid uptake over 24h was blunted in obesity (114).

Few studies have been published that compare abdominal and gluteofemoral postprandial fatty acid trafficking. When studied using radioactive tracers and timed biopsies after a single meal, abdominal adipose tissue appeared to take up fatty acids more avidly than femoral adipose tissue (104). The same study found that women take up a larger proportion of dietary fatty acids compared to men. Using the same radioactive tracer technique it was also found that body fat distribution influences regional fatty acid trafficking. Lower-body obese women took up more

dietary-derived fatty acids in gluteal adipose tissue than upper-body obese women and men (232). The uptake of dietary fatty acids in femoral adipose tissue increased in parallel with increasing leg fat mass (233). Furthermore, men were found to suppress abdominal lipolysis less than women after ingestion of a meal (234).

Recently, femoral and abdominal postprandial fatty acid trafficking and ATBF after a single mixed meal were studied using the AV difference technique and ^{133}Xe washout (106). Both abdominal and femoral ATBF increased similarly during the postprandial period, and direct NEFA and VLDL-derived TG uptake were similar between the two fat depots. However, abdominal adipose tissue showed a higher extraction rate of chylomicron-derived TG than femoral adipose tissue. This finding suggests that abdominal adipose tissue is more metabolically active with respect to short-term diet-related fatty acid trafficking, while femoral adipose tissue acts as a long-term store of circulating fatty acids that may have not been stored in adipose tissue immediately after a meal.

To date, there are no studies comparing abdominal and femoral fatty acid trafficking over a 24 h period. The study of regional fatty acid fluxes in relation to three meals and an overnight postabsorptive period could contribute significantly to our understanding of the physiological role of femoral adipose tissue as a distinct fat depot that acts as a “metabolic sink”.

6.2 Study design and participants

The study design comprised the feeding of three meals containing fatty acids labelled with isotope tracer and the investigation of abdominal and femoral ATBF and fatty acid trafficking over 24 h. The methods I used were the following:

- Recruitment of participants using the Oxford BioBank (see Section 2.7)
- Measurement of baseline anthropometric characteristics, including total body and regional fat mass with DXA (see Section 2.7.2)
- Insertion of an arterial catheter and two catheters into veins draining abdominal and femoral adipose tissue for AV difference calculation purposes (see Section 2.2)
- Monitoring of abdominal and femoral ATBF with ^{133}Xe washout (see Section 2.1.1)

- Feeding of three mixed meals containing fatty acids labelled with three different isotope tracers (see Section 2.4.2)
- Calculation of regional ATBF and fatty acid fluxes (see Section 2.6)

In total, eight healthy male volunteers were recruited. Their baseline characteristics are shown in Table 6.1.

Table 6.1: Baseline anthropometric and metabolic characteristics of subjects

	Male (n=8)
Age	39 (33-52)
BMI	25.2 (21.9-27.5)
WHR	0.95 (0.92-1.01)
Body fat %	26.8 (19.5-29.6)
Fasting TG (μmol/l)	900 (500-1400)
Fasting NEFA (μmol/l)	400 (190-570)
Fasting glucose (mmol/l)	5.3 (4.5-5.7)
Fasting insulin (mIU/l)	13.3 (5.2-16.8)

Median and range shown

The participants arrived after an overnight fast and the femoral artery and two veins draining abdominal and femoral adipose tissue were catheterised as described before (see Section 2.2). A further cannula was placed into an antecubital vein for infusion purposes. After a basal sample was taken, a continuous infusion of [$^2H_2$]-palmitate was commenced at a rate of 1 μmol.min^{-1}.kg FFM^{-1} and maintained until the end of the study (see Section 2.4.1). Xenon was injected 2-3 cm laterally of the umbilicus into abdominal adipose tissue and into femoral adipose tissue of the anterior aspect of the thigh for the measurement of ATBF (see Section 2.1.1). ATBF was measured throughout the study. After 60 min of equilibration, three mixed meals were given: Breakfast at 0h (9:00 h, Meal 1), lunch at 5h (14:00 h, Meal 2) and dinner at 10h (19:00 h, Meal 3). For data analysis, the five hours following each meal were regarded as postprandial periods (0-300 min, 300-600 min and 600-900 min respectively). The time from 900 min to the end of the study at 1440 min was regarded as the postabsorptive period.

The energy content of each meal was adjusted to the estimated basal metabolic rate of each participant as previously described (2, 114). Each meal contained fatty acids in the form of a drink labelled with a different isotope tracer (see Section 2.4.2 and Appendix). The breakfast drink contained 100 mg [U-^{13}C]linoleic acid, lunch and dinner drinks contained 100 mg [U-^{13}C]oleic acid and [U-^{13}C]palmitic acid respectively. Blood samples were taken from all three sites simultaneously at frequent intervals during the day and the night. Apart from three short bouts of gentle exercise (walking), the participants spent their time semirecumbent in bed.

Using the three different isotopes for labelling dietary fatty acids, it is possible to trace the fate of dietary fatty acids over the 24 h period (2). As described in Section 2.4, the [$^2H_2$]-palmitate infusion allows for the calculation of Ra_{NEFA}. Furthermore, [$^2H_2$]-labelled fatty acids are incorporated into VLDL-TG in the liver and it is therefore possible to measure VLDL-TG extraction and compare it to dietary (chylomicron) TG extraction across adipose tissue (2). Furthermore, [$^2H_2$]-labelled NEFA extraction across adipose tissue is a measure of direct NEFA uptake. For technical reasons, isotope data with regards to meal-derived fatty acids were available for n=7, while data based on the [$^2H_2$]-labelled palmitate infusion were available for n=6 studies.

6.3 Results

6.3.1 Systemic metabolic data

Each meal was followed by a physiological response in plasma glucose, insulin, NEFA and TG concentrations. Plasma glucose concentrations increased within 40 min after each meal to 40% ($p=0.003$), 46% ($p=0.001$) and 61% ($p<0.001$) above baseline respectively (see Figure 6.1). The rise in plasma glucose was matched with a consecutive rise of plasma insulin concentrations by 495% ($p=0.003$), 370% ($p=0.01$) and 590% ($p=0.001$) from baseline respectively (see Figure 6.1). The time-averaged AUC for glucose, as a marker of the overall glucose rise between meals, was comparable between all three meals (see Figure 6.2). There was a statistically significant difference between the time-averaged breakfast and dinner glucose rise ($p<0.05$; see Figure 6.3). The physiological relevance of this is questionable and the time-averaged insulin response was similar between all three meals (see Figure 6.3). During the nightly postabsorptive period, plasma glucose and insulin concentrations returned back to baseline ($p<0.05$ compared to postprandial concentrations for both glucose and insulin).

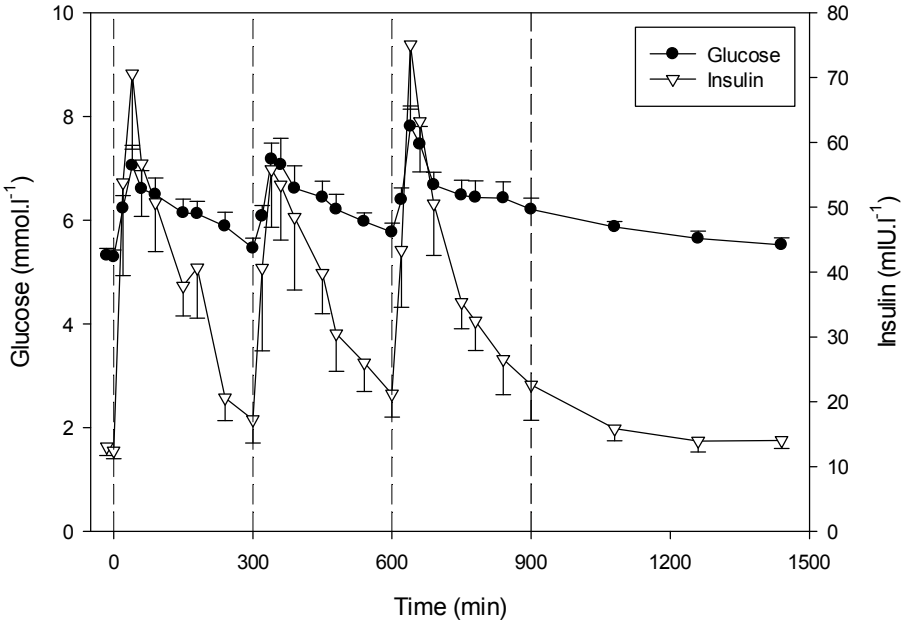

Figure 6.1: Plasma glucose and insulin concentrations over 24h (meals and start of postabsorptive period indicated by vertical lines).

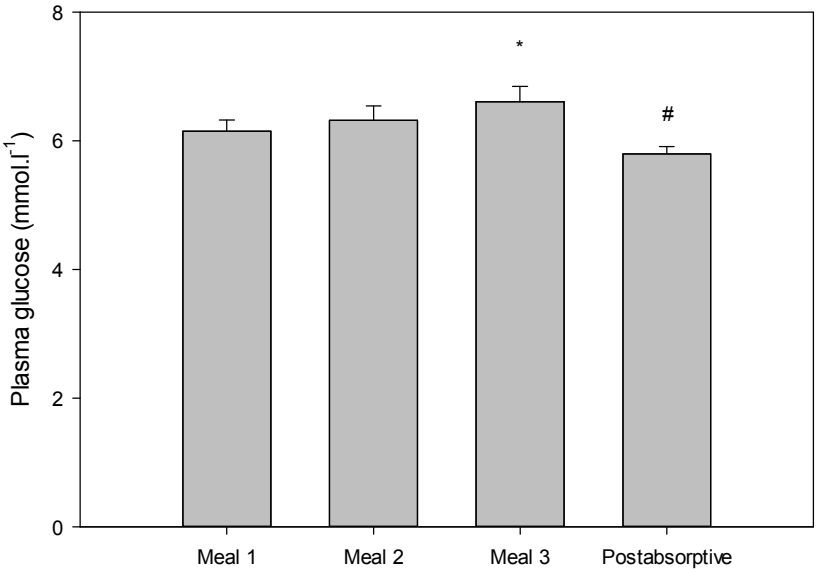

Figure 6.2: Time-averaged AUC for plasma glucose for each postprandial and the postabsorptive period (*p<0.05 compared to first meal, #p<0.05 compared to all three meals).

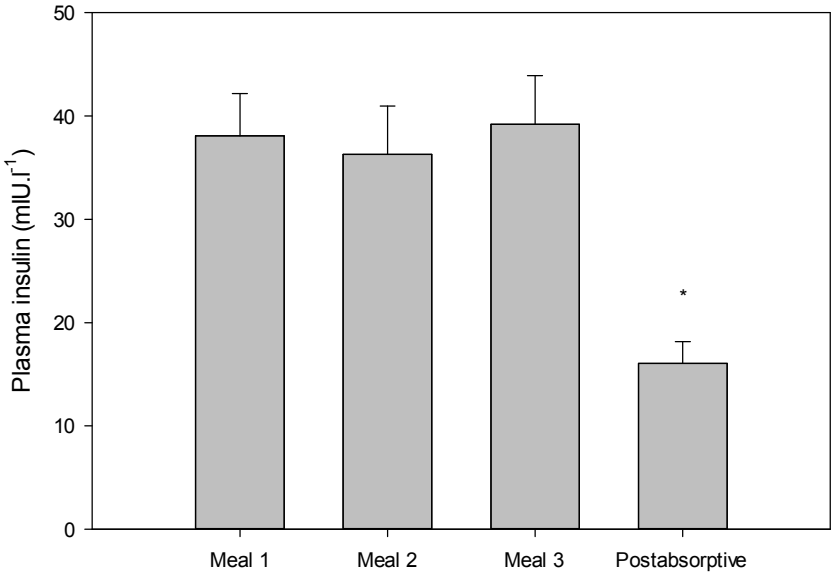

Figure 6.3: Time-averaged AUC for plasma insulin for each postprandial and the postabsorptive period (*p<0.05 compared to all three meals).

Systemic NEFA concentrations were highest in the fasting state before, and decreased rapidly after, breakfast and each of the following meals (see Figure 6.4). Given that lipolysis is suppressed by insulin (see Section 1.2.1), plasma NEFA concentrations rose before lunch and dinner and during the night in line with the decrease in plasma insulin concentrations (see Figure 6.4 and Figure 6.1 for insulin concentrations). Plasma NEFA concentrations naturally rose most during the postabsorptive period at night.

Expectedly, each meal led after 3-4h to an increase in plasma TG concentrations (see Figure 6.5). Plasma TG concentrations rose most after the second meal (see Figure 6.6; $p<0.05$ compared to first meal). During the postabsorptive period plasma TG concentrations returned to baseline ($p<0.001$ compared to postprandial concentrations).

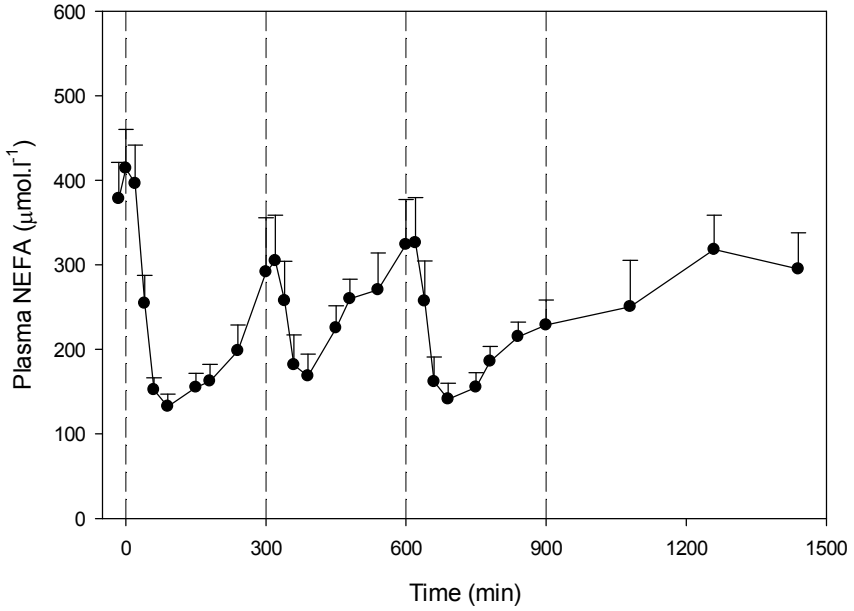

Figure 6.4: Plasma NEFA concentrations over 24h (meals and start of postabsorptive period indicated by vertical lines).

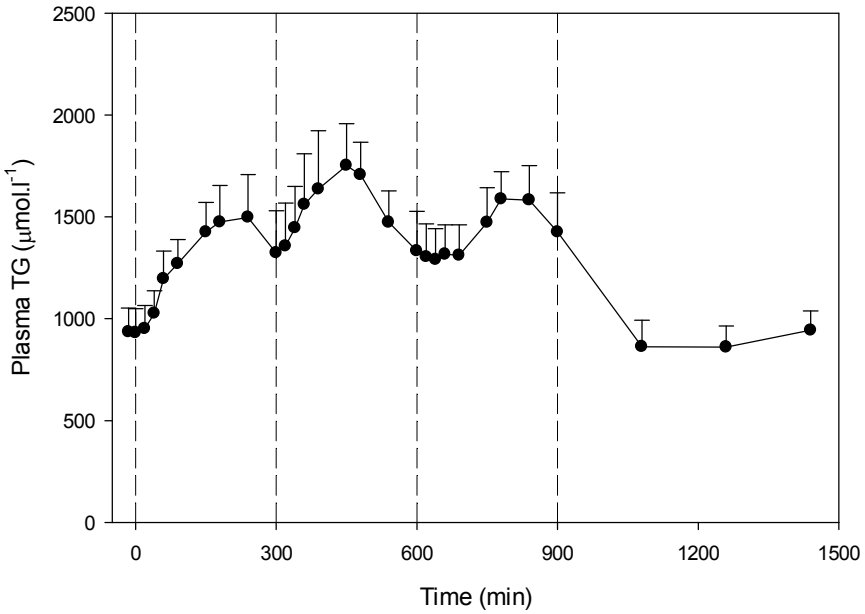

Figure 6.5: Plasma TG concentrations over 24h (meals and start of postabsorptive period indicated by vertical lines).

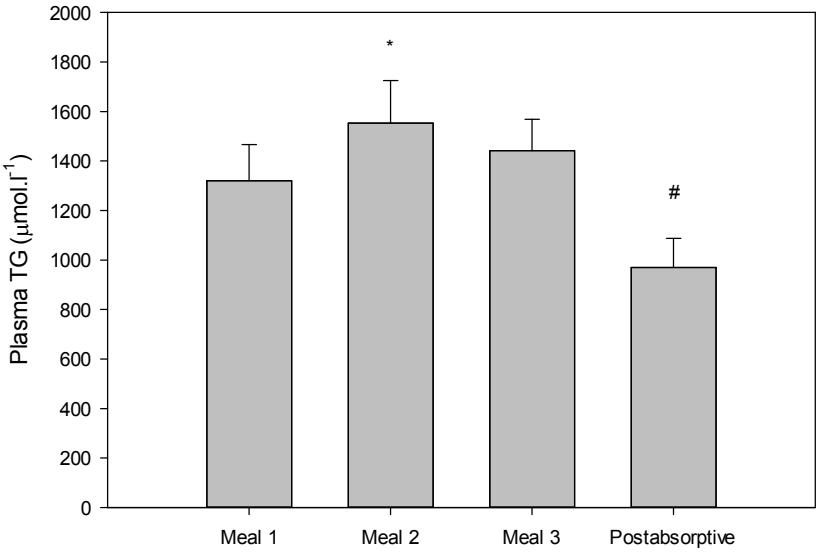

Figure 6.6: Time-averaged AUC for plasma TG for each postprandial and the postabsorptive period (*p<0.05 compared to first meal, #p<0.001 compared to all three meals).

6.3.2 Regional ATBF response

Abdominal basal ATBF was 3.1±0.5 ml.min^{-1}.100g tissue^{-1} and femoral basal ATBF was 2.6±0.5 ml.min^{-1}.100g tissue^{-1} (see Figure 6.8). There was a 2-fold increase in abdominal and femoral ATBF after each meal (ANOVA $p<0.05$ for time effect). There was no difference between the two adipose tissue depots with respect to the postprandial ATBF response after each meal or during the night period. However, the overall postprandial ATBF response and the ATBF response over the whole 24h period, calculated as the sum of postprandial AUC's and by comparison of the overall AUC respectively, was slightly lower in femoral adipose tissue ($p<0.05$ respectively; only data for postprandial AUC's shown in Figure 6.9). This is in line with the findings of the previous chapters, where femoral ATBF response was overall lower than abdominal.

Basal abdominal and femoral ATBF did not correlate with each other. There was a positive correlation between basal abdominal ATBF and the overall postprandial abdominal ATBF response (as AUC; Pearson $r=0.753$, $p<0.05$). The peak femoral ATBF after the first meal correlated positively with basal femoral ATBF (Pearson $r=0.836$, $p<0.05$). There was no association between regional ATBF responses to meals, with the exception of the peak ATBF after the second meal which correlated positively between abdominal and femoral adipose tissue (Pearson $r=0.753$, $p<0.05$). There was an inverse relationship between ATBF responses and measures of obesity. The peak abdominal ATBF response after the first meal was negatively

associated to BMI (Pearson r=-0.825, p<0.05), as was the peak femoral ATBF response after the third meal (Pearson r=-0.918, p=0.001). Finally, there was an inverse correlation between the peak femoral ATBF response after the first meal and WHR (Pearson r=-0.792, p<0.05).

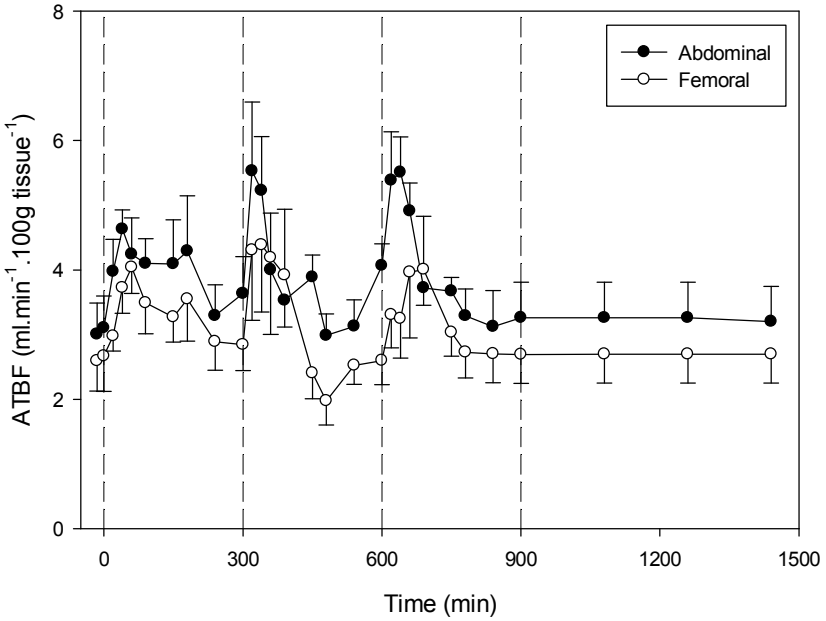

Figure 6.8: Abdominal and femoral ATBF over 24h (meals and start of postabsorptive period indicated by vertical lines).

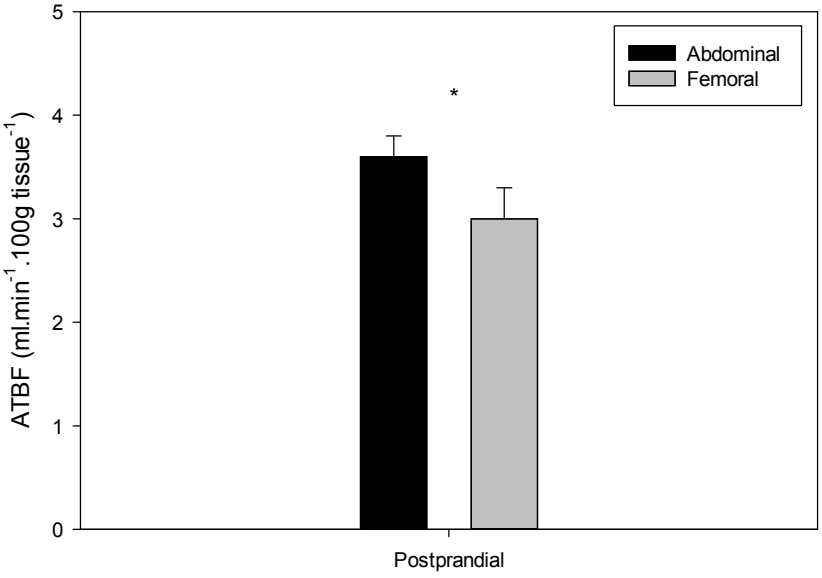

Figure 6.9: Comparison of total postprandial AUC's of regional ATBF (*p<0.05).

6.3.3 Regional metabolic non-isotope data

Abdominal and femoral glucose uptake increased significantly after each meal (see Figure 6.10). There was no difference in the regional glucose uptake between meals

(see Figure 6.11). As one would expect, glucose uptake was significantly lower during the postabsorptive period, where it remained stable around the baseline of 0.4 μmol.min^{-1}.100g tissue^{-1} in both adipose tissue depots ($p<0.05$ compared to postprandial concentrations).

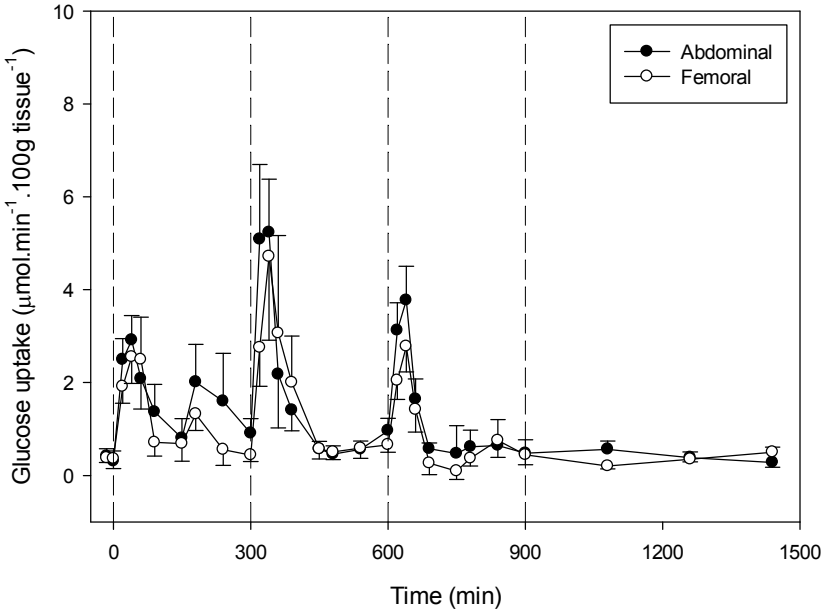

Figure 6.10: Abdominal and femoral glucose uptake over 24h (meals and start of postabsorptive period indicated by vertical lines).

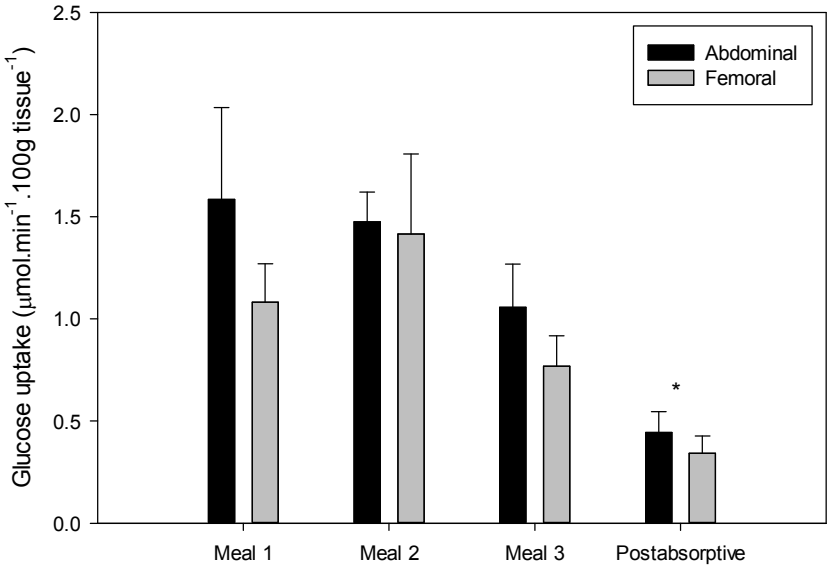

Figure 6.11: Time-averaged AUC for glucose uptake for each postprandial and the postabsorptive period (*p<0.05 compared to all three meals).

Regional NEFA release showed distinct depot-specific differences during the 24 h period. In both abdominal and femoral adipose tissue, NEFA release was rapidly suppressed after each meal (see Figure 6.12). However, femoral NEFA release was

lower in each postprandial period which resulted in smaller release rate changes postprandially (ANOVA $p<0.05$ for site by time interaction). During the nightly postabsorptive period, the NEFA release rate increased faster in the abdominal adipose tissue depot, while the femoral adipose tissue change in release rate was much less pronounced (Wilcoxon $p<0.05$ at 1260 min and $p=0.05$ at 1440 min; see Figure 6.12). The quiescence of femoral adipose tissue NEFA release becomes best evident when the time-averaged AUC for the total postprandial and the postabsorptive periods are compared between depots (see Figure 6.13; Wilcoxon $p<0.05$ for comparison of postprandial NEFA release, $p=0.05$ for postabsorptive period comparison).

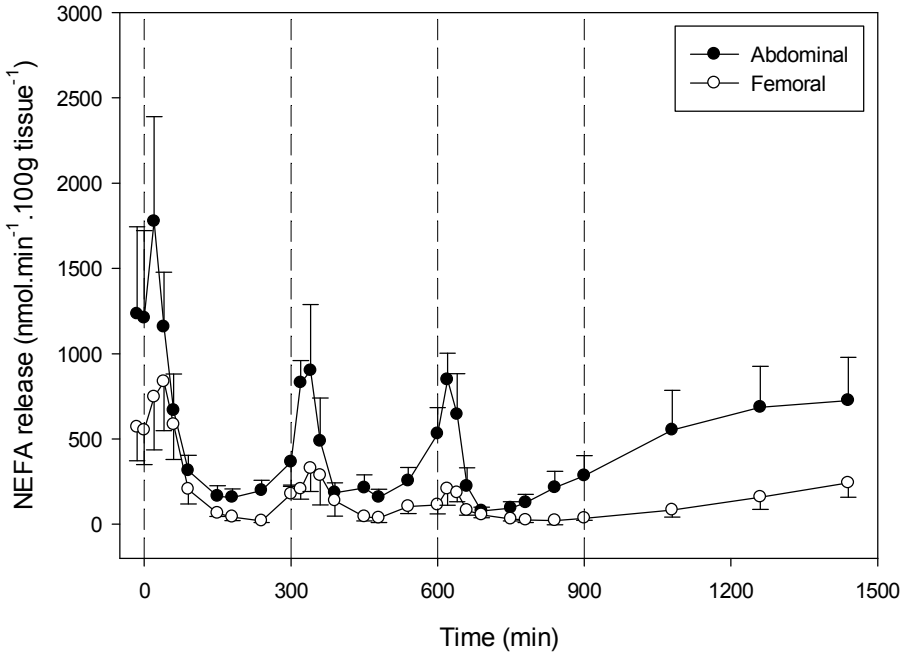

Figure 6.12: Abdominal and femoral NEFA release over 24h (meals and start of postabsorptive period indicated by vertical lines).

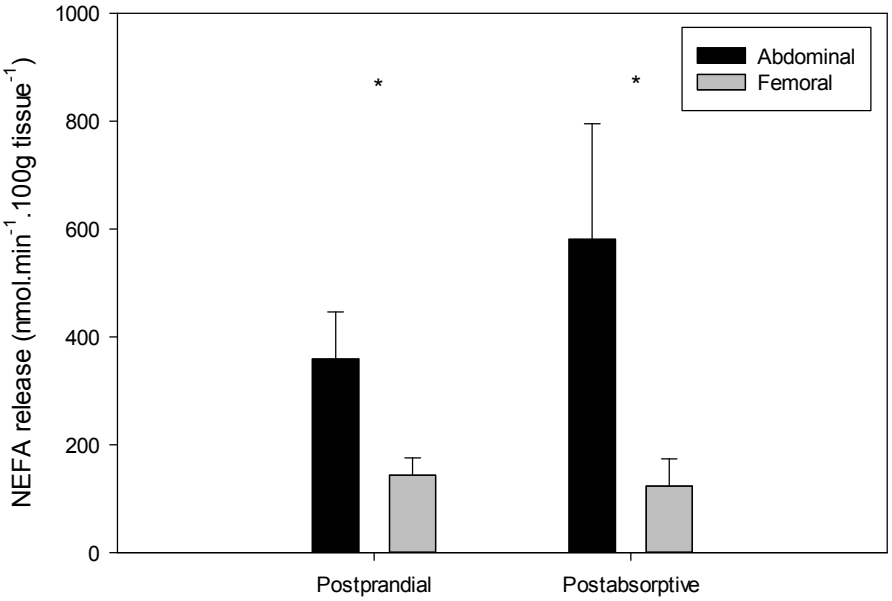

Figure 6.13: Time-averaged AUC for regional NEFA release for the total postprandial and the postabsorptive period (*p<0.05 between abdominal and femoral adipose tissue).

As described previously, abdominal and femoral adipose tissue show differential TG extraction rates after a meal, with femoral adipose tissue displaying a lower TG extraction rate (106). Over the 24 h period, femoral TG extraction remained lower than across abdominal adipose tissue (see Figure 6.14). Femoral adipose tissue TG extraction was lower after each meal, although it reached statistical significance after the first meal only ($p<0.05$ for AUC comparison). When the overall TG extraction rate (calculated as the sum of meal AUC's) was compared, femoral adipose tissue TG extraction rate was lower than in abdominal adipose tissue ($p<0.05$; see Figure 6.15). During the postabsorptive period, TG extraction rates were expectedly low and comparable between fat depots (Figure 6.15).

There was a negative correlation between basal abdominal TG extraction rate and BMI (Pearson $r=-0.769$, $p<0.05$). Apart from this, no other correlations between abdominal and femoral TG extraction rates or with regards to measures of obesity were found.

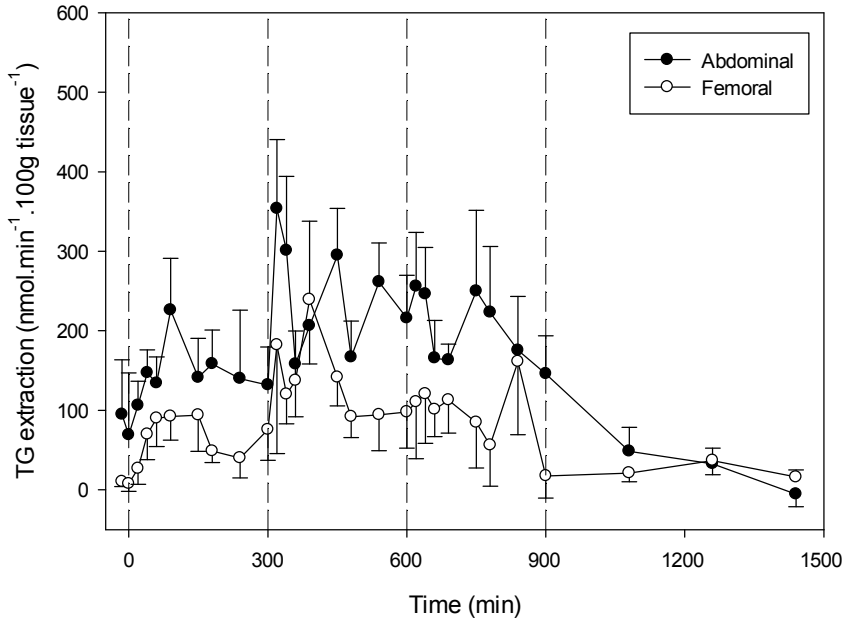

Figure 6.14: Abdominal and femoral TG extraction over 24h (meals and start of postabsorptive period indicated by vertical lines).

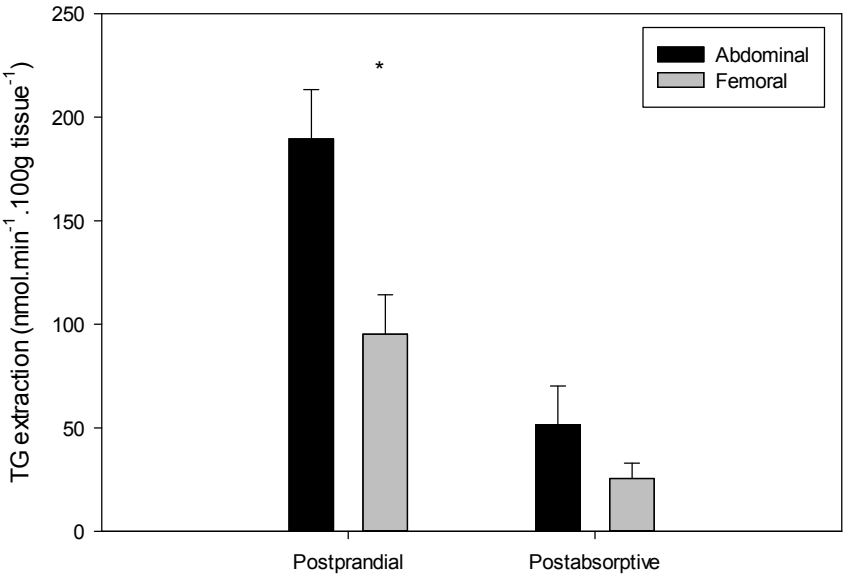

Figure 6.15: Time-averaged AUC for regional TG extraction for the total postprandial and the postabsorptive period (*p<0.05).

In order to assess the total fatty-acid movement across the two adipose tissue depots, I calculated the transcapillary flux (see Section 2.6). Before the first meal of the day, there was net outwards movement of fatty acids from both adipose tissue depots (see Figure 6.16). This changed soon after breakfast and from then on, there was net uptake into both abdominal and femoral adipose tissue throughout the day-

time. Once the postabsorptive period started, abdominal adipose tissue quickly returned to a net outward movement of fatty acids. However, femoral adipose tissue remained during most of the night in a state of inactivity, where fatty-acid trafficking stagnated. Only in the early hours of the morning, femoral fatty-acid trafficking returned to net release. In summary, fatty-acid trafficking during the postprandial periods was comparable between abdominal and femoral adipose tissue (see Figure 6.17). However, during the nightly postabsorptive period, abdominal and femoral adipose tissue fatty-acid trafficking was distinctly different, with femoral adipose tissue displaying the metabolic quiescence noted before (Wilcoxon $p<0.05$ for comparison between abdominal and femoral time-averaged postabsorptive transcapillary flux).

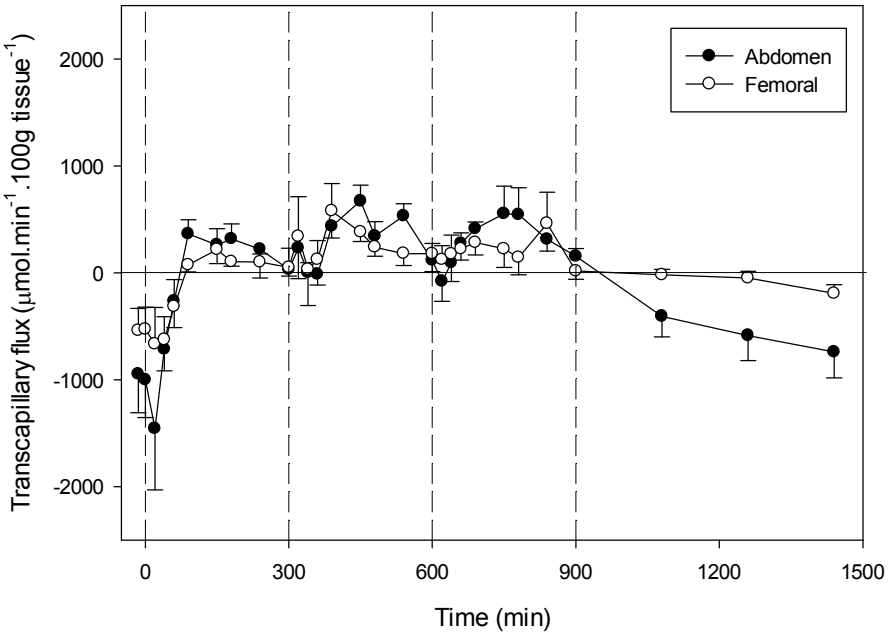

Figure 6.16: Transcapillary flux across abdominal and femoral adipose tissue over a 24h period (meals and start of postabsorptive period indicated by vertical lines).

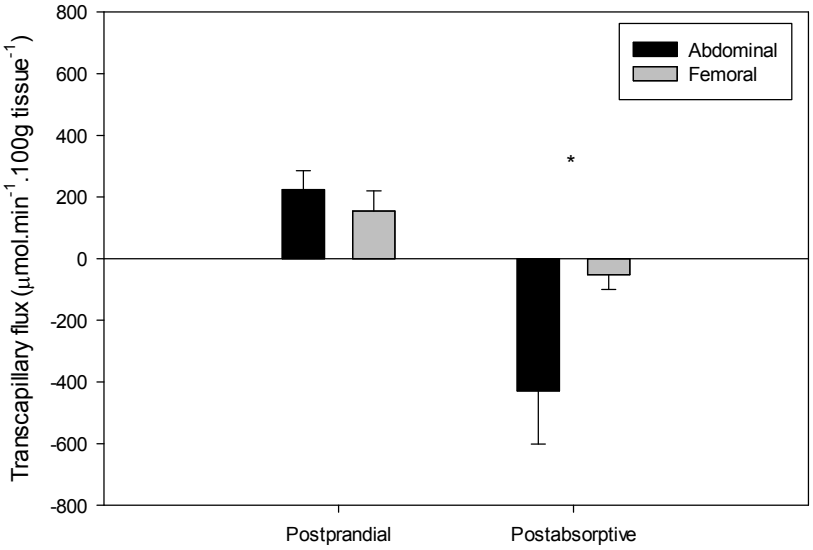

Figure 6.17: Time-averaged AUC for regional transcapillary flux for the total postprandial and the postabsorptive period (*p<0.05 between abdominal and femoral adipose tissue).

6.3.4 Regional metabolic isotope data

Whole body Ra_{NEFA} declined quickly after each meal in line with the postprandial suppression of adipose tissue lipolysis (see Figure 6.18). Despite a small increase in Ra_{NEFA} before lunch and dinner, it remained lower compared to the initial fasting value throughout the day. During the postabsorptive period, Ra_{NEFA} returned slowly back to the initial fasting levels in line with an increase in whole-body lipolysis.

As seen with the non-isotope data, regional Ra_{NEFA} was markedly different between abdominal and femoral adipose tissue (see Figure 6.19). In both adipose tissue depots Ra_{NEFA} declined rapidly after the first meal. In abdominal adipose tissue, there was a steady increase in Ra_{NEFA} during the postabsorptive period. In contrast, femoral adipose tissue remained suppressed up to the early hours of the morning (Wilcoxon $p<0.05$ for comparison between abdominal and femoral Ra_{NEFA} at 01:00 h (1080 min)).

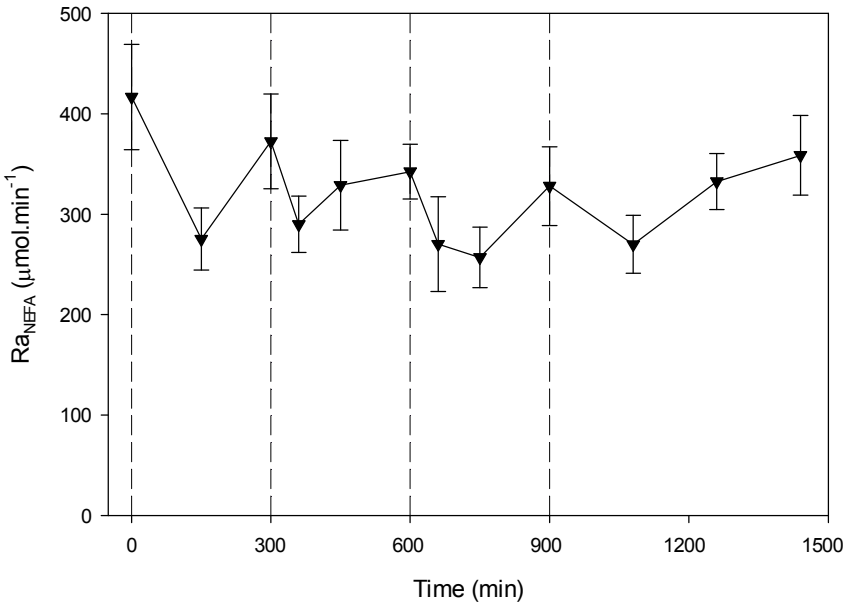

Figure 6.18: Whole body Ra_{NEFA} over a 24h period (meals and start of postabsorptive period indicated by vertical lines).

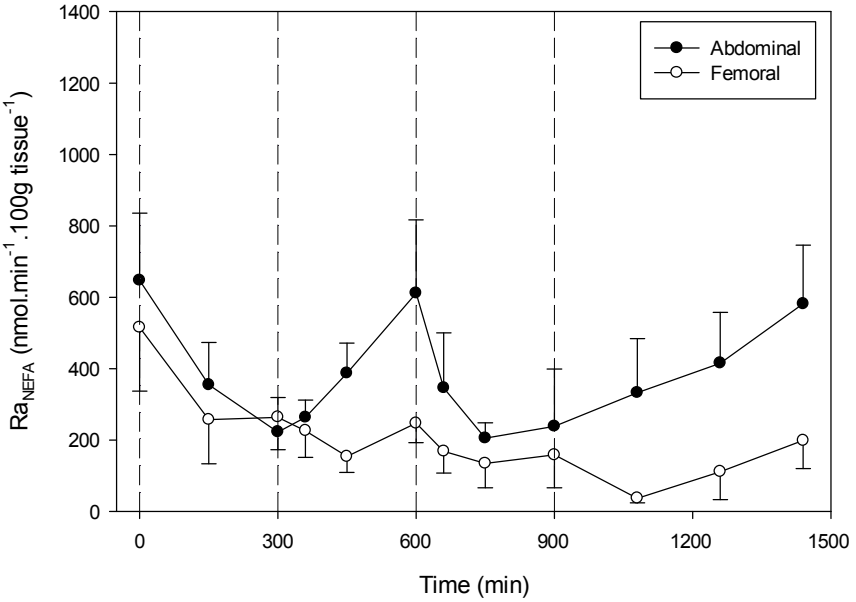

Figure 6.19: Regional Ra_{NEFA} over a 24h period (meals and start of postabsorptive period indicated by vertical lines). Note difference in units compared to Figure 6.18 (for calculations see Section 2.6.2).

Plasma TG concentration, labelled with the three different isotopic tracers (linoleic acid, oleic acid, palmitic acid at breakfast, lunch and dinner respectively) is shown in Figure 6.20. The first appearance of tracer in plasma is assumed to derive from chylomicron-TG, while later the tracers are likely to be found also in other lipoprotein classes (2).

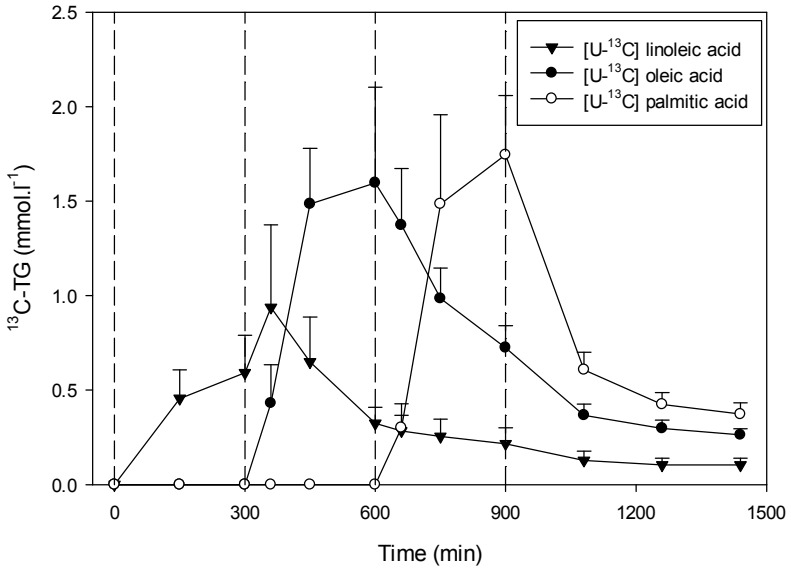

Figure 6.20: Plasma TG concentrations, labelled with three different stable isotopes (meals and start of postabsorptive period indicated by vertical lines).

Over the 24 h period, abdominal adipose tissue clearly extracted chylomicron-derived TG more avidly than femoral adipose tissue. This was seen both in the fractional extraction rate of TG labelled with each respective stable isotope (see Figure 6.21), as well as when comparing the total postprandial fractional extraction of TG (see Figure 6.22).

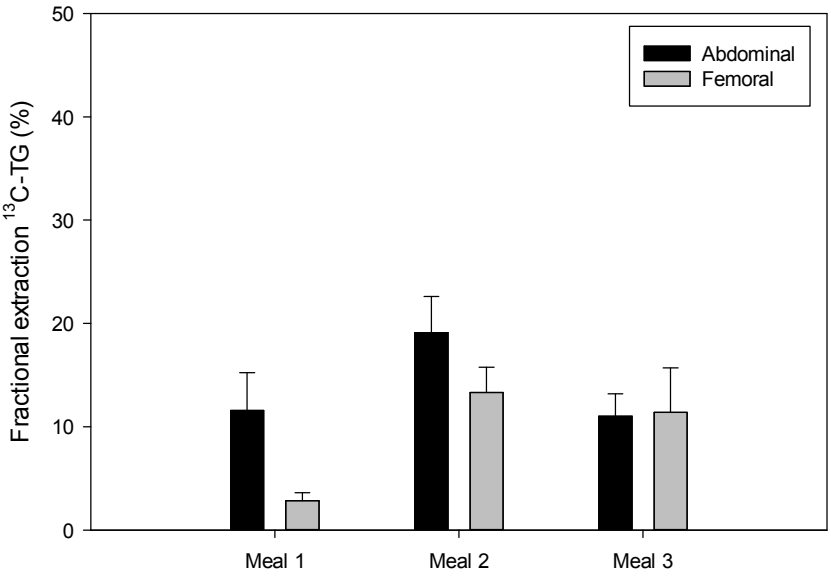

Figure 6.21: Regional fractional extraction of TG, labelled with [U-^{13}C]-linoleic acid (Meal 1), [U-^{13}C]-oleic acid (Meal 2) and [U-^{13}C]-palmitic acid (Meal 3).

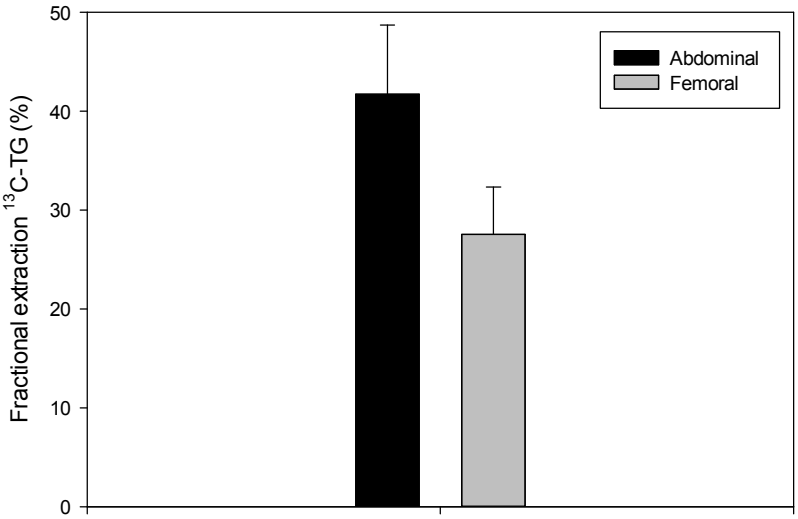

Figure 6.22: Regional fractional extraction of ^{13}C-TG for the total postprandial period (calculated as the sum of AUC of each postprandial period).

In contrast, when comparing VLDL-derived TG uptake and direct NEFA uptake, abdominal and femoral adipose tissue were similar (Figures 6.23 and 6.24). Given that the final participant numbers for this part of the data was very small, statistical analysis was not carried out. However, the findings are well in line with those of previous studies (2, 106, 114).

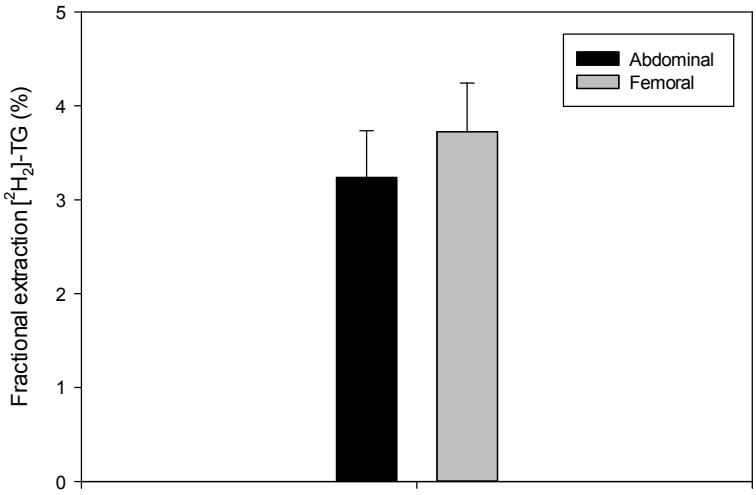

Figure 6.23: Regional fractional extraction of [$_2H^2$]-TG for the total 24h period (expressed as AUC).

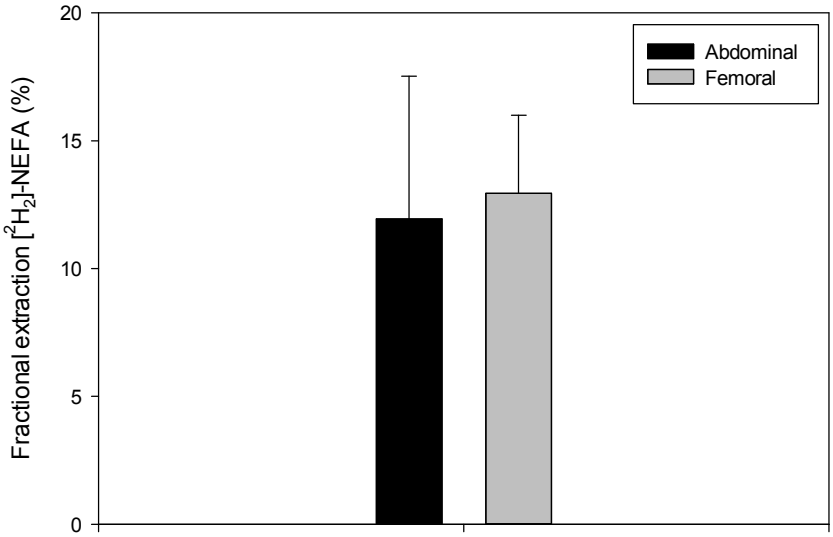

Figure 6.24: Regional fractional extraction of [$_2H^2$]-NEFA for the total 24h period (expressed as AUC).

6.4 Discussion

In this Chapter, I investigated the physiological fatty acid trafficking in abdominal and femoral adipose tissue that takes place over a 24 h period *in vivo*. The aim was to test the hypothesis that femoral adipose tissue is less metabolically active on a day-to-day basis and that it acts as a long-term store for fatty acids, thus preventing ectopic fatty acid deposition.

The results provide support for this hypothesis. Abdominal and femoral adipose tissue showed similar ATBF responses throughout the 24 h study period (Figure 6.8). This has been reported before in relation to the ATBF response after a single meal (106). Despite this, femoral adipose tissue showed a lower NEFA release rate and change in response to meals compared to abdominal adipose tissue (Figures 6.12 and 6.13). Furthermore, during the postabsorptive period, femoral adipose tissue did not switch to net release until the early hours of the morning (Figures 6.16 and 6.17), and then the NEFA release rate was still lower than in abdominal adipose tissue. This is in line with the findings of previous Chapters, where adrenaline-stimulated lipolysis was lower in femoral adipose tissue. It is known that lower-body fat is less metabolically active than abdominal fat in terms of fat mobilization (102). Here, for the first time, femoral adipose tissue is shown to display the same properties with regards to lipolysis in a physiological setting over 24 h.

In contrast, in the postprandial period, abdominal and femoral adipose tissue had comparable glucose uptake rates (Figures 6.10 and 6.11). A previous study using PET technology showed similar glucose uptake in abdominal and femoral adipose tissue during a normoglycaemic hyperinsulinaemic clamp (123). It was also comparable when studied with the AV difference technique after a single meal (106).

Abdominal adipose tissue was found to extract TG more avidly than femoral adipose tissue (Figure 6.15). The stable isotope data showed that this difference was accounted for largely by differential extraction of [U-^{13}C]-labelled (chylomicron) TG (Figure 6.22). In contrast, femoral adipose tissue extraction of [$^{2}H_{2}$]-TG (VLDL-derived TG) and of unbound NEFA was much more similar to that of the abdominal adipose tissue depot (Figures 6.23 and 6.24). These findings confirm previous studies of fatty acid trafficking across abdominal and femoral adipose tissue. The preferential uptake of chylomicron-derived fatty acids into abdominal adipose tissue after a single meal was reported by Bickerton *et al.* (134). McQuaid *et al.* confirmed that after a single meal femoral adipose tissue extracted less chylomicron-derived fatty acids compared to abdominal adipose tissue and that it might accumulate fatty acids not taken up by adipose tissue upon their first appearance in the circulation (106). Others have shown that in lower-body obese women more VLDL-TG, labelled *ex vivo* and given as a bolus infusion, is deposited in femoral than in abdominal adipose tissue (235). In addition, femoral VLDL-TG deposition appears to be a function of femoral adipose tissue mass, since the latter was found to be an independent predictor of VLDL-TG uptake efficiency (236).

Interestingly, it has been shown that abdominal adipose tissue is able to adapt its fatty acid extraction capabilities and that with each meal it becomes more effective in taking up dietary fatty acids (2). This feature of abdominal adipose tissue could only partially be replicated in my studies (Figure 6.21). The low fractional extraction of chylomicron-TG found during the postprandial period after dinner could be a result of the small numbers of available data sets for analysis and high background noise in the measurement of isotopic enrichment. In contrast, it was possible to show that important determinants of local adipose tissue function, i.e. ATBF response and basal TG-uptake, are inversely correlated with markers of obesity (Sections 6.3.2 and 6.3.3). It is known that dietary fatty acid uptake into abdominal adipose tissue is impaired in obesity (114).

Overall, the findings of this Chapter imply that once fatty acids have entered femoral adipose tissue, they are trapped and not released easily. Abdominal adipose tissue extracts preferentially diet-derived fatty acids and is the main source of NEFA during the night, acting as a short term buffer for fatty acids. Femoral adipose tissue may have a special role in taking up fatty acids that were not absorbed by adipose tissue in the first place and are recycled in the circulation either as VLDL-TG or as NEFA. This appears to be the physiological mechanism for the entrapment of fatty acids that would otherwise be deposited in organs other than adipose tissue, supporting the hypothesis that femoral adipose tissue acts as a “metabolic sink”.

7 Discussion

The aim of this thesis was to investigate fatty acid trafficking in abdominal and femoral adipose tissue *in vivo*, and to elucidate possible physiological mechanisms that render gluteofemoral adipose tissue protective against metabolic diseases. Differential adrenergic regulation *in vivo* appeared to be such a potential mechanism worth investigating, in light of its significant regulation of lipolysis and ATBF. A further objective was to investigate fatty-acid trafficking across abdominal and femoral adipose tissue over a 24 h period in order to establish whether there are any differences in the handling of fatty acids between the two fat depots over a longer period of time under "normal life" physiological conditions.

The studies of this thesis are based upon a large body of evidence showing that lower-body fat, i.e. gluteofemoral fat mass, is associated with a protective cardiovascular disease risk profile (see Section 1.3). In 2004, it was proposed that femoral adipose tissue acts as a metabolic sink, where TG-rich lipoproteins and dietary fatty acids are taken up, resulting in a favourable lipid profile in terms of cardiovascular risk (115). The storage of fatty acids in gluteofemoral adipose tissue would thus prevent ectopic fatty acid deposition in organs like the liver, skeletal muscle and pancreas, and also the accumulation of visceral adipose tissue – all factors that are clearly linked to insulin resistance and the metabolic syndrome (237). This hypothesis was supported by *in vitro* studies showing that gluteofemoral adipocytes display lower lipolytic rates than abdominal and visceral adipocytes (108, 238). Studies of fatty acid turnover suggested a slower turnover of dietary fatty acids in femoral than in abdominal adipose tissue (239). During periods of a negative energy balance, femoral fat mass was found to decrease more slowly than abdominal fat mass (240, 241).

A major finding of my studies was that, *in vivo,* femoral adipose tissue is less responsive to the stimulus of adrenaline compared to abdominal adipose tissue. Adrenaline resulted in a significant increase in abdominal ATBF and lipolysis rate, while femoral ATBF was slow to respond. The femoral lipolysis rate was found to be largely unchanged during adrenaline stimulation. Mechanistically, this is due to differences in the balance between local α- and β-adrenoceptor function, with femoral adipose tissue displaying a dominant α-adrenergic response during adrenaline stimulation. These findings are in line with a large body of evidence from *in vitro*

studies, showing that abdominal adipocytes have an increased β-adrenergic and decreased α_2-adrenergic sensitivity compared to gluteal/femoral adipocytes (108-110). Others, using microdialysis and radioactive tracer techniques, have also shown differential responses to adrenergic stimuli between abdominal and leg adipose tissue *in vivo* (111-113). However, there is not complete consistency in this area, probably due to methodological differences and limitations. In line with *in vitro* findings, Horowitz *et al.* found a blunted femoral lipolytic (measured as glycerol release with the microdialysis technique) and ATBF response to adrenaline in lean women (111). In contrast to my findings in Chapter 3, Guo *et al.* found decreased leg lipolysis (measured as palmitate release) compared to abdominal adipose tissue during β-adrenergic stimulation with isoprenaline in women (112). The same research group found that palmitate release from the leg increased in men, but not in women, during an adrenaline infusion (113). This was postulated to result in the typical female fat distribution phenotype of increased gluteofemoral fat mass. My studies confirmed some physiological differences in the lipolytic response to adrenaline between men and women. Women had a higher basal and adrenaline-stimulated femoral lipolysis rate, while, in terms of ATBF, responses to adrenaline were similar to those in men. I interpreted this as an indication of increased metabolic activity of female femoral adipose tissue. As discussed further below, regional fat depot formation and fat mass maintenance is determined by fat turnover, rather than just differences in the lipolytic rate. Clearly, male-female differences in regional fatty acid trafficking warrant further investigation.

My studies were the first to investigate adipose tissue lipolysis *in vivo* using an integrative physiological approach. The use of the AV difference technique allowed for the study of abdominal and femoral adipose tissue specifically. This is in contrast to using the whole leg model that has been used by other research groups. The proposed mechanism contributing to the protective role of femoral adipose tissue is that fatty acids, once stored in femoral adipose tissue, are not readily released upon adrenergic stimulation. Hence, the metabolic sink function of femoral adipose tissue might be based on a mechanism of decreased release. However, it is important to note that in addition to a differential release rate, there must also be a mechanism regulating femoral fatty acid uptake in a different way than in abdominal adipose tissue. An overall lower lipolysis rate must be balanced by an overall lower uptake rate. This is because otherwise femoral fat mass would increase steadily over time. In contrast, femoral fat mass remains stable over large time periods and changes

only in relation to hormonal changes, e.g. during lactation and menopause (242), or, of course, during positive energy balance.

Bickerton *et al.* studied postprandial fatty acid uptake into subcutaneous abdominal adipose tissue using the same integrative physiology methodology as I did in my studies (134). They reported that abdominal adipose tissue takes up both dietary (chylomicron-derived) and VLDL-derived fatty acids after ingestion of a meal. They also described for the first time direct NEFA uptake, i.e. the uptake of circulating plasma NEFA that were not contained in lipoprotein particles, by abdominal adipose tissue during this period. However, compared to chylomicron-derived fatty acids, the proportion of plasma NEFA taken up directly was minor. More recently, a study of fatty acid trafficking *in vivo* by McQuaid *et al.* showed that femoral adipose tissue does not extract dietary fatty acids to the same extent as abdominal adipose tissue (106). In contrast, the rates of VLDL-derived fatty acid extraction and direct NEFA uptake were comparable to abdominal adipose tissue. Hence, it was postulated that femoral adipose tissue preferentially takes up fatty acids that have been recycled through the liver or have been released by other adipose tissue depots.

Differential handling and turnover of fatty acids between abdominal and femoral fat depots was confirmed in my studies of 24 h duration described in Chapter 6. In contrast to abdominal adipose tissue, femoral adipose tissue did not switch to net fatty acid release during the postabsorptive period. This confirms that femoral adipose tissue acts as a long-term storage depot of fatty acids *in vivo*. Furthermore, I showed that over the course of 24 h, femoral adipose tissue preferentially extracts VLDL-derived fatty acids and plasma NEFA.

The findings of my studies support the metabolic sink hypothesis, and suggest that an important determinant of cardiovascular disease risk is the balance between subcutaneous adipose tissue depots with regards to fatty acid trafficking and turnover. Subcutaneous adipose tissue is the dedicated organ for fatty acid storage. Abdominal adipose tissue appears to be the primary store for dietary fatty acids upon their first entry into the circulation. Interestingly, this feature of abdominal adipose tissue is impaired in obesity (114). Furthermore, obesity is characterized by adipose tissue dysfunction, as seen in studies of ATBF, which is linked to insulin resistance (20, 21). Situations where there is loss of femoral adipose tissue function, as clinically seen in Cushing's syndrome and partial lipodystrophy, are also clearly linked with an increased cardiovascular disease risk and insulin resistance (see

Section 1.3.2). Femoral adipose tissue conveys protection because it may have a special role in the uptake of fatty acids that have been recycled in the body and were not taken up by other adipose tissue depots when first entering the circulation. Moreover, fatty acids are trapped in femoral adipose due to the lower lipolysis rate compared to abdominal adipose tissue.

Future research will need to focus on the physiology of fatty acid redistribution between fat depots. Direct NEFA uptake could be such a mechanism determining regional fat depot mass and its impact on metabolic health. For example, direct NEFA uptake has been proposed as a means of maintaining the increased gluteofemoral fat mass in women, since they displayed higher rates of direct NEFA uptake when investigated using radioactive tracers and timed biopsies (243). However, little is known as to whether this pathway also contributes e.g. to the increased visceral fat mass found in obesity (52). Recently, it was shown that direct NEFA uptake per unit fat mass is higher in visceral than in subcutaneous adipose tissue (244). Moreover, current physiological studies have focused around situations of energy balance, when fat depot mass should remain fairly constant and redistribution rates among fat depots should be low. A chronic positive energy balance, associated with the Western lifestyle and leading to obesity, could have significant implications in fatty acid trafficking pathways between adipose tissue depots. Of special interest is the ability of the femoral adipose tissue depot to expand in response to chronic positive energy balance, which could be beneficial with regards to cardiovascular and metabolic risk. Whether the inability of femoral adipose tissue to expand and buffer an increased flow of recycled fatty acids ultimately leads to ectopic fatty acid deposition, remains to be investigated. The study of upper-body versus lower-body obese individuals in chronic positive energy balance might provide further insight into the physiology of regional fatty acid trafficking.

8 References

1. KN Frayn, P Arner, H Yki-Jarvinen. Fatty acid metabolism in adipose tissue, muscle and liver in health and disease. Essays Biochem. 2006;42:89-103

2. T Ruge, L Hodson, J Cheeseman, AL Dennis, BA Fielding, SM Humphreys, KN Frayn, F Karpe. Fasted to fed trafficking of fatty acids in human adipose tissue reveals a novel regulatory step for enhanced fat storage. J Clin Endocrinol Metab. 2009;94:1781-1788

3. RV Farese, Jr., TJ Yost, RH Eckel. Tissue-specific regulation of lipoprotein lipase activity by insulin/glucose in normal-weight humans. Metabolism. 1991;40:214-216

4. M Febbraio, DP Hajjar, RL Silverstein. CD36: a class B scavenger receptor involved in angiogenesis, atherosclerosis, inflammation, and lipid metabolism. J Clin Invest. 2001;108:785-791

5. H Eriksson, M Ridderstrale, E Degerman, D Ekholm, CJ Smith, VC Manganiello, P Belfrage, H Tornqvist. Evidence for the key role of the adipocyte cGMP-inhibited cAMP phosphodiesterase in the antilipolytic action of insulin. Biochim Biophys Acta. 1995;1266:101-107

6. P Chakrabarti, KV Kandror. FoxO1 controls insulin-dependent adipose triglyceride lipase (ATGL) expression and lipolysis in adipocytes. J Biol Chem. 2009;284:13296-13300

7. KN Frayn. Metabolic regulation: a human perspective. 3rd edition. 2010; Wiley-Blackwell

8. R Zimmermann, JG Strauss, G Haemmerle, G Schoiswohl, R Birner-Gruenberger, M Riederer, A Lass, G Neuberger, F Eisenhaber, A Hermetter, R Zechner. Fat mobilization in adipose tissue is promoted by adipose triglyceride lipase. Science. 2004;306:1383-1386

9. C Londos, C Sztalryd, JT Tansey, AR Kimmel. Role of PAT proteins in lipid metabolism. Biochimie. 2005;87:45-49

10. KN Frayn, F Karpe, BA Fielding, IA Macdonald, SW Coppack. Integrative physiology of human adipose tissue. Int J Obes Relat Metab Disord. 2003;27:875-888

11. JT Tansey, AM Huml, R Vogt, KE Davis, JM Jones, KA Fraser, DL Brasaemle, AR Kimmel, C Londos. Functional studies on native and mutated forms of perilipins. A role in protein kinase A-mediated lipolysis of triacylglycerols. J Biol Chem. 2003;278:8401-8406

12. KN Frayn. Non-esterified fatty acid metabolism and postprandial lipaemia. Atherosclerosis. 1998;141 Suppl 1:S41-46

13. KN Frayn, S Shadid, R Hamlani, SM Humphreys, ML Clark, BA Fielding, O Boland, SW Coppack. Regulation of fatty acid movement in human adipose

tissue in the postabsorptive-to-postprandial transition. Am J Physiol. 1994;266:E308-317

14. M Lafontan, D Langin. Lipolysis and lipid mobilization in human adipose tissue. Prog Lipid Res. 2009;48:275-297

15. C Sengenes, M Berlan, I De Glisezinski, M Lafontan, J Galitzky. Natriuretic peptides: a new lipolytic pathway in human adipocytes. FASEB J. 2000;14:1345-1351

16. KN Frayn, IA MacDonald. Adipose tissue circulation. In: T Bennett and SM Gardiner, editors. Nervous control of blood vessels. 1st edition. 1996; Overseas Publishers Association

17. LK Summers, J Callow, JS Samra, IA Macdonald, DR Matthews, KN Frayn. The effect on adipose tissue blood flow of isoenergetic meals containing different amounts and types of fat. Int J Obes Relat Metab Disord. 2001;25:1294-1299

18. JL Ardilouze, BA Fielding, JM Currie, KN Frayn, F Karpe. Nitric oxide and beta-adrenergic stimulation are major regulators of preprandial and postprandial subcutaneous adipose tissue blood flow in humans. Circulation. 2004;109:47-52

19. GH Goossens, SE McQuaid, AL Dennis, MA van Baak, EE Blaak, KN Frayn, WH Saris, F Karpe. Angiotensin II: a major regulator of subcutaneous adipose tissue blood flow in humans. J Physiol. 2006;571:451-460

20. F Karpe, BA Fielding, V Ilic, IA Macdonald, LK Summers, KN Frayn. Impaired postprandial adipose tissue blood flow response is related to aspects of insulin sensitivity. Diabetes. 2002;51:2467-2473

21. LK Summers, JS Samra, SM Humphreys, RJ Morris, KN Frayn. Subcutaneous abdominal adipose tissue blood flow: variation within and between subjects and relationship to obesity. Clin Sci (Lond). 1996;91:679-683

22. F Karpe, BA Fielding, JL Ardilouze, V Ilic, IA Macdonald, KN Frayn. Effects of insulin on adipose tissue blood flow in man. J Physiol. 2002;540:1087-1093

23. P Perez-Matute, MJ Neville, GD Tan, KN Frayn, F Karpe. Transcriptional control of human adipose tissue blood flow. Obesity (Silver Spring). 2009;17:681-688

24. E Hagstrom-Toft, J Bolinder, U Ungerstedt, P Arner. A circadian rhythm in lipid mobilization which is altered in IDDM. Diabetologia. 1997;40:1070-1078

25. JS Samra, ML Clark, SM Humphreys, IA Macdonald, KN Frayn. Regulation of lipid metabolism in adipose tissue during early starvation. Am J Physiol. 1996;271:E541-546

26. JN Patel, SW Coppack, DS Goldstein, JM Miles, G Eisenhofer. Norepinephrine spillover from human adipose tissue before and after a 72-hour fast. J Clin Endocrinol Metab. 2002;87:3373-3377

27. KN Frayn. Fat as a fuel: emerging understanding of the adipose tissue-skeletal muscle axis. Acta Physiol (Oxf). 2010;199:509-518

28. M Lafontan, M Berlan. Fat cell adrenergic receptors and the control of white and brown fat cell function. J Lipid Res. 1993;34:1057-1091

29. J Ward, R Clarke, R Linden. Physiology at a glance. 1st edition. 2005; Blackwell Publishing

30. M Lafontan, P Barbe, J Galitzky, G Tavernier, D Langin, C Carpene, A Bousquet-Melou, M Berlan. Adrenergic regulation of adipocyte metabolism. Hum Reprod. 1997;12 Suppl 1:6-20

31. TW Burns, PE Langley, BE Terry, DB Bylund, BB Hoffman, MD Tharp, RJ Lefkowitz, JA Garcia-Sainz, JN Fain. Pharmacological characterizations of adrenergic receptors in human adipocytes. J Clin Invest. 1981;67:467-475

32. TJ Ulahannan, F Karpe, SM Humphreys, DR Matthews, KN Frayn. Effects of acute administration of doxazosin on fasting and postprandial haemodynamics and lipid metabolism in healthy subjects. Horm Metab Res. 2002;34:499-503

33. JG Salway. Metabolism at a glance. 3rd edition. 2004; Blackwell Publishing

34. C Holm, T Osterlund, H Laurell, JA Contreras. Molecular mechanisms regulating hormone-sensitive lipase and lipolysis. Annu Rev Nutr. 2000;20:365-393

35. H Olsson, P Stralfors, P Belfrage. Direct evidence for protein phosphatase-catalyzed dephosphorylation/deactivation of hormone-sensitive lipase from adipose tissue. Biochim Biophys Acta. 1984;794:488-491

36. E Degerman, P Belfrage, VC Manganiello. Structure, localization, and regulation of cGMP-inhibited phosphodiesterase (PDE3). J Biol Chem. 1997;272:6823-6826

37. C Wirsen. Adrenergic Innervation of Adipose Tissue Examined by Fluorescence Microscopy. Nature. 1964;202:913

38. BG Slavin, KW Ballard. Morphological studies on the adrenergic innervation of white adipose tissue. Anat Rec. 1978;191:377-389

39. M Rebuffe-Scrive. Neuroregulation of adipose tissue: molecular and hormonal mechanisms. Int J Obes. 1991;15 Suppl 2:83-86

40. TG Youngstrom, TJ Bartness. Catecholaminergic innervation of white adipose tissue in Siberian hamsters. Am J Physiol. 1995;268:R744-751

41. B Cousin, L Casteilla, M Lafontan, L Ambid, D Langin, MF Berthault, L Penicaud. Local sympathetic denervation of white adipose tissue in rats induces preadipocyte proliferation without noticeable changes in metabolism. Endocrinology. 1993;133:2255-2262

42. TJ Bartness. Dual innervation of white adipose tissue: some evidence for parasympathetic nervous system involvement. J Clin Invest. 2002;110:1235-1237

43. GA Hawkins, ST Weiss, ER Bleecker. Clinical consequences of ADRbeta2 polymorphisms. Pharmacogenomics. 2008;9:349-358

44. CM Drysdale, DW McGraw, CB Stack, JC Stephens, RS Judson, K Nandabalan, K Arnold, G Ruano, SB Liggett. Complex promoter and coding region beta 2-adrenergic receptor haplotypes alter receptor expression and predict in vivo responsiveness. Proc Natl Acad Sci U S A. 2000;97:10483-10488

45. P Eriksson, I Dahlman, M Ryden, J Hoffstedt, P Arner. Relationship between beta-2 adrenoceptor gene haplotypes and adipocyte lipolysis in women. Int J Obes Relat Metab Disord. 2004;28:185-190

46. WC Willett, WH Dietz, GA Colditz. Guidelines for healthy weight. N Engl J Med. 1999;341:427-434

47. DP Guh, W Zhang, N Bansback, Z Amarsi, CL Birmingham, AH Anis. The incidence of co-morbidities related to obesity and overweight: a systematic review and meta-analysis. BMC Public Health. 2009;9:88

48. J Vague. The degree of masculine differentiation of obesities: a factor determining predisposition to diabetes, atherosclerosis, gout, and uric calculous disease. Am J Clin Nutr. 1956;4:20-34

49. P Bjorntorp. The regulation of adipose tissue distribution in humans. Int J Obes Relat Metab Disord. 1996;20:291-302

50. KN Frayn. Regulation of fatty acid delivery in vivo. Adv Exp Med Biol. 1998;441:171-179

51. KN Manolopoulos, F Karpe, KN Frayn. Gluteofemoral body fat as a determinant of metabolic health. Int J Obes (Lond). 2010;34:949-959

52. BL Wajchenberg. Subcutaneous and visceral adipose tissue: their relation to the metabolic syndrome. Endocr Rev. 2000;21:697-738

53. SE Taksali, S Caprio, J Dziura, S Dufour, AM Cali, TR Goodman, X Papademetris, TS Burgert, BM Pierpont, M Savoye, M Shaw, AA Seyal, R Weiss. High visceral and low abdominal subcutaneous fat stores in the obese adolescent: a determinant of an adverse metabolic phenotype. Diabetes. 2008;57:367-371

54. T Hayashi, EJ Boyko, MJ McNeely, DL Leonetti, SE Kahn, WY Fujimoto. Visceral adiposity, not abdominal subcutaneous fat area, is associated with an increase in future insulin resistance in Japanese Americans. Diabetes. 2008;57:1269-1275

55. S Sam, S Haffner, MH Davidson, RB D'Agostino, Sr., S Feinstein, G Kondos, A Perez, T Mazzone. Relationship of abdominal visceral and subcutaneous adipose tissue with lipoprotein particle number and size in type 2 diabetes. Diabetes. 2008;57:2022-2027

56. P Arner. Catecholamine-induced lipolysis in obesity. Int J Obes Relat Metab Disord. 1999;23 Suppl 1:10-13

57. P Bjorntorp. "Portal" adipose tissue as a generator of risk factors for cardiovascular disease and diabetes. Arteriosclerosis. 1990;10:493-496

58. ML Martin, MD Jensen. Effects of body fat distribution on regional lipolysis in obesity. J Clin Invest. 1991;88:609-613

59. Z Guo, DD Hensrud, CM Johnson, MD Jensen. Regional postprandial fatty acid metabolism in different obesity phenotypes. Diabetes. 1999;48:1586-1592

60. KN Frayn, JS Samra, LK Summers. Visceral fat in relation to health: is it a major culprit or simply an innocent bystander? Int J Obes Relat Metab Disord. 1997;21:1191-1192

61. KN Frayn. Visceral fat and insulin resistance--causative or correlative? Br J Nutr. 2000;83 Suppl 1:S71-77

62. JM Miles, MD Jensen. Counterpoint: visceral adiposity is not causally related to insulin resistance. Diabetes Care. 2005;28:2326-2328

63. D Canoy, R Luben, A Welch, S Bingham, N Wareham, N Day, KT Khaw. Fat distribution, body mass index and blood pressure in 22,090 men and women in the Norfolk cohort of the European Prospective Investigation into Cancer and Nutrition (EPIC-Norfolk) study. J Hypertens. 2004;22:2067-2074

64. SM Grundy, B Adams-Huet, GL Vega. Variable contributions of fat content and distribution to metabolic syndrome risk factors. Metab Syndr Relat Disord. 2008;6:281-288

65. S Yusuf, S Hawken, S Ounpuu, L Bautista, MG Franzosi, P Commerford, CC Lang, Z Rumboldt, CL Onen, L Lisheng, S Tanomsup, P Wangai, Jr., F Razak, AM Sharma, SS Anand. Obesity and the risk of myocardial infarction in 27,000 participants from 52 countries: a case-control study. Lancet. 2005;366:1640-1649

66. C Meisinger, A Doring, B Thorand, M Heier, H Lowel. Body fat distribution and risk of type 2 diabetes in the general population: are there differences between men and women? The MONICA/KORA Augsburg cohort study. Am J Clin Nutr. 2006;84:483-489

67. JC Seidell, L Perusse, JP Despres, C Bouchard. Waist and hip circumferences have independent and opposite effects on cardiovascular disease risk factors: the Quebec Family Study. Am J Clin Nutr. 2001;74:315-321

68. RB Terry, ML Stefanick, WL Haskell, PD Wood. Contributions of regional adipose tissue depots to plasma lipoprotein concentrations in overweight men and women: possible protective effects of thigh fat. Metabolism. 1991;40:733-740

69. MJ Williams, GR Hunter, T Kekes-Szabo, S Snyder, MS Treuth. Regional fat distribution in women and risk of cardiovascular disease. Am J Clin Nutr. 1997;65:855-860

70. MB Snijder, M Visser, JM Dekker, BH Goodpaster, TB Harris, SB Kritchevsky, N De Rekeneire, AM Kanaya, AB Newman, FA Tylavsky, JC Seidell. Low subcutaneous thigh fat is a risk factor for unfavourable glucose and lipid levels, independently of high abdominal fat. The Health ABC Study. Diabetologia. 2005;48:301-308

71. B Buemann, A Astrup, O Pedersen, E Black, C Holst, S Toubro, S Echwald, JJ Holst, C Rasmussen, TI Sorensen. Possible role of adiponectin and insulin sensitivity in mediating the favorable effects of lower body fat mass on blood lipids. J Clin Endocrinol Metab. 2006;91:1698-1704

72. JE Yim, S Heshka, JB Albu, S Heymsfield, D Gallagher. Femoral-gluteal subcutaneous and intermuscular adipose tissues have independent and opposing relationships with CVD risk. J Appl Physiol. 2008;104:700-707

73. I Ferreira, MB Snijder, JW Twisk, W van Mechelen, HC Kemper, JC Seidell, CD Stehouwer. Central fat mass versus peripheral fat and lean mass: opposite (adverse versus favorable) associations with arterial stiffness? The Amsterdam Growth and Health Longitudinal Study. J Clin Endocrinol Metab. 2004;89:2632-2639

74. MB Snijder, RM Henry, M Visser, JM Dekker, JC Seidell, I Ferreira, LM Bouter, JS Yudkin, N Westerhof, CD Stehouwer. Regional body composition as a determinant of arterial stiffness in the elderly: The Hoorn Study. J Hypertens. 2004;22:2339-2347

75. LB Tanko, YZ Bagger, P Alexandersen, PJ Larsen, C Christiansen. Peripheral adiposity exhibits an independent dominant antiatherogenic effect in elderly women. Circulation. 2003;107:1626-1631

76. LB Tanko, YZ Bagger, P Alexandersen, PJ Larsen, C Christiansen. Central and peripheral fat mass have contrasting effect on the progression of aortic calcification in postmenopausal women. Eur Heart J. 2003;24:1531-1537

77. T Okura, Y Nakata, K Yamabuki, K Tanaka. Regional body composition changes exhibit opposing effects on coronary heart disease risk factors. Arterioscler Thromb Vasc Biol. 2004;24:923-929

78. RE Van Pelt, EM Evans, KB Schechtman, AA Ehsani, WM Kohrt. Contributions of total and regional fat mass to risk for cardiovascular disease in older women. Am J Physiol Endocrinol Metab. 2002;282:E1023-1028

79. MB Snijder, JM Dekker, M Visser, LM Bouter, CD Stehouwer, JS Yudkin, RJ Heine, G Nijpels, JC Seidell. Trunk fat and leg fat have independent and opposite associations with fasting and postload glucose levels: the Hoorn study. Diabetes Care. 2004;27:372-377

80. MB Snijder, JM Dekker, M Visser, JS Yudkin, CD Stehouwer, LM Bouter, RJ Heine, G Nijpels, JC Seidell. Larger thigh and hip circumferences are associated with better glucose tolerance: the Hoorn study. Obes Res. 2003;11:104-111

81. PM Rocha, JT Barata, PJ Teixeira, R Ross, LB Sardinha. Independent and opposite associations of hip and waist circumference with metabolic syndrome components and with inflammatory and atherothrombotic risk factors in overweight and obese women. Metabolism. 2008;57:1315-1322

82. MB Snijder, PZ Zimmet, M Visser, JM Dekker, JC Seidell, JE Shaw. Independent and opposite associations of waist and hip circumferences with diabetes, hypertension and dyslipidemia: the AusDiab Study. Int J Obes Relat Metab Disord. 2004;28:402-409

83. D Canoy, SM Boekholdt, N Wareham, R Luben, A Welch, S Bingham, I Buchan, N Day, KT Khaw. Body fat distribution and risk of coronary heart disease in men and women in the European Prospective Investigation Into Cancer and Nutrition in Norfolk cohort: a population-based prospective study. Circulation. 2007;116:2933-2943

84. D Canoy, N Wareham, A Welch, S Bingham, R Luben, N Day, KT Khaw. Plasma ascorbic acid concentrations and fat distribution in 19,068 British men and women in the European Prospective Investigation into Cancer and Nutrition Norfolk cohort study. Am J Clin Nutr. 2005;82:1203-1209

85. MG Burt, J Gibney, KK Ho. Characterization of the metabolic phenotypes of Cushing's syndrome and growth hormone deficiency: a study of body composition and energy metabolism. Clin Endocrinol (Oxf). 2006;64:436-443

86. DP Macfarlane, S Forbes, BR Walker. Glucocorticoids and fatty acid metabolism in humans: fuelling fat redistribution in the metabolic syndrome. J Endocrinol. 2008;197:189-204

87. M Rebuffe-Scrive, M Krotkiewski, J Elfverson, P Bjorntorp. Muscle and adipose tissue morphology and metabolism in Cushing's syndrome. J Clin Endocrinol Metab. 1988;67:1122-1128

88. JS Samra, ML Clark, SM Humphreys, IA MacDonald, PA Bannister, KN Frayn. Effects of physiological hypercortisolemia on the regulation of lipolysis in subcutaneous adipose tissue. J Clin Endocrinol Metab. 1998;83:626-631

89. W Mayo-Smith, CW Hayes, BM Biller, A Klibanski, H Rosenthal, DI Rosenthal. Body fat distribution measured with CT: correlations in healthy subjects, patients with anorexia nervosa, and patients with Cushing syndrome. Radiology. 1989;170:515-518

90. BL Wajchenberg, A Bosco, MM Marone, S Levin, M Rocha, AC Lerario, M Nery, J Goldman, B Liberman. Estimation of body fat and lean tissue distribution by dual energy X-ray absorptiometry and abdominal body fat evaluation by computed tomography in Cushing's disease. J Clin Endocrinol Metab. 1995;80:2791-2794

91. TC Friedman, G Mastorakos, TD Newman, NM Mullen, EG Horton, R Costello, NM Papadopoulos, GP Chrousos. Carbohydrate and lipid metabolism in endogenous hypercortisolism: shared features with metabolic syndrome X and NIDDM. Endocr J. 1996;43:645-655

92. BR Walker. Cortisol--cause and cure for metabolic syndrome? Diabet Med. 2006;23:1281-1288

93. AG Rockall, SA Sohaib, D Evans, G Kaltsas, AM Isidori, JP Monson, GM Besser, AB Grossman, RH Reznek. Computed tomography assessment of fat distribution in male and female patients with Cushing's syndrome. Eur J Endocrinol. 2003;149:561-567

94. A Garg. Acquired and inherited lipodystrophies. N Engl J Med. 2004;350:1220-1234

95. A Garg, RM Peshock, JL Fleckenstein. Adipose tissue distribution pattern in patients with familial partial lipodystrophy (Dunnigan variety). J Clin Endocrinol Metab. 1999;84:170-174

96. H Bays, L Mandarino, RA DeFronzo. Role of the adipocyte, free fatty acids, and ectopic fat in pathogenesis of type 2 diabetes mellitus: peroxisomal proliferator-activated receptor agonists provide a rational therapeutic approach. J Clin Endocrinol Metab. 2004;89:463-478

97. JP Montani, JF Carroll, TM Dwyer, V Antic, Z Yang, AG Dulloo. Ectopic fat storage in heart, blood vessels and kidneys in the pathogenesis of cardiovascular diseases. Int J Obes Relat Metab Disord. 2004;28 Suppl 4:S58-65

98. HH Schmidt, J Genschel, P Baier, M Schmidt, J Ockenga, UJ Tietge, M Propsting, C Buttner, MP Manns, H Lochs, G Brabant. Dyslipemia in familial partial lipodystrophy caused by an R482W mutation in the LMNA gene. J Clin Endocrinol Metab. 2001;86:2289-2295

99. I Barroso, M Gurnell, VE Crowley, M Agostini, JW Schwabe, MA Soos, GL Maslen, TD Williams, H Lewis, AJ Schafer, VK Chatterjee, S O'Rahilly. Dominant negative mutations in human PPARgamma associated with severe insulin resistance, diabetes mellitus and hypertension. Nature. 1999;402:880-883

100. DB Savage, GD Tan, CL Acerini, SA Jebb, M Agostini, M Gurnell, RL Williams, AM Umpleby, EL Thomas, JD Bell, AK Dixon, F Dunne, R Boiani, S Cinti, A Vidal-Puig, F Karpe, VK Chatterjee, S O'Rahilly. Human metabolic syndrome resulting from dominant-negative mutations in the nuclear receptor peroxisome proliferator-activated receptor-gamma. Diabetes. 2003;52:910-917

101. A Misra, A Peethambaram, A Garg. Clinical features and metabolic and autoimmune derangements in acquired partial lipodystrophy: report of 35 cases and review of the literature. Medicine (Baltimore). 2004;83:18-34

102. GD Tan, GH Goossens, SM Humphreys, H Vidal, F Karpe. Upper and lower body adipose tissue function: a direct comparison of fat mobilization in humans. Obes Res. 2004;12:114-118

103. J Gjedsted, LC Gormsen, S Nielsen, O Schmitz, CB Djurhuus, S Keiding, H Orskov, E Tonnesen, N Moller. Effects of a 3-day fast on regional lipid and glucose metabolism in human skeletal muscle and adipose tissue. Acta Physiol (Oxf). 2007;191:205-216

104. C Koutsari, CL Snozek, MD Jensen. Plasma NEFA storage in adipose tissue in the postprandial state: sex-related and regional differences. Diabetologia. 2008;51:2041-2048

105. SA Romanski, RM Nelson, MD Jensen. Meal fatty acid uptake in adipose tissue: gender effects in nonobese humans. Am J Physiol Endocrinol Metab. 2000;279:E455-462

106. SE McQuaid, SM Humphreys, L Hodson, BA Fielding, F Karpe, KN Frayn. Femoral adipose tissue may accumulate the fat that has been recycled as VLDL and nonesterified fatty acids. Diabetes. 2010;59:2465-2473

107. SE McQuaid, L Hodson, MJ Neville, AL Dennis, J Cheeseman, SM Humphreys, T Ruge, M Gilbert, BA Fielding, KN Frayn, F Karpe. Downregulation of Adipose Tissue Fatty Acid Trafficking in Obesity: A Driver for Ectopic Fat Deposition? Diabetes. 2010;60:47-55

108. H Wahrenberg, F Lonnqvist, P Arner. Mechanisms underlying regional differences in lipolysis in human adipose tissue. J Clin Invest. 1989;84:458-467

109. P Arner, L Hellstrom, H Wahrenberg, M Bronnegard. Beta-adrenoceptor expression in human fat cells from different regions. J Clin Invest. 1990;86:1595-1600

110. M Lafontan, L Dang-Tran, M Berlan. Alpha-adrenergic antilipolytic effect of adrenaline in human fat cells of the thigh: comparison with adrenaline responsiveness of different fat deposits. Eur J Clin Invest. 1979;9:261-266

111. JF Horowitz, S Klein. Whole body and abdominal lipolytic sensitivity to epinephrine is suppressed in upper body obese women. Am J Physiol Endocrinol Metab. 2000;278:E1144-1152

112. Z Guo, CM Johnson, MD Jensen. Regional lipolytic responses to isoproterenol in women. Am J Physiol. 1997;273:E108-112

113. MD Jensen, PE Cryer, CM Johnson, MJ Murray. Effects of epinephrine on regional free fatty acid and energy metabolism in men and women. Am J Physiol. 1996;270:E259-264

114. SE McQuaid, L Hodson, MJ Neville, AL Dennis, J Cheeseman, SM Humphreys, T Ruge, M Gilbert, BA Fielding, KN Frayn, F Karpe. Down-regulation of adipose tissue fatty acid trafficking in obesity: a driver for ectopic fat deposition? Diabetes. 2010;

115. I Lemieux. Energy partitioning in gluteal-femoral fat: does the metabolic fate of triglycerides affect coronary heart disease risk? Arterioscler Thromb Vasc Biol. 2004;24:795-797

116. J Galitzky, M Lafontan, J Nordenstrom, P Arner. Role of vascular alpha-2 adrenoceptors in regulating lipid mobilization from human adipose tissue. J Clin Invest. 1993;91:1997-2003

117. P Lonnroth. Microdialysis in adipose tissue and skeletal muscle. Horm Metab Res. 1997;29:344-346

118. P Barbe, C Darimont, P Saint-Marc, J Galitzky. Measurements of white adipose tissue metabolism by microdialysis technique. Methods Mol Biol. 2001;155:305-321

119. F Karpe, BA Fielding, V Ilic, SM Humphreys, KN Frayn. Monitoring adipose tissue blood flow in man: a comparison between the (133)xenon washout method and microdialysis. Int J Obes Relat Metab Disord. 2002;26:1-5

120. PA Jansson, A Larsson, U Smith, P Lonnroth. Glycerol production in subcutaneous adipose tissue in lean and obese humans. J Clin Invest. 1992;89:1610-1617

121. PA Jansson, A Larsson, U Smith, P Lonnroth. Lactate release from the subcutaneous tissue in lean and obese men. J Clin Invest. 1994;93:240-246

122. AD Jaskille, JC Ramella-Roman, JW Shupp, MH Jordan, JC Jeng. Critical review of burn depth assessment techniques: part II. Review of laser doppler technology. J Burn Care Res. 31:151-157

123. KA Virtanen, P Lonnroth, R Parkkola, P Peltoniemi, M Asola, T Viljanen, T Tolvanen, J Knuuti, T Ronnemaa, R Huupponen, P Nuutila. Glucose uptake and perfusion in subcutaneous and visceral adipose tissue during insulin stimulation in nonobese and obese humans. J Clin Endocrinol Metab. 2002;87:3902-3910

124. L Tobin, L Simonsen, J Bulow. Real-time contrast-enhanced ultrasound determination of microvascular blood volume in abdominal subcutaneous adipose tissue in man. Evidence for adipose tissue capillary recruitment. Clin Physiol Funct Imaging. 2010;30:447-452

125. K Wei, AR Jayaweera, S Firoozan, A Linka, DM Skyba, S Kaul. Quantification of myocardial blood flow with ultrasound-induced destruction of microbubbles administered as a constant venous infusion. Circulation. 1998;97:473-483

126. SS Kety. The theory and applications of the exchange of inert gas at the lungs and tissues. Pharmacol Rev. 1951;3:1-41

127. OA Larsen, NA Lassen, F Quaade. Blood flow through human adipose tissue determined with radioactive xenon. Acta Physiol Scand. 1966;66:337-345

128. GH Goossens, F Karpe. Human adipose tissue blood flow and micromanipulation of human subcutaneous blood flow. Methods Mol Biol. 2008;456:97-107

129. J Bülow, R Jelnes, A Astrup, J Madsen, P Vilmann. Tissue/blood partition coefficients for xenon in various adipose tissue depots in man. Scand J Clin Lab Invest. 1987;47:1-3

130. EE Blaak, MA van Baak, GJ Kemerink, MT Pakbiers, GA Heidendal, WH Saris. Beta-adrenergic stimulation and abdominal subcutaneous fat blood flow in lean, obese, and reduced-obese subjects. Metabolism. 1995;44:183-187

131. SY Yeh, RE Peterson. Solubility of krypton and xenon in blood, protein solutions, and tissue homogenates. J Appl Physiol. 1965;20:1041-1047

132. AM Andersen, J Ladefoged. Partition coefficient of 133-xenon between various tissues and blood in vivo. Scand J Clin Lab Invest. 1967;19:72-78

133. JS Samra, EJ Simpson, ML Clark, CD Forster, SM Humphreys, IA Macdonald, KN Frayn. Effects of epinephrine infusion on adipose tissue: interactions between blood flow and lipid metabolism. Am J Physiol. 1996;271:E834-839

134. AS Bickerton, R Roberts, BA Fielding, L Hodson, EE Blaak, AJ Wagenmakers, M Gilbert, F Karpe, KN Frayn. Preferential uptake of dietary Fatty acids in adipose tissue and muscle in the postprandial period. Diabetes. 2007;56:168-176

135. RY Chen, FC Fan, S Kim, KM Jan, S Usami, S Chien. Tissue-blood partition coefficient for xenon: temperature and hematocrit dependence. J Appl Physiol. 1980;49:178-183

136. JS Samra, KN Frayn, JA Giddings, ML Clark, IA Macdonald. Modification and validation of a commercially available portable detector for measurement of adipose tissue blood flow. Clin Physiol. 1995;15:241-248

137. P Wellhoner, D Rolle, P Lonnroth, L Strindberg, M Elam, C Dodt. Laser-Doppler flowmetry reveals rapid perfusion changes in adipose tissue of lean and obese females. Am J Physiol Endocrinol Metab. 2006;291:E1025-1030

138. G Clough, A Chipperfield, C Byrne, F de Mul, R Gush. Evaluation of a new high power, wide separation laser Doppler probe: potential measurement of deeper tissue blood flow. Microvasc Res. 2009;78:155-161

139. NA Monteiro-Riviere, DG Bristol, TO Manning, RA Rogers, JE Riviere. Interspecies and interregional analysis of the comparative histologic thickness and laser Doppler blood flow measurements at five cutaneous sites in nine species. J Invest Dermatol. 1990;95:582-586

140. MJ Daly, RE Henry. Quantitative measurement of skin perfusion with xenon-133. J Nucl Med. 1980;21:156-160

141. A Astrup, J Bulow, J Madsen. Skin temperature and subcutaneous adipose blood flow in man. Scand J Clin Lab Invest. 1980;40:135-138

142. KN Frayn, SW Coppack, SM Humphreys, PL Whyte. Metabolic characteristics of human adipose tissue in vivo. Clin Sci (Lond). 1989;76:509-516

143. S Klein, SW Coppack, V Mohamed-Ali, M Landt. Adipose tissue leptin production and plasma leptin kinetics in humans. Diabetes. 1996;45:984-987

144. V Mohamed-Ali, S Goodrick, A Rawesh, DR Katz, JM Miles, JS Yudkin, S Klein, SW Coppack. Subcutaneous adipose tissue releases interleukin-6, but not tumor necrosis factor-alpha, in vivo. J Clin Endocrinol Metab. 1997;82:4196-4200

145. K Evans, ML Clark, KN Frayn. Effects of an oral and intravenous fat load on adipose tissue and forearm lipid metabolism. Am J Physiol. 1999;276:E241-248

146. RS Gordon, Jr. Unesterified fatty acid in human blood plasma. II. The transport function of unesterified fatty acid. J Clin Invest. 1957;36:810-815

147. MD Jensen, N Moller, KS Nair, P Eisenberg, M Landt, S Klein. Regional leptin kinetics in humans. Am J Clin Nutr. 1999;69:18-21

148. KN Frayn, SW Coppack, SM Humphreys. Subcutaneous adipose tissue metabolism studied by local catheterization. Int J Obes Relat Metab Disord. 1993;17 Suppl 3:S18-21; discussion S22

149. SE McQuaid, KN Manolopoulos, AL Dennis, J Cheeseman, F Karpe, KN Frayn. Development of an arterio-venous difference method to study the metabolic physiology of the femoral adipose tissue depot. Obesity (Silver Spring). 2010;18:1055-1058

150. JE Dimsdale, JA Herd. Variability of plasma lipids in response to emotional arousal. Psychosom Med. 1982;44:413-430

151. JA Sirs. The flow of human blood through capillary tubes. J Physiol. 1991;442:569-583

152. SS Jolly, S Amlani, M Hamon, S Yusuf, SR Mehta. Radial versus femoral access for coronary angiography or intervention and the impact on major bleeding and ischemic events: a systematic review and meta-analysis of randomized trials. Am Heart J. 2009;157:132-140

153. IW Gallen, IA Macdonald. Effect of two methods of hand heating on body temperature, forearm blood flow, and deep venous oxygen saturation. Am J Physiol. 1990;259:E639-643

154. T Lewis, GW Pickering. Vasodilation in the limbs in response to warming the body, with evidence for sympathetic vasodilator nerves in man. Heart. 1931;16:33-51

155. KN Frayn, IA Macdonald. Methodological considerations in arterialization of venous blood. Clin Chem. 1992;38:316-317

156. EA McGuire, JH Helderman, JD Tobin, R Andres, M Berman. Effects of arterial versus venous sampling on analysis of glucose kinetics in man. J Appl Physiol. 1976;41:565-573

157. MA Nauck, H Liess, EG Siegel, PD Niedmann, W Creutzfeldt. Critical evaluation of the 'heated-hand-technique' for obtaining 'arterialized' venous blood: incomplete arterialization and alterations in glucagon responses. Clin Physiol. 1992;12:537-552

158. GE Sonnenberg, U Keller. Sampling of arterialized heated-hand venous blood as a noninvasive technique for the study of ketone body kinetics in man. Metabolism. 1982;31:1-5

159. MD Jensen, VJ Heiling. Heated hand vein blood is satisfactory for measurements during free fatty acid kinetic studies. Metabolism. 1991;40:406-409

160. D Liu, K Andreasson, PE Lins, UC Adamson, IA Macdonald. Adrenaline and noradrenaline responses during insulin-induced hypoglycaemia in man: should the hormone levels be measured in arterialized venous blood? Acta Endocrinol (Copenh). 1993;128:95-98

161. A Astrup, L Simonsen, J Bulow, NJ Christensen. Measurement of forearm oxygen consumption: role of heating the contralateral hand. Am J Physiol. 1988;255:E572-578

162. PN Bramley, RW Heighton, JH Green. Methodological considerations in arterialization of venous blood. Clin Chem. 1991;37:1139-1140

163. EE Blaak, MA Van Baak, KP Kempen, WH Saris. Effect of hand heating by a warm air box on O2 consumption of the contralateral arm. J Appl Physiol. 1992;72:2364-2368

164. GA Zello, JM Smith, PB Pencharz, RO Ball. Development of a heating device for sampling arterialized venous blood from a hand vein. Ann Clin Biochem. 1990;27 (Pt 4):366-372

165. EE Blaak, MA Van Baak, GJ Kemerink, MT Pakbiers, GA Heidendal, WH Saris. Beta-adrenergic stimulation of energy expenditure and forearm skeletal muscle metabolism in lean and obese men. Am J Physiol. 1994;267:E306-315

166. JW Jocken, GH Goossens, AM van Hees, KN Frayn, M van Baak, J Stegen, MT Pakbiers, WH Saris, EE Blaak. Effect of beta-adrenergic stimulation on whole-body and abdominal subcutaneous adipose tissue lipolysis in lean and obese men. Diabetologia. 2008;51:320-327

167. JW Jocken, C Roepstorff, GH Goossens, P van der Baan, M van Baak, WH Saris, B Kiens, EE Blaak. Hormone-sensitive lipase serine phosphorylation and glycerol exchange across skeletal muscle in lean and obese subjects: effect of beta-adrenergic stimulation. Diabetes. 2008;57:1834-1841

168. P Mauriege, J Galitzky, M Berlan, M Lafontan. Heterogeneous distribution of beta and alpha-2 adrenoceptor binding sites in human fat cells from various fat deposits: functional consequences. Eur J Clin Invest. 1987;17:156-165

169. WE Clutter, DM Bier, SD Shah, PE Cryer. Epinephrine plasma metabolic clearance rates and physiologic thresholds for metabolic and hemodynamic actions in man. J Clin Invest. 1980;66:94-101

170. AD Galster, WE Clutter, PE Cryer, JA Collins, DM Bier. Epinephrine plasma thresholds for lipolytic effects in man: measurements of fatty acid transport with [l-13C]palmitic acid. J Clin Invest. 1981;67:1729-1738

171. J Webber, J Taylor, H Greathead, J Dawson, PJ Buttery, IA Macdonald. A comparison of the thermogenic, metabolic and haemodynamic responses to infused adrenaline in lean and obese subjects. Int J Obes Relat Metab Disord. 1994;18:717-724

172. C Hertel, JP Perkins. Receptor-specific mechanisms of desensitization of beta-adrenergic receptor function. Mol Cell Endocrinol. 1984;37:245-256

173. S Forbes, S Robinson, J Dungu, V Anyaoku, P Bannister, D Forster, S Dissanayake, MI McCarthy, IA MacDonald, S Venkatesan, DG Johnston. Sustained endogenous glucose production, diminished lipolysis and non-esterified fatty acid appearance and oxidation in non-obese women at high risk of type 2 diabetes. Eur J Endocrinol. 2006;155:469-476

174. P Bougneres, CL Stunff, C Pecqueur, E Pinglier, P Adnot, D Ricquier. In vivo resistance of lipolysis to epinephrine. A new feature of childhood onset obesity. J Clin Invest. 1997;99:2568-2573

175. LH Enevoldsen, L Simonsen, B Stallknecht, H Galbo, J Bulow. In vivo human lipolytic activity in preperitoneal and subdivisions of subcutaneous abdominal adipose tissue. Am J Physiol Endocrinol Metab. 2001;281:E1110-1114

176. G Cohen, B Holland, J Sha, M Goldenberg. Plasma concentrations of epinephrine and norepinephrine during intravenous infusions in man. J Clin Invest. 1959;38:1935-1941

177. AV Kurpad, RN Kulkarni, M Vaz, PS Shetty. Repeated infusions of identical doses of norepinephrine show potentiation of metabolic responses in human subjects. Metabolism. 1989;38:979-982

178. J Webber, IA Macdonald. A comparison of the cardiovascular and metabolic effects of incremental versus continuous dose adrenaline infusions in men and women. Int J Obes Relat Metab Disord. 1993;17:37-43

179. JR Smythies. Molecular mechanisms of adrenergic receptors. J Theor Biol. 1972;35:93-101

180. B Green, SB Duffull. What is the best size descriptor to use for pharmacokinetic studies in the obese? Br J Clin Pharmacol. 2004;58:119-133

181. H Schott. Osmolality/osmolarity data and calculations. Pharmazie. 1979;34:257-259

182. RR Wolfe, DL Chinkes. Isotope tracers in metabolic research. 2nd edition. 2005; John Wiley and Sons

183. L Hagenfeldt. Turnover of individual free fatty acids in man. Fed Proc. 1975;34:2246-2249

184. JL Vincent, MM Wilkes, RJ Navickis. Safety of human albumin--serious adverse events reported worldwide in 1998-2000. Br J Anaesth. 2003;91:625-630

185. I von Hoegen, C Waller. Safety of human albumin based on spontaneously reported serious adverse events. Crit Care Med. 2001;29:994-996

186. A Farrugia. Safety of Plasma Volume Expanders. J Clin Pharmacol. 2011;51:292-300

187. J Folch, M Lees, GH Sloane Stanley. A simple method for the isolation and purification of total lipides from animal tissues. J Biol Chem. 1957;226:497-509

188. RB Heath, F Karpe, RW Milne, GC Burdge, SA Wootton, KN Frayn. Selective partitioning of dietary fatty acids into the VLDL TG pool in the early postprandial period. J Lipid Res. 2003;44:2065-2072

189. RS Dillon. Importance of the hematocrit in interpretation of blood sugar. Diabetes. 1965;14:672-674

190. GD Tan, MJ Neville, E Liverani, SM Humphreys, JM Currie, L Dennis, BA Fielding, F Karpe. The in vivo effects of the Pro12Ala PPARgamma2 polymorphism on adipose tissue NEFA metabolism: the first use of the Oxford Biobank. Diabetologia. 2006;49:158-168

191. P Chomczynski, N Sacchi. Single-step method of RNA isolation by acid guanidinium thiocyanate-phenol-chloroform extraction. Anal Biochem. 1987;162:156-159

192. GW Dorn, 2nd. Adrenergic signaling polymorphisms and their impact on cardiovascular disease. Physiol Rev. 2010;90:1013-1062

193. JR Docherty. Subtypes of functional alpha1-adrenoceptor. Cell Mol Life Sci. 2010;67:405-417

194. JH Pinkney, SW Coppack, V Mohamed-Ali. Effect of isoprenaline on plasma leptin and lipolysis in humans. Clin Endocrinol (Oxf). 1998;48:407-411

195. P Barbe, L Millet, J Galitzky, M Lafontan, M Berlan. In situ assessment of the role of the beta 1-, beta 2- and beta 3-adrenoceptors in the control of lipolysis and nutritive blood flow in human subcutaneous adipose tissue. Br J Pharmacol. 1996;117:907-913

196. L Hellstrom, D Langin, S Reynisdottir, M Dauzats, P Arner. Adipocyte lipolysis in normal weight subjects with obesity among first-degree relatives. Diabetologia. 1996;39:921-928

197. P Barbe, V Stich, J Galitzky, M Kunesova, V Hainer, M Lafontan, M Berlan. In vivo increase in beta-adrenergic lipolytic response in subcutaneous adipose tissue of obese subjects submitted to a hypocaloric diet. J Clin Endocrinol Metab. 1997;82:63-69

198. V Stich, I de Glisezinski, J Galitzky, J Hejnova, F Crampes, D Riviere, M Berlan. Endurance training increases the beta-adrenergic lipolytic response in subcutaneous adipose tissue in obese subjects. Int J Obes Relat Metab Disord. 1999;23:374-381

199. SL Schiffelers, JA Akkermans, WH Saris, EE Blaak. Lipolytic and nutritive blood flow response to beta-adrenoceptor stimulation in situ in subcutaneous abdominal adipose tissue in obese men. Int J Obes Relat Metab Disord. 2003;27:227-231

200. EE Blaak, GJ Kemerink, MT Pakbiers, BH Wolffenbuttel, GA Heidendal, WH Saris. Microdialysis assessment of local adipose tissue lipolysis during beta-

adrenergic stimulation in upper-body-obese subjects with type II diabetes. Clin Sci (Lond). 1999;97:421-428

201. DP van Aggel-Leijssen, WH Saris, M Homan, MA van Baak. The effect of exercise training on beta-adrenergic stimulation of fat metabolism in obese men. Int J Obes Relat Metab Disord. 2001;25:16-23

202. B Richelsen. Increased alpha 2- but similar beta-adrenergic receptor activities in subcutaneous gluteal adipocytes from females compared with males. Eur J Clin Invest. 1986;16:302-309

203. FC Brunicardi, YS Sun, P Druck, RJ Goulet, D Elahi, DK Andersen. Splanchnic neural regulation of insulin and glucagon secretion in the isolated perfused human pancreas. Am J Surg. 1987;153:34-40

204. TT Chuang, L Iacovelli, M Sallese, A De Blasi. G protein-coupled receptors: heterologous regulation of homologous desensitization and its implications. Trends Pharmacol Sci. 1996;17:416-421

205. J Rowe, J Young, K Minaker, A Stevens, J Pallotta, L Landsberg. Effect of insulin and glucose infusions on sympathetic nervous system activity in normal man. Diabetes. 1981;30:219-225

206. G Lewis, K Uffelman, L Szeto, G Steiner. Effects of acute hyperinsulinemia on VLDL triglyceride and VLDL apoB production in normal weight and obese individuals. Diabetes. 1993;42:833-842

207. J Bülow, L Simonsen, D Wiggins, S Humphreys, K Frayn, D Powell, G Gibbons. Co-ordination of hepatic and adipose tissue lipid metabolism after oral glucose. J Lipid Res. 1999;40:2034-2043

208. K Nonogaki. New insights into sympathetic regulation of glucose and fat metabolism. Diabetologia. 2000;43:533-549

209. JE Gerich, JH Karam, PH Forsham. Stimulation of glucagon secretion by epinephrine in man. J Clin Endocrinol Metab. 1973;37:479-481

210. W Malaisse, F Malaisse-Lagae, PH Wright, J Ashmore. Effects of adrenergic and cholinergic agents upon insulin secretion in vitro. Endocrinology. 1967;80:975-978

211. AH Rosengren, R Jokubka, D Tojjar, C Granhall, O Hansson, DQ Li, V Nagaraj, TM Reinbothe, J Tuncel, L Eliasson, L Groop, P Rorsman, A Salehi, V Lyssenko, H Luthman, E Renstrom. Overexpression of alpha2A-adrenergic receptors contributes to type 2 diabetes. Science. 2010;327:217-220

212. RL Lerner, D Porte, Jr. Epinephrine: selective inhibition of the acute insulin response to glucose. J Clin Invest. 1971;50:2453-2457

213. DE Harrison, MR Christie, DW Gray. Properties of isolated human islets of Langerhans: insulin secretion, glucose oxidation and protein phosphorylation. Diabetologia. 1985;28:99-103

214. IW Fellows, T Bennett, IA MacDonald. The effect of adrenaline upon cardiovascular and metabolic functions in man. Clin Sci (Lond). 1985;69:215-222

215. MJ Brown, CT Dollery. Adrenaline and hypertension. Clin Exp Hypertens A. 1984;6:539-549

216. P Hjemdahl, T Akerstedt, T Pollare, M Gillberg. Influence of beta-adrenoceptor blockade by metoprolol and propranolol on plasma concentrations and effects of noradrenaline and adrenaline during i.v. infusion. Acta Physiol Scand Suppl. 1983;515:45-53

217. E Blaak. Gender differences in fat metabolism. Curr Opin Clin Nutr Metab Care. 2001;4:499-502

218. FD Martinez, PE Graves, M Baldini, S Solomon, R Erickson. Association between genetic polymorphisms of the beta2-adrenoceptor and response to albuterol in children with and without a history of wheezing. J Clin Invest. 1997;100:3184-3188

219. JW Jocken, EE Blaak, S Schiffelers, P Arner, MA van Baak, WH Saris. Association of a beta-2 adrenoceptor (ADRB2) gene variant with a blunted in vivo lipolysis and fat oxidation. Int J Obes (Lond). 2007;31:813-819

220. RL Leibel, J Hirsch. Site- and sex-related differences in adrenoreceptor status of human adipose tissue. J Clin Endocrinol Metab. 1987;64:1205-1210

221. M Rosenbaum, E Presta, J Hirsch, RL Leibel. Regional differences in adrenoreceptor status of adipose tissue in adults and prepubertal children. J Clin Endocrinol Metab. 1991;73:341-347

222. M Berlan, M Lafontan. Evidence that epinephrine acts preferentially as an antilipolytic agent in abdominal human subcutaneous fat cells: assessment by analysis of beta and alpha 2 adrenoceptor properties. Eur J Clin Invest. 1985;15:341-348

223. DM Berman, BJ Nicklas, EM Rogus, KE Dennis, AP Goldberg. Regional differences in adrenoceptor binding and fat cell lipolysis in obese, postmenopausal women. Metabolism. 1998;47:467-473

224. P Arner, E Kriegholm, P Engfeldt, J Bolinder. Adrenergic regulation of lipolysis in situ at rest and during exercise. J Clin Invest. 1990;85:893-898

225. F Lonnqvist, H Wahrenberg, L Hellstrom, S Reynisdottir, P Arner. Lipolytic catecholamine resistance due to decreased beta 2-adrenoceptor expression in fat cells. J Clin Invest. 1992;90:2175-2186

226. M Lafontan, M Berlan. Fat cell alpha 2-adrenoceptors: the regulation of fat cell function and lipolysis. Endocr Rev. 1995;16:716-738

227. L Millet, P Barbe, M Lafontan, M Berlan, J Galitzky. Catecholamine effects on lipolysis and blood flow in human abdominal and femoral adipose tissue. J Appl Physiol. 1998;85:181-188

228. P Mauriege, G De Pergola, M Berlan, M Lafontan. Human fat cell beta-adrenergic receptors: beta-agonist-dependent lipolytic responses and characterization of beta-adrenergic binding sites on human fat cell membranes with highly selective beta 1-antagonists. J Lipid Res. 1988;29:587-601

229. MD Jensen, MW Haymond, JE Gerich, PE Cryer, JM Miles. Lipolysis during fasting. Decreased suppression by insulin and increased stimulation by epinephrine. J Clin Invest. 1987;79:207-213

230. LK Summers, SC Barnes, BA Fielding, C Beysen, V Ilic, SM Humphreys, KN Frayn. Uptake of individual fatty acids into adipose tissue in relation to their presence in the diet. Am J Clin Nutr. 2000;71:1470-1477

231. SW Coppack, RM Fisher, GF Gibbons, SM Humphreys, MJ McDonough, JL Potts, KN Frayn. Postprandial substrate deposition in human forearm and adipose tissues in vivo. Clin Sci (Lond). 1990;79:339-348

232. S Santosa, DD Hensrud, SB Votruba, MD Jensen. The influence of sex and obesity phenotype on meal fatty acid metabolism before and after weight loss. Am J Clin Nutr. 2008;88:1134-1141

233. SB Votruba, RS Mattison, DA Dumesic, C Koutsari, MD Jensen. Meal fatty acid uptake in visceral fat in women. Diabetes. 2007;56:2589-2597

234. MD Jensen. Gender differences in regional fatty acid metabolism before and after meal ingestion. J Clin Invest. 1995;96:2297-2303

235. LC Gormsen, B Nellemann, LP Sorensen, MD Jensen, JS Christiansen, S Nielsen. Impact of body composition on very-low-density lipoprotein-triglycerides kinetics. Am J Physiol Endocrinol Metab. 2009;296:E165-173

236. B Nellemann, LC Gormsen, JS Christiansen, MD Jensen, S Nielsen. Postabsorptive VLDL-TG fatty acid storage in adipose tissue in lean and obese women. Obesity (Silver Spring). 2010;18:1304-1311

237. JP Despres, I Lemieux. Abdominal obesity and metabolic syndrome. Nature. 2006;444:881-887

238. B Richelsen, SB Pedersen, T Moller-Pedersen, JF Bak. Regional differences in triglyceride breakdown in human adipose tissue: effects of catecholamines, insulin, and prostaglandin E2. Metabolism. 1991;40:990-996

239. P Marin, M Rebuffe-Scrive, P Bjorntorp. Uptake of triglyceride fatty acids in adipose tissue in vivo in man. Eur J Clin Invest. 1990;20:158-165

240. PR Jones, DA Edwards. Areas of fat loss in overweight young females following an 8-week period of energy intake reduction. Ann Hum Biol. 1999;26:151-162

241. BH Goodpaster, DE Kelley, RR Wing, A Meier, FL Thaete. Effects of weight loss on regional fat distribution and insulin sensitivity in obesity. Diabetes. 1999;48:839-847

242. JC Wells, L Griffin, P Treleaven. Independent changes in female body shape with parity and age: A life-history approach to female adiposity. Am J Hum Biol. 2010;22:456-462

243. S Shadid, C Koutsari, MD Jensen. Direct free fatty acid uptake into human adipocytes in vivo: relation to body fat distribution. Diabetes. 2007;56:1369-1375

244. JC Hannukainen, KK Kalliokoski, RJ Borra, AP Viljanen, T Janatuinen, UM Kujala, J Kaprio, OJ Heinonen, T Viljanen, M Haaparanta, P Iozzo, R Parkkola, P Nuutila. Higher free fatty acid uptake in visceral than in abdominal subcutaneous fat tissue in men. Obesity (Silver Spring). 2010;18:261-265

245. G Bos, MB Snijder, G Nijpels, JM Dekker, CD Stehouwer, LM Bouter, RJ Heine, H Jansen. Opposite contributions of trunk and leg fat mass with plasma lipase activities: the Hoorn study. Obes Res. 2005;13:1817-1823

246. JB Albu, S Kenya, Q He, M Wainwright, ES Berk, S Heshka, DP Kotler, ES Engelson. Independent associations of insulin resistance with high whole-body intermuscular and low leg subcutaneous adipose tissue distribution in obese HIV-infected women. Am J Clin Nutr. 2007;86:100-106

247. K Evans, GC Burdge, SA Wootton, ML Clark, KN Frayn. Regulation of dietary fatty acid entrapment in subcutaneous adipose tissue and skeletal muscle. Diabetes. 2002;51:2684-2690

248. DM Wallace. Precipitation of nucleic acids. Methods Enzymol. 1987;152:41-48

9 Appendix

9.1 Tables

Table 1 (on following page): Protective properties of the gluteofemoral fat depot – overview of studies (from (51))

Author (year)	n	male/female	age	BMI	Population	Method	Measurement	Association
Terry (1991)[68]	263	133/130	39.6±6.3	29.3±2.2	Overweight	Tape measure, DXA	TC, leg AT mass	↑ HDL, ↑ HDL mass, ↑ LDL size in women
Williams (1997)[69]	224	0/244	44.2±14.1	23.9±4.5	General population	CT, DXA	Leg AT mass	↓ total cholesterol, ↓ LDL, ↓ VLDL, ↓ IDL, ↓ TG
Seidell (2001)[67]	695	313/382	42.9±17.0	27.1±7.1	General population	Tape measure	HC	↓ TG, ↓ insulin in both genders; ↑ HDL, ↓ glucose in men
van Pelt (2002)[78]	166	0/166	66.0±4.0	26.6±4.7	General population	DXA	Leg AT mass	↓ post-OGTT insulin, ↓ insulin resistance, ↓ TG, ↑ HDL
Snijder (2003)[80]	2380	1099/1281	61.5±7.4	26.5±3.4	General population	Tape measure	TC	↓ fasting and post-OGTT glucose; ↓ HbA1c in women
							HC	↓ fasting and post-OGTT glucose, ↓ HbA1c in both genders; ↓ insulin in women
Tanko (2003)[75]	1356	0/1356	71.4±5.2	26.2±3.8	General population	DXA	Peripheral (arm and leg) AT mass	↓ TG, ↓ total cholesterol, ↓ glucose, ↓ aortic calcification
Tanko (2003)[76]	316	0/316	62.3±5.8	25.5±3.8	General population	DXA	Peripheral (arm and leg) AT mass	↓ progression of aortic calcification over 7.7 years
Ferreira (2004)[73]	336	161/175	36.6±0.6	24.0±3.1	General population	DXA	Peripheral (arm and leg) AT mass	↓ arterial stiffness
Okura (2004)[77]	128	0/128	50.0±7.0	29.0±2.8	Obese women to undergo diet and exercise programme	DXA	Leg AT mass change (increase)	↓ diastolic blood pressure, ↓ LDL, ↓ glucose, ↓ no of CHD-factors
Snijder (2004)[79]	556	275/281	69.6±6.3	27.2±3.7	General population, incl. IGT and DM	DXA	Leg AT mass	↓ fasting and post-OGTT glucose
Snijder (2004)[82]	8400	3818/4582	48.3±13.3	26.4±4.7	General population	Tape measure	HC	↓ prevalence of undiagnosed DM and dyslipidaemia

Snijder (2004)[74]	484	244/240	69.1±6.1	26.4±3.1	General population	DXA	Leg AT mass	↓ arterial stiffness
Bos (2005)[245]	406	197/209	69.3±6.0	27.0±2.4	General population	DXA	Leg AT mass	↑ LPL activity in women, ↓ hepatic lipase activity in women
Canoy (2005)[84]	19068	8593/10475	59.3±8.5	26.3±3.8	General population	Tape measure	HC	↑ ascorbic acid
Snijder (2005)[70]	2106	1019/1087	73.6±2.9	27.0±4.5	General population	CT	Thigh s.c. AT area	↓ TG, ↑ HDL; ↓ fasting and post-OGTT glucose levels in men
Yusuf (2005)[65]	27098	20310/6788	57.5±12.2	25.8±0.05	MI patients and healthy controls	Tape measure	HC	↓ OR for MI
Buemann (2005)[71]	443	443/0	48.8±5.5	29.6±4.3	General population	DXA	Gluteofemoral AT mass	↓ total cholesterol, ↓ TG, ↑ HDL
Albu (2007)[246]	49	0/49	37.9±6.8	35.4±3.1	HIV+ women and healthy controls	MRI	Leg s.c. AT %	↑ insulin sensitivity in both groups combined
Canoy (2007)[83]	24508	11117/13391	59.9±8.8	26.4±3.8	General population	Tape measure	HC	↓ OR for CHD
Rocha (2008)[81]	140	0/140	38.3±0.5	30.4±0.3	Healthy overweight and obese women	CT	HC	↓ insulin, ↓ HbA1c, ↓ PAI-1
							Thigh total and s.c. AT mass	↓ Hba1c, ↓ LDL/HDL-ratio
							Thigh total AT mass	↑ leptin
							Thigh s.c. AT mass	↓ insulin
Yim (2008)[72]	319	104/215	45.1±17.5	25.7±4.4	General population	MRI	Thigh s.c. AT mass	↓ insulin, ↓ TG

Table 2: Calculation of maximum radiation dose for study participants (from ethics application)

Modality	Dose per Exam (mSv)	Procedure	Number of Procedures	Estimated Maximum Dose (mSv)
DEXA	0.01	Body Composition	1	0.01 mSv
Nuclear Medicine	0.001	Xe-133 adipose tissue blood flow	4	0.004 mSv
			TOTAL	**0.014**

Dose Constraint	**1 DEXA Body Composition Study (0.01 mSv)** **4 Xe-133 sub-cutaneous injections (0.004mSv)**

Risk Assessment for Research involving Ionising Radiation

Study Title and Reference	Relationship between regional adiposity and metabolism: an integrative approach
Age range of participants	18-65

Dose and Risk

Total effective dose (Research Only)	**0.014**	**mSv**
Cancer induction risk approx 1 in	1,000,000	

1 DEXA body composition study is additional to routine care

4 Xe133 subcutaneous injections are additional to routine care

9.2 Preparation of [$^2H_2$] palmitate infusion

The infusion is prepared within a laminar flow cabinet that is dedicated for the preparation of drugs or isotopes for infusion only. Gloves should be worn during the preparation of the infusion.

Equipment:

1 x 500 ml 4% human albumin solution
(Check expiry date and that it is clear and yellow).
1 x weigh boat
Potassium Palmitate – 2,2-D2
10 ml vial sterile water
1 x 20 ml syringe
3 x 50 ml syringe
5 x green needle
3 x orange needle
1 Falcon tube in a rack
1 filter – 0.20 µm (Sartorius Minisart non-pyrogenic)
Alcohol swabs
Label

Prior to preparation:

Clean flow cabinet with 70% industrial methylated spirits (IMS)
Place equipment in cabinet
Turn on UV light for 10 min, then turn on air flow for a further 10 min.
Turn on the two water baths. Check water levels.

Method:

Place albumin bottle in large water bath.
Put 10 ml sterile water into falcon tube.
Place falcon tube in the rack in the small water bath.
Turn on scales and place weigh boat on and tare balance to 00.000
Turn off air flow to cabinet.
Carefully weigh out Potassium Palmitate – 2,2-D2
Add carefully to hot sterile water in the falcon tube and mix gently.
If it does not dissolve immediately then put back into the small water bath for a further 5-10 min.

Turn flow cabinet back on.
Check temperature of large water bath and when at correct temperature (56ºC) remove albumin bottle.
Wipe albumin bung with alcohol swab and insert an orange needle.
Assemble green needle and filter.
Using a green needle and 20 ml syringe aspirate the palmitate from the falcon tube plus some air to clear the needle.
Remove needle from syringe and attach to the assembled filter and green needle.
Add palmitate to albumin carefully through filter.
Agitate albumin gently, label and replace into large water bath until needed.

9.3 Preparation of stable isotope drink

Ingredients:
Fat used for the emulsion:

Tesco olive oil, light and mild (73 g mono-unsaturated fatty acids, 14.3 g saturated fatty acids, 8.2 g polyunsaturated fatty acids per 100 g) for enrichment in [U-13C]oleic acid in plasma.

Purified safflower oil (Anglia) for enrichment in [u-13C]linoleic acid in plasma

Palm stearin (Anglia) for enrichment in [U-13C]palmitic acid in plasma

Myverol 18-04K emulsifier (Quest International)
Cocoa powder (Cadburys, 322 kcal, 23.1 g protein, 10.5 g CHO, 20.8 g fat per 100 g)
Granulated sweetener, aspartame (Canderal)
Hot water
Stable isotopically-labelled fatty acids or triglycerides (tracers).

Storage of isotopes:
[U-^{13}C]palmitic acid (powder): This should be stored/standing at room temperature for at least 30 min prior to use. Each bottle should be kept in a sealed plastic bag which will need to be replaced each time isotope is removed.

[U-^{13}C]linoleic acid (liquid): Unopened bottle stored in fridge. Once opened should be allocated into Eppendorf tubes and stored at -80 °C, defrost before use.

[U-^{13}C]oleic (liquid): Stored in the fridge in solid form, needs to stand at room temperature prior to use to become liquid.

Equipment :

Accurate scale
600 ml thick walled Pyrex beaker
Beakers to heat water and weigh oil
Spoon spatula for weighing powdered form isotope
Pipette and tips for liquid isotope
Teaspoon for weighing other powder ingredients
Hand mixer
Plastic bottle for the finished emulsion
Disposable plastic cups
Digital food thermometer
Microwave
Weighing boats
100 ml measuring cylinder
Baby bottle warmer

Preparation:

Preparation can be done one or two hours in advance but is better just before the drink is needed (emulsion with saturated fat needs to be made just before consumption).

Fill the bottle warmer with water and set to heat to 65 °C
Place all equipment and ingredients on a piece of blue roll.
Using the kitchen scales: Tare the scales with a plastic cup/weigh boat and weight out appropriate oil or fat, pour into 600 ml Pyrex beaker.
Using the accurate scales weigh out the following:

Emulsifier in weighing boat.
Cocoa powder in weighing boat.
Sweetener in weighing boat.
The appropriate amount of tracer(s) if required. The tracer and amount weighed should be checked by two appropriately trained staff.

Heat the 600 ml beaker containing the oil in the microwave for 20 sec. Check the temperature is between 50 and 60 °C.
Add the emulsifier (and tracer(s) if using) to the hot oil, swirl gently and dispose of weight boat/pipette tips immediately.
Put the beaker back into the microwave and heat for 10 sec, recheck the temperature; if the oil temperature is at or very close to 70 °C and the emulsifier has not dissolved then transfer to a pan of hot water and warm through until the emulsifier has dissolved. If the temperature is less than 65 °C and the emulsifier has not dissolved reheat for another 10 sec in the microwave. Repeat with 10 sec bursts until the emulsifier has dissolved. Do not let the oil heat above 70 °C as it will oxidise the fatty acids in the oil and tracer(s), and spoil the taste.
Remove the beaker and place in a pan of hot water to keep it warm.
Measure hot water into 100 ml cylinder.
Add the cocoa to the hot oil.
Add the sweetener to the hot oil.
Add most of the hot water to the hot oil mixture.
Mix everything with the handmixer for 2 min to achieve a good emulsion.
Transfer to a bottle, rinse the mixer with a few millilitres of the remaining hot water and add to bottle, then rinse the beaker with hot water and also add to the bottle.
Put the lid on the bottle.
Place in the bottle warmer to keep warm until needed.
The finished product should be light in colour (like milk chocolate) and not dark like the cocoa.

Suppliers:

Aarhus United Uk Ltd (Anglia Oils Limited)
King George Dock
Kingston-upon-Hull
HU9 5PX
Telephone: 01482 701271
Fax: 01482 709447
Contact : Norman Harris

Quest International
PO Box 18
3330 AA Zwijndrecht
The Netherlands

or
Lindtsedijk 8
3336 LE tZwijndrecht,
The Netherlands
Telephone: +31 78 610 9920
Fax: +31 78 619 5279
HYMONO 8903K Cat. no: 5Z10398 for 1 x 250 grams

9.4 Measurements of fatty acid composition and isotopic enrichment

Analysis of specific fatty acid composition of TG and NEFA by gas chromatography:

Total lipids extraction from plasma and lipoprotein fractions, and the preparation of methyl esters from NEFA and TG fractions in order to determine fatty acid composition and isotopic enrichment has been described previously (247). Fatty acid compositions (μmol.100 μmol total fatty acids^{-1}) were determined by gas chromatography (GC), and palmitate concentrations calculated by multiplying the proportion of palmitate by the corresponding plasma concentration of NEFA or TG determined enzymatically.

Analysis of [^{13}C]-enriched triglyceride rich lipoprotein-TG samples by GC-IRMS

The [^{13}C]/[^{12}C] ratio in the fatty acid methyl ester (FAME) derivatives were determined by combustion isotope-ratio mass spectrometry using a 'Delta Plus XP' GC-C-IRMS (Thermo Electron Corporation) in order to trace incorporation of the [^{13}C]-fatty acids into lipoprotein fractions. FAMEs were resolved using a Varian CP-FFAP CB capillary column (Varian Limited, Oxford) with dimensions of 25 m x 0.32 mm x 0.3 μm fitted in the GC (Agilent Technologies UK Limited, Cheadle Royal Business Park, Stockport, Cheshire). The sample (1 μl) was introduced using splitless injection mode, injector temperature of 250 °C and initial oven temperature of 80 °C for 1 min. The oven temperature was increased by 25 °C.min^{-1} to 200 °C, and after holding for 15 min, the temperature was increased again by 25 °C.min^{-1} to 240 °C and held for 7.6 min. The column flow was held constant at 1.2 ml.min^{-1}. FAMEs were converted to CO_2 by heating at 940 °C in the presence of Pt/CuO/NiO, and the [$^{13}CO_2$]/[$^{12}CO_2$] ratio was determined using tricosanoic acid methyl ester as an isotopic enrichment standard (247).This was verified on each run by including a certified standard of eicosanoic

acid FAME with $\delta^{13}C\ ^{0}/_{00}$ v Vienna-PeeDee Belemnite of -25.38 (The Department of Geological Sciences, Indiana University, USA). The retention times of individual fatty acids were verified using a reference material (AOCS#6, RM-6, Thames Restek UK Ltd, Bucks) containing known proportions of the fatty acids of interest. Results expressed as with $\delta^{13}C\ ^{0}/_{00}$ were converted to TTR using the following formula:

$$TTR\ (^{13}C/^{12}C) = (\delta^{13}C\ ^{0}/_{00}/1000)+1)*0.0112372$$

The TTR for a baseline sample (before administration of the stable isotope tracer) was subtracted from each TTR to account for naturally occurring [^{13}C] enrichment.

Analysis of [$^{2}H_2$]- and [U-^{13}C]-enriched plasma TG and triglyceride-rich lipoprotein samples by GC-MS

[U-^{13}C] and [$^{2}H_2$]palmitate enrichments were determined simultaneously by GC-mass spectrometry (GC-MS) using a 5890 GC coupled to a 5973N MSD (Agilent Technologies, UK). The GC was equipped with a DB-Wax 30 m capillary column (from Agilent, i.d. 0.25 mm, film thickness 0.25 µm) and ions with mass-to-charge ratios (m/z) of 270 (M+0), 272 (M+2) and 286 (M+16) were determined by selected ion monitoring. Dwell time was 100 ms. TTRs for [U-^{13}C]palmitate (M+16)/(M+0) and [$^{2}H_2$]palmitate (M+2)/(M+0) were multiplied by the corresponding palmitate-NEFA or palmitate-TG concentrations to give plasma tracer concentration.

9.5 RNA extraction from adipose tissue biopsies

Equipment

TRI reagent (Sigma Cat. No.T9424 or Ambion Cat. No. AM9738)
80% ethanol
100% ethanol
Isopropanol
mirVana™ miRNA Isolation Kit (Ambion Cat no. 1561)
1-bromo-3-chloro propane (Sigma Cat. No. 085K3767)
Sodium Acetate 5M, pH 5.5 (Ambion)
RNA storage solution – freezer (Ambion).
DNA-free™ (Ambion Cat. No. AM1906)
Homogeniser (Mixer Mill MM 400, Retsch, Haan, Germany)

Homogenization of fresh tissue samples

Add a ball bearing and 1 ml of TRI reagent to a 2 ml Eppendorf tube.

Weigh the tube and record (can be frozen for later use).

Transfer fresh biopsy directly into tube. For large biopsies split between multiple tubes.

Immediately close lid, place in tube adaptor of homogeniser.

Place adaptor in homogeniser tightening clamp so it is tight but not too tight.

Make sure the balancing adapter is in place in the other clamp of the homogeniser.

Homogenise for 1 min at frequency 25.sec^{-1}.

Re-weigh tube to determine weight of fat biopsy.

Dilute the homogenate with TRI reagent such that there is at least 1 ml per 100 mg of tissue. Place in a strong 15 ml tube with a blue lid (can be frozen at -80 °C).

Separation of lipids

In preparation, label fresh high speed-compatible 15 ml tubes and 1.5 ml Eppendorf tubes for lipid layer.

Place 15 ml tubes containing thawed homogenized fat biopsy in cooled centrifuge and spin at 9500g for 20-40 min at 4 °C.

Remove lower pink layer, and the pellet at bottom, from under the upper lipid layer and place into the fresh labelled 15 ml tube – avoid pipetting any lipid by pipetting out an air bubble when introducing pipette through lipid layer (the lipid layer may not be visible on small samples). Store fat layer and remnant homogenate left behind at -80 °C for lipid analysis.

Separation of aqueous phase

Measure approximate volume of homogenate and record (better to overestimate slightly rather than underestimate).

Add 0.1 x volume of 1-bromo-3-chloro propane.

Mix samples by hand for 15 sec. Leave 5 min on the bench.

Place in a cooled centrifuge and spin at 9500g for at least 20 min at 4 °C

Whilst spinning samples, label and weigh empty 15 ml tubes (or 2 mL Eppendorf tubes if small sample) for aqueous phase, and 2 ml Eppendorf tubes for organic protein/DNA phase – if keeping for protein analysis or DNA-extraction.

Remove upper aqueous layer (using a 1000 µl pipette) and place in weighed tubes. Be careful not to transfer the interphase or organic phase (pink). If using the next back extraction step, more aqueous layer can be left behind. Keep the pink organic layer for protein extraction.

Back-extraction for maximum RNA recovery

Add 750 µl of TRI reagent and 75 µl of 1-bromo-3-chloro-propane to fresh 2 ml Eppendorf tubes. (N.B if small samples, add 400-500 µl TRI reagent and 40-50 µl of 1-bromo-3-chloro-propane).

Add 750 µl of remaining aqueous layer, interphase and organic phase to these tubes. Mix samples by hand for 15 sec. Leave on the bench for 5 min.

Place in a cooled centrifuge and spin at maximum speed at 4 °C for at least 15 min.

Remove upper aqueous layer (using a 200 µl pipette) and place in the weighed tubes with the aqueous phase from the 15 ml phase separation. Add the remaining organic layer and interphase to the previous organic layer and store at -80 ºC for later protein extraction.

Re-weigh aqueous phase tubes and calculate weight of aqueous phase. Divide this by 1.076 to achieve true volume and record.

RNA purification

At this point the RNA is present in the aqueous phase. A standard isopropanol precipitation and 70% ethanol wash following the TRI reagent standard protocol was used (248).

9.6 Real time PCR

The Applied Biosystems (ABI; Life Technologies Corporation, Carlsbad, CA, USA) platform was used. For cDNA synthesis the manufacturer's High Capacity cDNA Reverse Transcription Kit (ABI product code 4368813) was used. For real time PCR the TaqMan® Gene Expression assay was used. All procedures were performed according to the manufacturer's instructions. The following primers were used (exact primer sequences retained by manufacturer):

Gene	**ABI assay ID**
ADRA1A	*Hs00169865_m1*
ADRA2A	*Hs00265081_s1*
ADRB1	*Hs00265096_s1*
ADRB2	*Hs00240532_s1*